Cooperative Research Centre for Coastal Zone, Estuary & Waterway Management

Technical Report 34

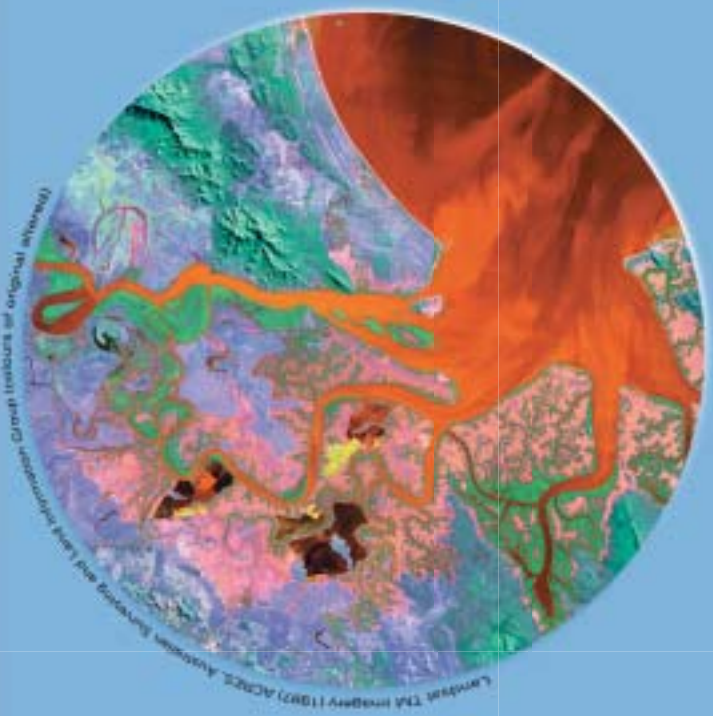

Keppel Bay: physical processes and biogeochemical functioning

L.C. Radke,
P.W. Ford,
I.T. Webster,
I. Atkinson
K. Oubelkheir

2006

CSIRO
Central Queensland University Where Students Come First.
Queensland Government Natural Resources, Mines and Water
Australian Government Geoscience Australia
Griffith University
CRC for Coastal Zone Estuary & Waterway Management

Keppel Bay: physical processes and biogeochemical engineering

L.C. Radke[1], P.W. Ford[2], I.T. Webster[2], I. Atkinson[1], K.Oubelkheir[2]

[1] Geoscience Australia, Canberra, ACT

[2] CSIRO Land and Water, Canberra, ACT

2006

Keppel Bay: physical processes and biogeochemical functioning

Written by:

L.C. Radke

P.W. Ford

I,T, Webster

I. Atkinson

K. Oubelkheir

Published by the Cooperative Research Centre for Coastal Zone, Estuary

and Waterway Management (Coastal CRC)

Indooroopilly Sciences Centre

80 Meiers Road

Indooroopilly Qld 4068

Australia

www.coastal.crc.org.au

National Library of Australia Cataloguing-in-Publication data

Keppel Bay: physical processes and biogeochemical functioning

QNRM06356

ISBN 1 921017759 (print and online)

Acknowledgements

The work described in this report was funded by the CRC for Coastal Zone, Estuary and Waterway Management and relied on extensive inputs of data and ideas from members of other components of the Fitzroy Contaminants subproject (described in CRC Reports 34 to 37). We acknowledge and thank the following other people for their various contributions to this work:

Kirrod Broadhurst, Graham Wassell, Paul Ridett and David Munro, the captain and deckhands of the *Rum Rambler*, managed navigation, shared local knowledge and provided assistance during the sampling.

Lesley Clementson of CSIRO Marine and Atmospheric Research undertook the phytoplankton pigment analyses.

Ray Degraaf, Stan Rucinski, Andrew Hislop, Tim Johnson and Craig Wintle of the Field and Engineering Support Group at Geoscience Australia developed and produced equipment used on the survey (sediment grab, continuous flow apparatus and filtering apparatus).

Miles Furnas (AIMS) and David Haynes (GBRMPA) for access to data and helpful advice.

Nicky Grigg saved our bacon in formatting Word.

Ralf Haese engaged in helpful discussions pertaining to science and methods, and provided constructive criticism to an earlier version of this report.

Alan Hinde (Geoscience Australia) wrote a macro that calculates PSUs.

Danny Hunt provided advice on preparing samples for surface area analysis and Adrian Beech (CSIRO) undertook these analyses.

Angie Jaensch, Veronika Galinec and Heinz Buettikofer drafted the figures.

Algis Juoldvalkis (Geoscience Australia) prepared and analysed samples by XRD/SiroQuant. Tan Kok Piang (Geoscience Australia) provided some advice on the methods.

John Pyke, Liz Webber and Bill Pappas (Geoscience Australia) prepared and analysed the XRF and LECO-TOC samples. Liz Webber conducted FeO analyses. Richard Phillips (CSIRO PI) carried out the C and N isotopic analyses.

Andy Longmore (MAFRI) undertook analysis of the different types of sediment P.

Alex McLachlan and Neil Ramsay (Geoscience Australia) conducted the grain size analyses.

Luis Neumann and David Page (The University of Queensland) provided advice on quality control measures for grain size analysis.

Bob Noble, Bob Packett and Peter Verwey (DNRMW Queensland) assisted with logistics and provided local knowledge.

Rachel Davenport and Carolyn Sandison (Geoscience Australia) ran the mass spectrometer, and provided advice on the analysis of carbon isotopes in sediments with low TOC contents.

Darren Skene, Brendan Brooke, David Ryan and the crew of the *Pacific Conquest* collected box core and vibro-cores.

Peter Taylor (Geoscience Australia) milled the sediment samples.

Colin Tindall provided support in the field and with the survey logistics.

I.T. Webster and P.W. Ford led the design of this study, with contributions from I. Atkinson, K. Oubelkheir and L.C. Radke. The report was written and compiled by P.W. Ford, L.C. Radke and I.T. Webster: P.W. Ford led Chapters 6 and 7; L.C. Radke led Chapter 5 and I.T. Webster led Chapters 3 and 4. All authors contributed to the final synthesis (Conceptual Models) in Chapter 8. I. Atkinson was a key participant and organiser of the field work. K. Oubelkheir contributed to the pigment analysis and provided a link to the remote sensing activity.

Table of contents

Table of figures

Table of tables

Non-technical summary

In recent years there has been concern that catchment-derived nutrients and sediments discharged by rivers into the lagoon of the Great Barrier Reef are having a deleterious impact on near-shore reef ecosystems. On average, the Fitzroy River delivers the second largest quantity of these materials to the lagoon after the Burdekin River. The Fitzroy Agricultural Contaminants Project (AC), which is a Coastal CRC project, included amongst its aims the development of an understanding of the fate and impact of these agricultural contaminants (nutrients and sediments) within the Fitzroy Estuary-Keppel Bay system.

One activity in Project AC is aimed at providing an understanding of the functioning of Keppel Bay and adjacent waterways from the physical, chemical, and biological-ecological perspective. It considers the sources, forms, and availability (for primary production) of nutrients (both dissolved and attached to particulates), the physical processes moving these substances throughout Keppel Bay and the growth of phytoplankton in the bay. The results described here were applied in the conceptualisation, validation, and calibration of computer models used to make predictions of the response of Keppel Bay to changes in loads delivered from the catchments. This report is one of a suite of final milestone reports summarising the findings and developing conceptual models of the inter-relationship of the various processes.

The Fitzroy River flows as a series of one or more ‘flood’ events most commonly during the summer months. Virtually all the nutrients and fine sediments are delivered to its estuary during these events; for most of the rest of the year, river flows are small and provide insignificant contaminants inputs. Large freshwater flows can fill the estuary and discharge fresh water, nutrients and fine sediments directly into Keppel Bay. The resulting freshwater plumes are gradually dispersed within Keppel Bay by the strong tidal currents and by wind-driven flows. Most of the nutrient material that is transported down the river is in organic form attached to fine sediment particles. Flocculation causes these fine sediments and attached nutrients to be deposited fairly near the mouth of the Fitzroy Estuary.

During the dry-season, the deposited organic material breaks down through bacterial action releasing nutrients into the water column. In turn, these nutrients are consumed by phytoplankton and eventually converted to dissolved form when the phytoplankton die and are decomposed. Through mixing processes and currents much of the nutrients in their various forms are dispersed throughout Keppel Bay and to other parts of the GBR lagoon. In effect, Keppel Bay acts as a biogeochemical reactor, which transforms particulate and dissolved organic material input by the Fitzroy River and gradually ‘leaks’ it to

other parts of the GBR lagoon. However, much of the nutrient input during floods in the form of organic matter attached to fine particles is buried within the bay and tidal creeks and takes little or no further part in biogeochemical cycling. The following findings of the biogeochemical activity should be considered in the light of this conceptual model.

1. With tidal ranges of up to five metres at spring tides, the tidal currents within the bay are strong and are certain to be a major agent for the mixing of dissolved and suspended particulate material throughout Keppel Bay. The prevailing winds in the Capricornia Region are southeasterly and will tend to steer contaminants ultimately derived from the Fitzroy River northwards along the coast.
2. Annual evaporation exceeds precipitation in the Keppel bay area. Under dry-season conditions, the salinity of the inshore waters (western edge of Keppel Bay) is higher than the deeper and more marine eastern edge. The estimated time to replace the water in Keppel Bay is ~20 days.
3. Under wet season conditions, the inshore waters have a lower salinity than the eastern (marine) waters. Most of the (small) flood waters remained within Keppel Bay for at least 10 days after the event.
4. Earlier work has shown that during major flood events the flood plume exists as a freshwater layer spreading seaward over largely marine waters. During our investigations undertaken during a year of less-than-average river discharge, the plume did not exist as a distinct freshwater surface layer.
5. The tides are semi-diurnal and have a 14-day spring-neap cycle. King tides occur in February and August and, in addition to the astronomical components, wind effects can produce a further 20 cm increase in sea level. This is significant in affecting inundation and establishing connectivity in the wetlands adjoining Keppel Bay and the tidal creeks.
6. The wave climate in Keppel Bay is such that under reasonably frequently occurring wind conditions wave driven processes are likely to be the dominant mode of fine-sediment resuspension along the western side of Keppel Bay.
7. The sediments entering Keppel Bay from the Fitzroy catchment in the freshwater are predominantly fine particles (>80% are <10 µm). The particles rapidly aggregate on mixing with relatively small amounts of salt water (flocculation). The settling speed of the aggregates is much faster than that of their individual constituent particles.

8. The concentration of suspended sediments in the water column varies greatly over the daily tidal cycles and over the spring-neap cycle. This variation reflects the combined effects of local resuspension, the advection of resuspended material from up-current, and the settling of aggregates (at about two m/day) from the water column.
9. Due to the active resuspension processes, there is a strong correlation between the mud content of the sediments and the turbidity of the water column, with the suspended sediment concentrations highest in the channel approaches to the Fitzroy Estuary.
10. During the dry season, there is net export of suspended sediments out of Keppel Bay through the Timandra channel equivalent to an annual rate of approximately two million tonnes, and a smaller quantity is exported past Buoy 1.
11. Keppel Bay sediments are a mixture of sediment types. In addition to the areas of high mud content, there are large areas of relict sands and zones of intermediate composition. The major sediment geochemical characteristics reflect the sediment fabric with the highest nitrogen, phosphorus, organic carbon and iron contents all associated with the highest mud content consistent with the high surface area of the muds.
12. All sediment classifications have large proportions of biologically-unavailable phosphorus bound to calcium. The carbon and nitrogen contents of the sediments are low relative to other estuarine systems and the content of the incoming particulates. These differences reflect the net loss of C, N and P due to decomposition processes in sediments.
13. The highest concentrations of dissolved nutrients in the dry season occur in the zones of highest turbidity reflecting the highest mud contents and resuspension. Particulate nutrients in the water column are the principal nutrient form available in the dry season and the concentrations are strongly correlated with the concentration of suspended sediment.
14. In the wet season, reflecting the delivery of nutrients in the flood waters, the zones of lowest salinity have the highest nutrient concentration. There is some release to the water of nitrogen nutrient species attached the incoming particles and there is enhanced microbial break down of unreactive forms of nitrogen to produce biological available forms immediately post flood.
15. Integrating all the biogeochemical results leads to the definition of three zones within Keppel Bay: Zone of Maximum Resuspension (ZMR); Blue Water Zone (BWZ): and a Coastal Transition Zone (CTZ) with

intermediate properties reflecting the broad band of the tidal excursion between the two end members. This is a powerful organising principle as numerous other biogeochemical characteristics such as the distribution of phytoplankton and the various phytoplankton functional groups, optical properties of the water column all differ between these three zones but are coherent within the zone.

16. The ZMR is the zone of highest dissolved nutrient concentration, highest phytoplankton biomass, and highest turbidity and encompasses the sediments with a relatively high proportion of mud. The BWZ is the zone of sands and greatest water clarity, the lowest dissolved nutrient concentrations, and the lowest concentration of phytoplankton.
17. Four major coastal creeks (Connor, Casuarina, and the Raglan-Inkerman Creek system) enter the south western corner of Keppel Bay in close proximity to the mouth of the Fitzroy estuary. Their combined volumes and surface areas are comparable to that of the estuary and they play a substantial role in the dry season processing of nutrients.
18. All creeks have very small catchments and their hydrology is dominated by inputs of salt water (dry season) and freshwater (wet season) at the mouth together with suspended sediments. Raglan Creek has an upstream source of fresh water. These factors lead to a wide range of salinity zones in the creeks and make them an important area ecologically by providing diverse habitats.
19. The creeks differ in depth and the extent of tidal resuspension of fine sediment, and water turbidity varies correspondingly. Connor Creek is the deepest creek. It has the lowest turbidity, highest primary production, and removes dissolved nutrients entering from Keppel Bay, while Casuarina Creek has high turbidity, low primary production, and exports dissolved nutrients to Keppel Bay
20. The measured rates of oxygen evolution demonstrate that photosynthesis occurs at similar rates in the ZMR and BWZ despite the ZMR having significantly higher chlorophyll concentrations. The nutrient concentrations differ widely between zones with the ZMR having sufficient bioavailable nitrogen to sustain a further two days production. In the BWZ however, the nitrogen supply is small and would be consumed in a fraction of a day. These results imply that the ZMR is light limited while the BWZ is nutrient limited.
21. Different phytoplankton functional groups dominate the different zones - diatoms in the ZMR, and small cyanobacteria in the BWZ.

22. In addition to the *in situ* primary production the filamentous cyanobacterium *Trichodesmium* is driven onshore by the prevailing winds. This represents a nutrient subsidy to Keppel Bay from the off shore areas and although it increases local nutrient bioavailability by orders of magnitude it is small compared to the inputs from the Fitzroy River.

23. Preliminary budgets have been established for nitrogen and phosphorus. They show that about ¾ of the entering materials derived from the catchment are ultimately exported from Keppel Bay albeit in changed chemical forms while the remainder is buried in the sediments of Keppel Bay.

Introduction

Project origins and aims

The Fitzroy catchment is the largest Queensland catchment (144 000 km^2) discharging to the Great Barrier Reef Lagoon and the second largest seaward draining catchment in Australia. Sediments, nutrients (both particulate and dissolved), together with anthropogenic pollutants originating upstream in the catchment are discharged via the Fitzroy Estuary into Keppel Bay. The bay and the estuary act as natural chemical reactors where the materials delivered undergo chemical and physical transformations before being stored in the growing deltaic and beach areas, or are transported eastward to the southern zone of the Great Barrier Reef (GBR) Lagoon. There is growing evidence (summarised in Furnas, 2003) that sediments, pollutants, and nutrients generated by human activities in tropical catchments and then transported by rivers into the GBR Lagoon have the potential to exert a deleterious impact on the basic reef ecosystems. In especially severe occurrences, these materials have the capacity to irreversibly affect the structure and function of central components of the reef ecology such as corals and sea grasses with ultimate loss of the natural ecosystem.

Substantial resources have been provided recently under the auspices of Reef Water Quality Protection Plan (http://www.deh.gov.au/coasts/pollution/reef/) to improve land-use management practices within many of the Queensland catchments with the intent of reducing loads of potentially deleterious substances entering the GBR lagoon. The Fitzroy catchment and the adjacent Burdekin catchment, are the two largest sources of sediments and nutrients to the GBR Lagoon (Furnas, 2003). Accordingly, these two systems were given special prominence for reduction in sediment and nutrient loads through funding of improved catchment management. However, the requisite background knowledge to make realistic predictions of the response of the estuarine and Keppel Bay ecosystems to different sediment and nutrient loads, and to evaluate the consequences of altered water deliveries to the GBR lagoon did not exist when this project started. The Agricultural Contaminants Project (AC) was developed to address these knowledge gaps and to produce the requisite predictive framework to aid managers in the evaluation of various load reduction strategies and therefore of the various alternative proposed changes in the catchment management.

Project AC has five broad objectives:

1. How are nutrients and sediments transported and transformed within the Fitzroy Estuary and Keppel Bay?
2. How are variations in nutrient and sediment delivery likely to impact on ecological function and primary production within the system?
3. How are variations in riverine loads of sediment and nutrients likely to alter delivery to the GBR
4. What pesticides are delivered to, and remain in the Fitzroy Estuary and Keppel Bay?
5. How should managers monotor ecosytem health and function?

Project AC builds on previous projects undertaken by the Coastal CRC in the Fitzroy Estuary (Currie and Small, 2002; Margvelashvili *et al*., 2003; Webster *et al*., 2004; Douglas *et al*., 2005b) by extending the focus to include Keppel Bay. It is complemented by two concurrent projects in the estuary, namely Environmental Flows (AF) and Floodplain Wetlands (AW). The project comprised a series of field-based measurement programs which were undertaken to develop an understanding of various facets of the system dynamics. These studies were also used to support the development of linked computer models of the hydrodynamics, fine-sediment dynamics and the biogeochemistry of the Fitzroy Estuary-Keppel Bay system. The models provide a predictive framework as well as diagnostic support for the measurement-based studies.

Relationship of the contents of this report to the scientific questions

This report fulfils the obligations of milestone AC66. It presents the results and interpretation of the project activity that investigated the biogeochemistry of Keppel Bay and the adjacent tidal creeks. This activity was primarily concerned with developing an understanding of the cycling of nutrients and primary production in the bay. Measurements were obtained on the physical and chemical properties of the water column (as well as phytoplankton concentrations), and on bottom sediments from throughout the bay. The report presents an interpretation of these measurements in the context of currents and mixing, fine-sediment dynamics, biogeochemical function and primary production. The measurements were also used to validate and calibrate all three computer models as well as to facilitate the use of remotely sensed chlorophyll and suspended sediment concentrations to provide synoptic data for the whole of Keppel Bay.

Structure of this report

In Chapter 2, we provide an overview of the principal and geological characteristics of the Fitzroy catchment and of Keppel Bay (the Fitzroy Estuary was investigated in an earlier project undertaken through the Coastal CRC and is thoroughly described in Douglas *et al.* (2005b)). The next section describes the hydrological characteristics of the catchment. River floods are the mechanism by which sediments, nutrients, and pollutants are moved from the catchment into the coastal area and these intermittent deliveries are key drivers of biogeochemical processes within Keppel Bay. This chapter concludes with a summary of the experimental methods, especially those used in our field investigations.

Chapter 3 starts with an account of currents and mixing including within Keppel Bay. The tidal currents are discussed as well as wind-driven currents along the coast. These processes are responsible for transport of nutrients, both dissolved and particulate, both within Keppel Bay and along the coast, as well as controlling the amount of material suspended in the water column. Water properties within the bay are considered for the dry season and for the time following summer flows in the Fitzroy River. The salinity regime within Keppel Bay is examined and is used to derive an estimate of exchange time for the bay. The results of the hydrodynamic modelling of the Fitzroy Estuary and Keppel Bay is presented in Report 38 (Herzfeld *et al.*, 2006)

The next chapter (Chapter 4) considers the temporal and spatial distributions of fine suspended sediments in Keppel Bay. These sediments with particle sizes less than 63 µm are carried down the Fitzroy River, through the estuary and eventually some of them are deposited in Keppel Bay where they are a major component of the seabed over much of the bay. Fine sediments are readily suspended by the currents within the bay and, due to their relatively slow sinking rates, can remain in suspension for some time before settling back to the bottom. High concentrations of sediments in the water column lead to high turbidity and a consequent reduction in light necessary for photosynthesis by benthic plants and microalgae and by phytoplankton. Further, organic material adsorbs to the surfaces of the sediment particles in sufficient amounts so that the transport of these sediments represents a major pathway for the movement of these organic materials from one part of the bay to another. Thus, behaviour of fine sediments is an important determinant of the biogeochemistry of Keppel Bay both through its potential impact on primary production and on nutrient cycling. The modelling of the resuspension, settling and transport of fine sediments is treated in a separate Report 39 for the project (Margvelashvili *et al.*).

Chapter 5 deals with the biogeochemistry of both the sediments, and the dissolved phases in Keppel Bay. It uses statistical techniques to examine the spatial distribution of the various nutrients in the solid phase within the sediments, with emphasis on the role of iron as the major oxidant. Attention is then focussed on the biogeochemical character of the suspended solids and useful predictive relations are established between the surface area of the sediments (and surrogates) and the content of the major nutrients and iron. These relationships are used to deduce the role of microbial mediated processes which are converting particulate attached nutrients into dissolved nutrients and thus into forms available for ready uptake by phytoplankton. The existence of strong spatial gradients in the distribution of dissolved nutrients is then demonstrated and the implications for nutrient sources and sinks discussed. The chapter concludes with a zonation of Keppel Bay based on an integration of the sediment characteristics and the water column properties, which are controlled by the sediment.

Chapter 6 examines the biogeochemical behaviour of the major tidal creeks. These creeks have a combined area, which is similar to the area of the Fitzroy Estuary. Nutrients and fine sediments are transported in and out of them by the tides and by freshwater flows so these creeks are potentially important areas for the mineralisation and storage of organic particulate matter and for primary production. Their role determining the fate of material discharged from the Fitzroy Estuary is significant. Further, they represent unique aquatic systems that have hardly been studied.

Chapter 7 provides an outline of the spatial distribution of primary production by the various major functional groups throughout Keppel Bay, and looks at the implications for coastal nutrient budgets of the delivery of large amounts of the nitrogen fixing cyanobacterium *Trichodesmium* spp. to the shoreline.

The concluding Chapter 8 provides a summary of our conceptual understanding of the oceanographic processes, the fine sediment dynamics, and the processes controlling the biogeochemistry and primary production across the Bay. It draws together key features of the knowledge gained from the study particularly as this knowledge addresses the overall objectives of the Agricultural Contaminants project.

Background

Fitzroy River catchment and hydrological behaviour

The Fitzroy River has the largest Queensland catchment (144 000 km^2) draining to the Great Barrier Reef Lagoon. Four major rivers (Connor-Isaacs, Nogoa, Comet, and the Dawson) join to form the Fitzroy, which discharges into its estuary at Rockhampton (Figure 2.1).

Rainfall in the catchments is highly episodic and is concentrated in the austral summer (December to March). The rainfall pattern arises from the competing influences of the different climate zones within the large catchment and reflects both the continental scale low pressure frontal systems which deliver rainfall predominantly into the southern parts of the catchment, and monsoonal rainfall (including occasional cyclones) which deliver water predominantly to the more northern sub-catchments.

Although there are numerous weirs on the various rivers draining the Fitzroy catchment, they are all small and essentially “transparent” to large flow events. The only large storage, capable of retaining large water volumes, is Fairbairn Dam on the upper reaches of the Nogoa. Large-scale events are relatively rare and consequently only one or two events per year are sufficiently large to produce sufficient runoff to completely fill the Fitzroy estuary below the barrage (~$2.5x10^8$ m^3) and produce a large delivery of fresh water into Keppel Bay. Consequently, inflows into Keppel Bay are infrequent and short lived (Figure 2.2), and, for most of the year, the only fresh water entering the estuary (and thus ultimately Keppel Bay) is small discharges of treated waste water from Rockhampton, and limited flows (18 000 m^3d^{-1}) over the fish-ladder at the barrage.

Because the inflows are dependent on relatively infrequent generalised rainfall events in the catchment, the annual discharge of freshwater into Keppel Bay is also highly variable.

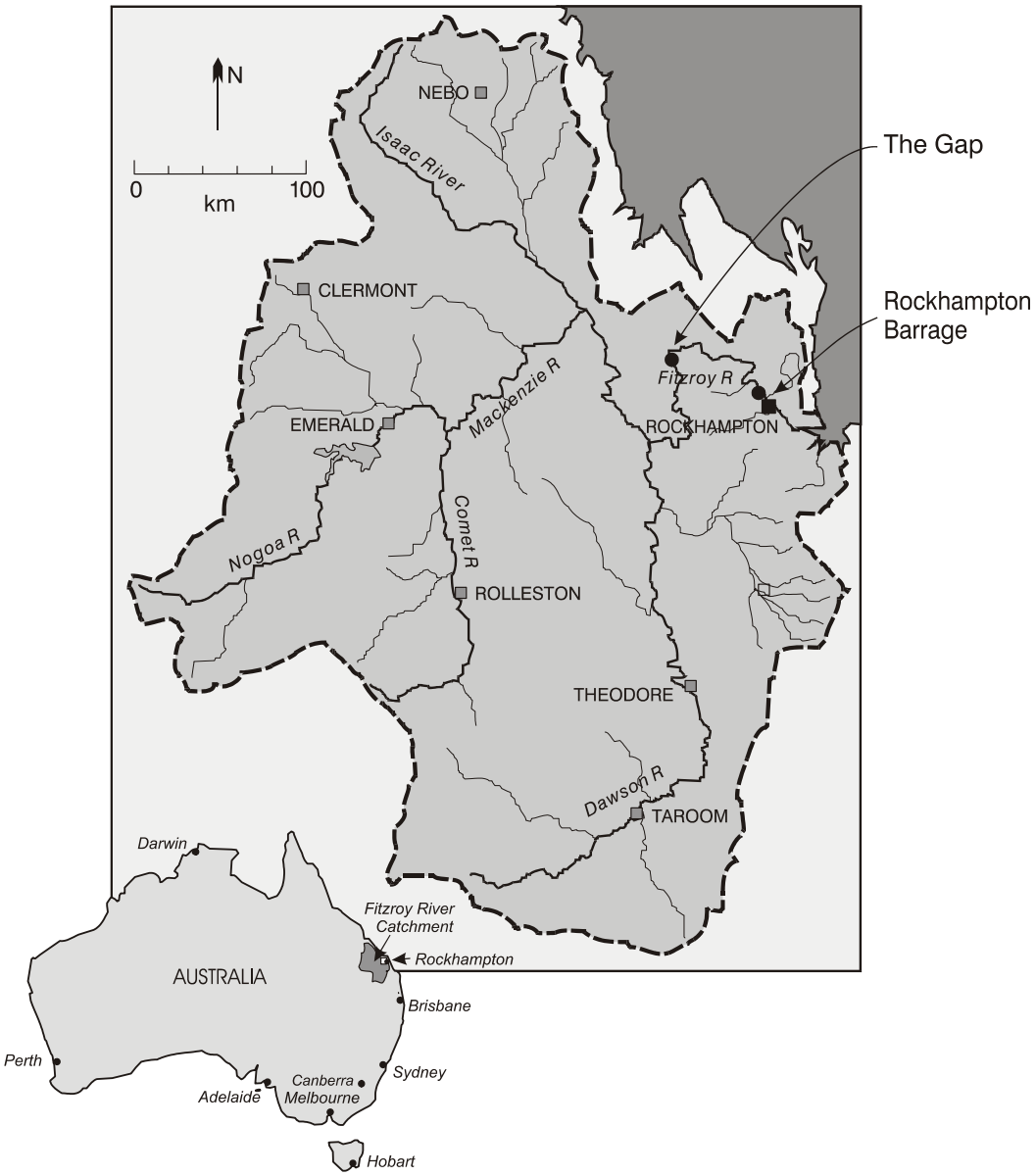

Figure 2.1: The major tributaries of the Fitzroy catchment and the entry of the Fitzroy Estuary into Keppel Bay.

The annual average discharge has varied (Figure 2.3) by more than two orders of magnitude, and deliveries of sediments and pollutants are likely to have varied on the same scale. This intrinsic variability underlines the value of the combined observation and modelling approach adopted in this work. The parametrised model allows us to explore what happens over a realistic sequence of different annual inflows rather than mounting long-term observational programs to measure them *in situ*.

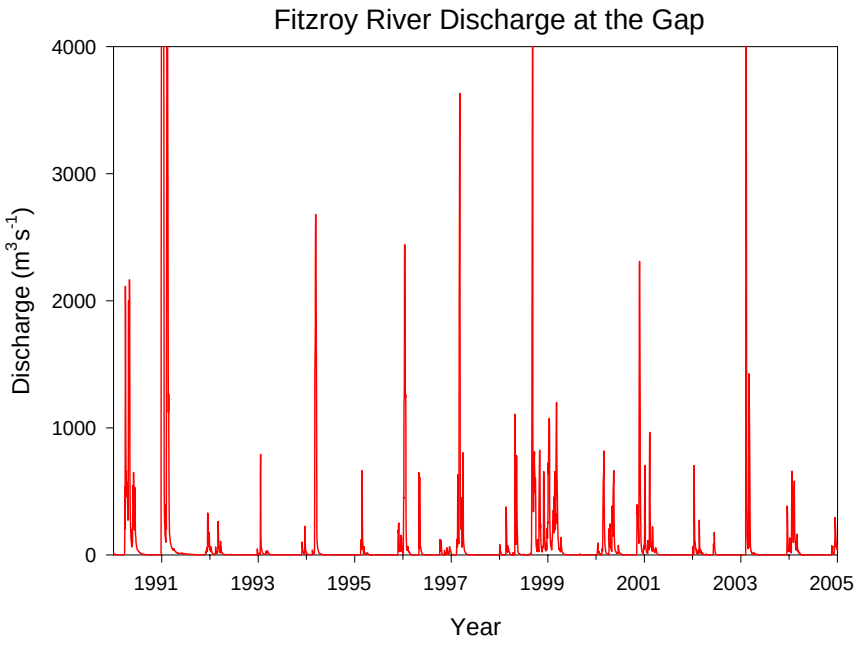

Figure 2.2: Instantaneous Discharge at the Gap. Note that the discharge during the 1991 event (3rd largest flood on record) peaked at ~15 000 m^3s^{-1}

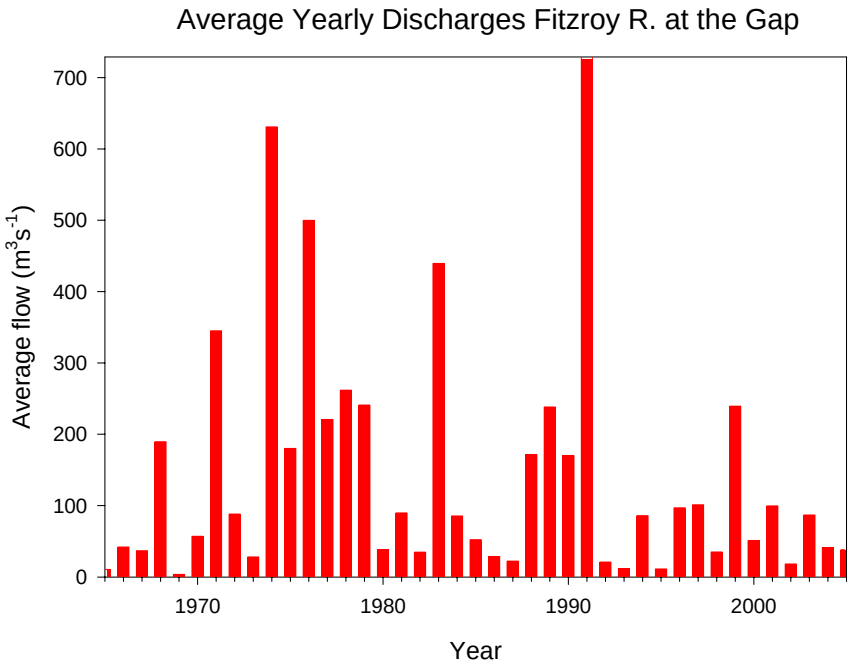

Figure 2.3: Average annual discharge from the Fitzroy River measured at the Gap.

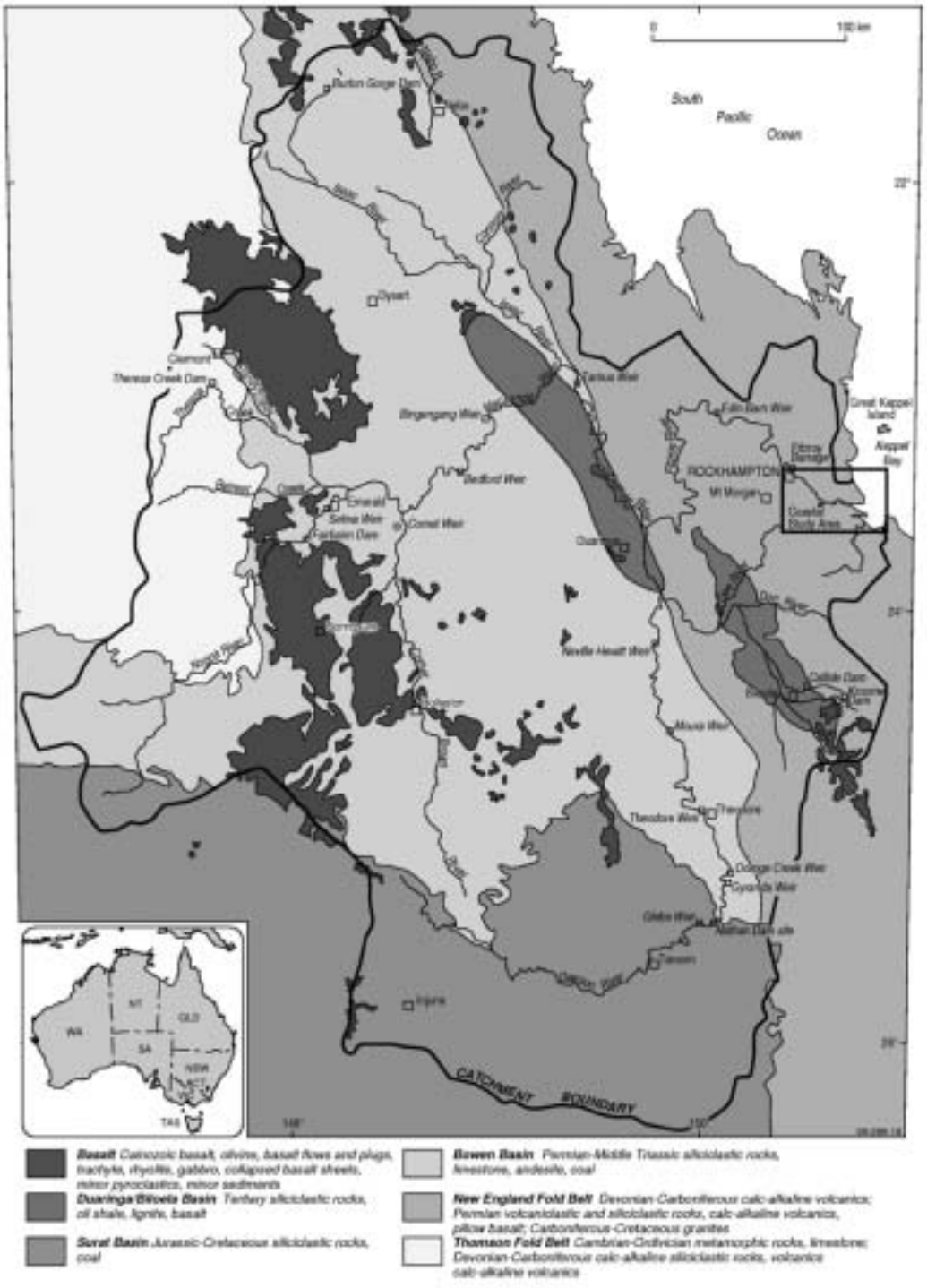

Figure 2.4: Major geological features of the Fitzroy catchment (after Douglas et al.*, 2005)*

Geology of the Fitzroy catchment

The geology of the Fitzroy River Basin (FRB) comprises more than 100 different types of rocks and has been divided into 5 major structural units (Figure 2.4; Douglas *et al.*, 2005a): The Thomson Fold Belt, the New England Fold Belt, the Bowen Basin, the Surat Basin and the Tertiary Basins. The Thomson Fold Belt (TFB) is found in the western-most part of the catchment and comprises

Cambrian-Ordovician metamorphic rocks, Devonian-Carboniferous siliclastics and calc-alkaline volcanic rocks. The New England Fold Belt (NEFB) is found in the easternmost part of the FRB and is composed of Devonian-Carboniferous calc-alkaline volcanics, Permian siliclastics and volcaniclastics and Carboniferous-Cretaceous granitoids. The Tertiary Basin occurs within and sub-parallel to the strike of the NEFB, and comprises the Tertiary siliciclastics, lignites, oil shales and basalts of the Duaringa Formation and the mudstones, sandstones, oil shales and lignites of the Biloela Formation. Permian-Triassic siliclastics, limestone, coal and andesite are found in the Bowen Basin (BB), in the central FRB, while Jurassic-Cretaceous siliclastic rocks and coal are found in the Surat Basin (SB) in the south of the catchment. Cainozoic volcanics (principally basalts) occur in isolated patches throughout the basin, but cover large patches of the BB.

An extensive Cainozoic weathering sequence also overlies the major structural units and may include duricrust, laterite, local scree deposits and soils. Clay and duplex soils account for more than half the area of soil cover (Furnas, 2003). Average TOC, TN and TP contents of soils in FRB are 1.3%, 0.09% and 0.042% respectively (data compiled by Furnas, 2003).

The Fitzroy Estuary

The upstream extent of the Fitzroy Estuary is defined by the barrage across the Fitzroy River at Rockhampton 60 km from the coast. At its coastal end, the estuary connects to the south-western corner of Keppel Bay in the vicinity of the major tidal creeks. Under flood conditions, relatively large volumes of water pass through the estuary and the residence time for water and pollutants is short (Webster *et al.*, 2004). Consequently, there is very limited opportunity for biogeochemical transformations to take place and most of the material is transmitted through to Keppel Bay unchanged. In contrast, immediately post flood, the estuary is filled with freshwater, and this is slowly displaced by exchange with seawater. This process takes about 100 days for the salinity at Rockhampton to approach that of seawater. During this extended period, there is ample time for the materials in the water, or settling out onto the estuarine sediments, to undergo chemical changes due to microbial processes. This (partially) transformed material is gradually transferred into Keppel Bay during the freshwater seawater exchanges. At the same time, the incoming seawaters bring a different mix of nutrients, sediments from Keppel Bay into the estuary and the creeks.

From a system perspective, the catchment can be considered as purely a source of materials to Keppel Bay. Under flood conditions, these materials go straight through to Keppel Bay. However, under low flow conditions, the estuary (and the

tidal creeks) and Keppel Bay are dynamically exchanging and transforming materials. As we will show later some of this material ultimately escapes from Keppel Bay although much of the material is deposited in the growing deltaic region. Overall, Keppel Bay functions to modulate (and reduce) the delivery of materials off shore to the Great Barrier Reef.

Keppel Bay

Keppel Bay is a relatively shallow embayment (Figure 2.5) with water depth slowly increasing seaward. At its northern end, our study area is defined approximately by the parallel of latitude running through the northern end of Great Keppel Island and its eastern boundary by the line joining Great Keppel Island to Cape Keppel on Curtis Island. Its offshore extent is ~20 km and the distance between its southern end near the mouth of the Fitzroy to Great Keppel Island is ~40 km. Depths near the offshore boundary are ~15 m.

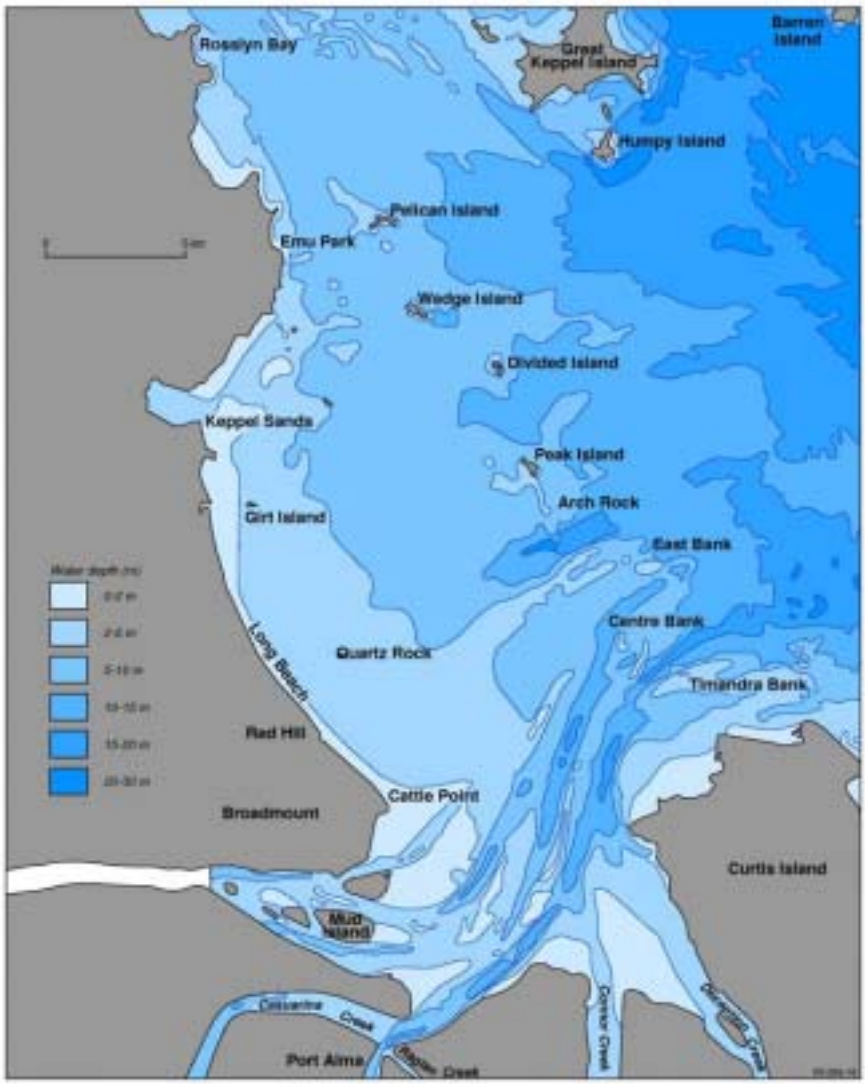

Figure 2.5: Bathymetry of Keppel Bay. Site locations are also provided (modified after Ryan et al.*, in prep).*

Extending from the mouth of the Fitzroy are three relatively deep channels with depths ~10 m or more. One of these is the main shipping channel into Port Alma and is dredged. The principal physical processes governing the transport of water and materials within the Bay are the large tides (maximum 5.4 m) and wind driven water circulation. The three largest coastal creeks (Casuarina, Raglan-Inkerman and Connor Creeks) together are of comparable size to the Fitzroy Estuary and all enter Keppel Bay in close proximity to the Fitzroy Estuary. The other, more northerly, coastal creeks entering directly into Keppel Bay are all small and ephemeral with very small catchments. The nutrient load delivered by them is assumed small relative to the load from the Fitzroy via the estuary.

Sampling strategy

Teams from Geoscience Australia (GA) and CSIRO Land & Water undertook three surveys of the Fitzroy Estuary and Keppel Bay in the periods from September 4–12, 2003, August 15 to September 1, 2004 and February 6–10, 2005. The first two surveys formed the 'dry season' component of the project. The February 2005 survey occurred just after approximately one estuary volume of freshwater entered the Fitzroy estuary (in the first few days of February). As the estuary was already largely filled with fresh water, it was expected that a small flood plume would be generated in Keppel Bay. Given the lack of wet season observations in the previous two years of the project AC, this flood presented the last opportunity to gather important wet season data. The *Rum Rambler*, a 42 ft motor vessel, was chartered for all three surveys.

The activities undertaken in Keppel Bay included measurements of water column physical and biogeochemical properties at a series of locations situated along a set of daily transects (all three surveys). The field campaigns, methods of analysis and results of analysis have already been reported (Radke *et al.*, 2004a and 2005a, b, and c; Ford *et al.* 2005b). *In situ* conductivity, water temperature, turbidity and position data were recorded continuously along the daily tracks using sondes housed in a continuous flow apparatus. The bottom sediment composition and texture data (Radke *et al.*, 2004a and 2005a) were investigated at sites throughout Keppel Bay. This bottom sediment data set was enlarged with the inclusion of grab sample collections made by Skene et al. (2004) in near shore waters alongside Long Beach (these numbers are followed by an a) and with inter-tidal sediments collected by Brooke et al., (2005) along the Capricorn Coast.

During the August 2004 survey, the boat was anchored at seven stations and an upward-looking Acoustic Doppler Current Profiler was placed on the sea floor. The ADCP measured current speed and direction at a series of depths through the water column over 24-hour periods coinciding with spring tide conditions at

the first three stations and neap tide conditions at the next four stations (Figure 2.6). The ADCP also measured water pressure. Sondes attached to the ADCP and located on the boat recorded turbidity at 10-second intervals, while samples for nutrients, TSM, chlorophyll *a* and TOC&DOC (from surface and bottom water) were collected at hourly intervals over the initial 12-hour periods. Detailed measurements of particle characteristics (size and settling velocities) and vertical profiles of salinity, water temperature, fluorescence, dissolved oxygen and scattering were also made at half-hourly intervals over the same 12-hour period. The same suite of physical and chemical measurements was made at a single 24-hour station during the wet season survey, with the exception of ADCP measurements.

A sediment biogeochemistry component of the survey was also conducted in conjunction with the Keppel Bay Vibracoring survey (Skene *et al.*, 2004), from aboard the *Pacific Conquest*. Sediment cores were collected by vibra- and box coring techniques. Cylindrical cores of sediment were removed from the box corer and incubated for 24 hours at *in situ* temperatures. Changes in physical and chemical properties in the water column overlying these sediments were used to estimate carbon decomposition, denitrification/nitrogen fixation and nutrient release rates. The raw data from the core incubation experiments have already been reported (Radke *et al.*, 2005b).

Casuarina Creek was sampled in August 2003 and twice in August–September 2004. Casuarina and Connor Creeks were sampled in collaboration with the Queensland EPA in September 2004. In all cases, filtered and unfiltered samples were collected at stations spaced along the creek and profiles of physical properties were measured at each station as well.

Maps showing the sampling locations and graphs showing fluctuations in tidal height during the different surveys are provided in Figure 2.6. The tidal plots are based on output from the WXTide32 program (http://www.wxtide32.com). Both neap and spring tide conditions were encountered during all three surveys.

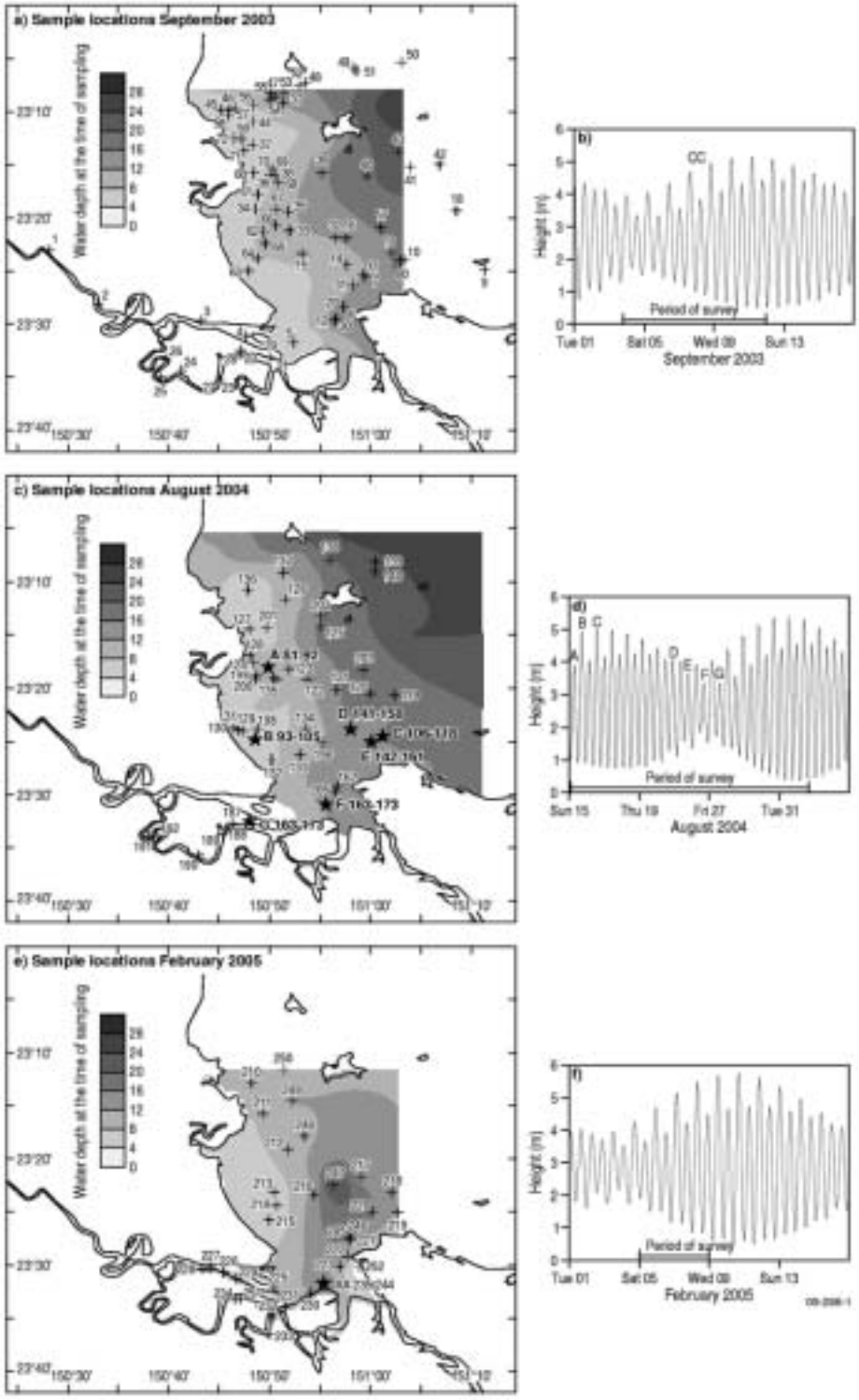

Figure 2.6: Maps showing water depths, tide heights and sampling location for each of the September 2003, August 2004, and February 2005 surveys.

Physical oceanography

Introduction

This section treats the physical oceanography of Keppel Bay and the Capricornia Region. Its information derives from studies undertaken by other investigators, from analyses of available meteorological data as well as from measurements obtained during the Fitzroy Contaminants study in Keppel Bay and the tidal creeks.

The chapter begins with a discussion of the meteorology of the region. Winds are important drivers of ocean currents and waves. Ultimately, how contaminants and phytoplankton are transported along the coast will be strongly affected by the strength and direction of the coastal currents. We provide an outline of the evaporation and precipitation climate of the region. Evaporation will be shown to have a significant impact on the salinity regime within Keppel Bay and the tidal creeks. The river flows deriving from summer rainfall is a central dynamic of the Fitzroy Estuary-Keppel Bay system.

Next, we consider the character of the tides and the currents associated with them. The region has large tidal ranges, which result in vigorous tidal currents. Even though the currents are oscillatory, they are likely to be the main agents for horizontal mixing of contaminants in Keppel Bay especially near the mouth of the Fitzroy Estuary. Tidal currents in the inner parts of the bay are responsible for suspending large amounts of fine sediments with consequent impacts on fine-sediment transport and on the underwater light climate. Waves are another agent for resuspension of fine sediments so we consider their character also.

The analyses of salinity measurements provides information on the rates at which mixing processes are occurring within the bay. The results from the dry and wet seasons are presented separately since the salinity characteristics of the Keppel Bay are quite different for these two seasons. Temperature is also considered, as it is a major determinant of the rate at which biogeochemical transformation processes occur.

The final section addresses the regional oceanography beyond Keppel Bay. Ultimately, we expect that the trajectories of dissolved contaminants derived from the Fitzroy Estuary will be carried by the more slowly varying currents that run past the offshore boundary of the bay. We present an analysis that shows that the longshore component of these currents is well correlated with the wind stress. It is shown that longer-term variations in sea level also have a clear association with the wind. The significance of sea level variation is that it will affect the likelihood of inundation of wetlands on the Fitzroy delta.

Meteorology

Winds

The Capricornia Coast, which encompasses the study region, extends approximately between latitudes 22 and 25º S. Lying across the Tropic of Capricorn, the region is tropical with hot summers tempered by sea breezes near the coast and mild winters. The mean daily temperature range in Yeppoon on the coast for July is 11–21° C (Bureau of Meteorology, 2005), whereas the mean January temperatures have a range of 23–29° C. Heron Island, 60 km offshore, demonstrates the moderating effect of the sea with daily July and January temperature ranges of 17–24° C and 21–30° C.

The region lies within the Southeast Trade Wind belt. Winds at Rockhampton are dominantly from the southeast and east, summer winds tending to be more easterly and winter winds more southeasterly (Gentilli, 1971). South of 18° S, monsoonal winds are uncommon, but they may be detected in the deflected trade winds, which may become easterlies or even northeasterlies in summer. Under these conditions, northwest winds around the heat low in central Queensland turn the Southeast Trades into a northeast monsoon and it is these latter winds that are the main factor causing the maxima in rainfall in summer (Gentilli, 1972). During spring and summer, late afternoon northeast sea breezes are frequent. The dominance of southerlies and southeasterlies for most of the year at this site is demonstrated in Figure 3.1. Pickard *et al.* (1977) state that south of 15°, the SE Trade winds prevail over the Great Barrier Reef Lagoon with wind direction generally between east and south; easterly being more common from August to February becoming more southerly for the remainder of the year.

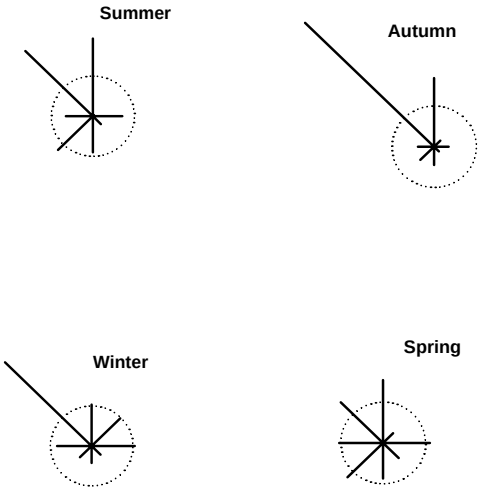

Figure 3.1: Frequency of occurrence of daily-averaged wind directions for a 200 km square located 60km east of Gladstone. The circles represent an occurrence frequency of 12.5%. Note that the oceanographic convention has been used for wind directions; that is, the lines represent directions towards which the wind blows. Data were derived from hind-casted wind stress obtained from the National Centres for Environmental Prediction.

Rainfall and evaporation

Monthly rainfall averages at Rockhampton, Heron Island, and Yeppoon suggest a distinct wet and dry season, with the wettest months generally occurring through the summer months December to March and the rest of the year being drier (Figure 3.2). Inland Rockhampton has an average annual precipitation of ~800 mm which is the lowest of these three sites. Yeppoon located on the coast has the highest annual precipitation of ~1300 mm, whereas Heron Island located 60km offshore has an average annual precipitation of ~1050 mm (Bureau of Meteorology, 2005). Presumably, much of the differences in precipitation is due to orographic effects. The measured average annual evaporation in Rockhampton is ~2100 mm so approximately twice as much water evaporates in the region as falls as rainfall. Monthly evaporation is highest in summer and falls to about half the summer rate in winter (Figure 3.2).

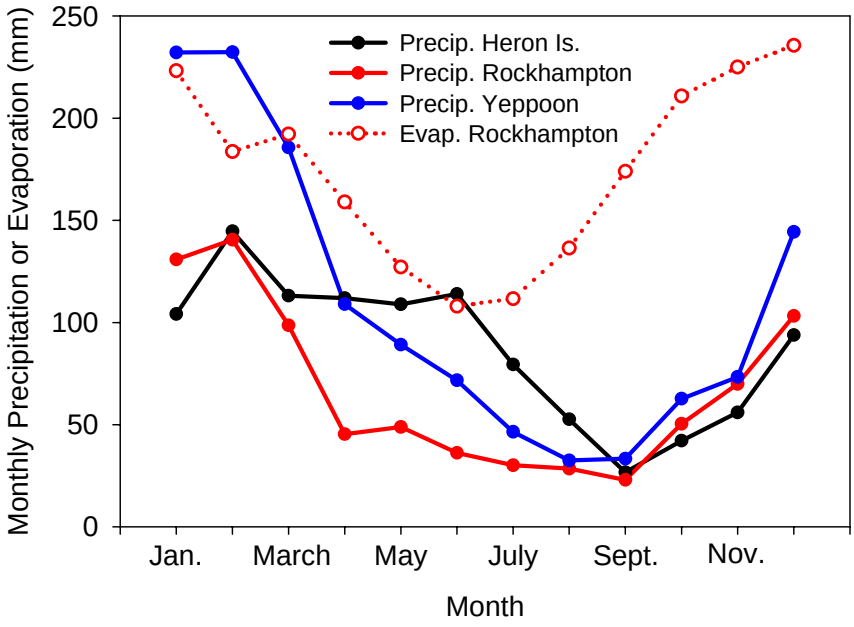

Figure 3.2: Average monthly precipitation at Heron Island (1956-2004), Rockhampton Airport (1939–2004) and at Yeppoon (1891–2004). Also shown is evaporation measured at Rockhampton (Bureau of Meteorology, 2005).

Cyclones

Rockhampton lies within the cyclone risk zone (Figure 3.3). A tropical cyclone is a tropical depression of sufficient intensity to produce sustained gale force winds (at least 63 km/h). There is considerable year-to-year variability in cyclone numbers, but in a typical year, ~6 tropical cyclones cross the Australian coast with about half of these crossing the northeast Queensland coast mostly between about Mossman and Maryborough. Tropical cyclones approaching the coast usually produce very heavy rain and high winds in coastal areas. Some cyclones move inland, losing intensity but still producing widespread heavy rainfall and, occasionally, moderate to severe damage.

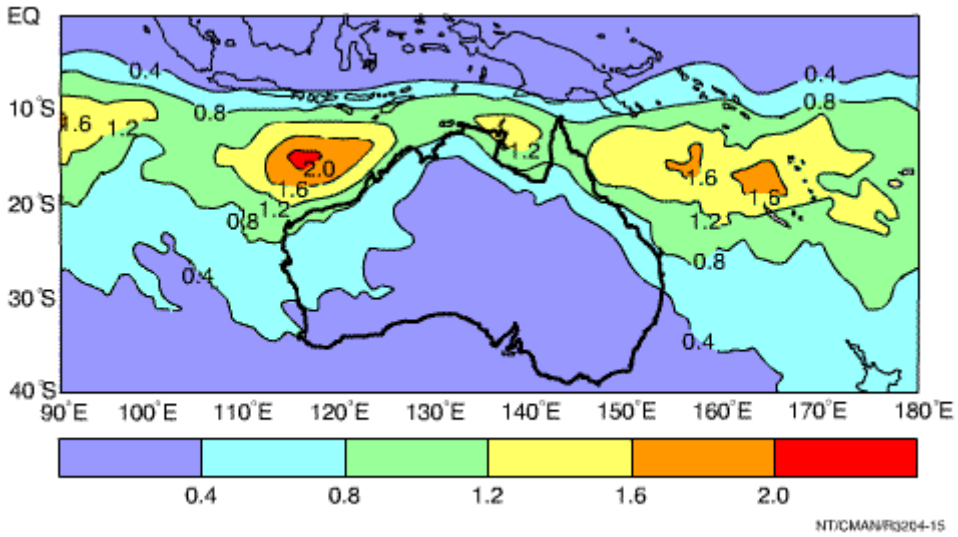

Figure 3.3: Map showing average annual frequency of tropical cyclones in the Australian region. (Jon Gill, Bureau of Meteorology http://www.bom.gov.au/lam/climate/levelthree/c20thc/cyclone.htm).

Tides

Tides – water levels

Pickard *et al.* (1977) report on the character of the tides along the Great Barrier Reef as derived from the work of Maxwell (1968) and Easton (1970). According to Pickard *et al.*, the tidal wave propagates westward from the Coral Sea and then north westward north of Cairns and south eastward south of Cairns. Over most of the length of the GBR, the tidal range at its edge is ~3 m which is similar to the range at the coast. However, in the vicinity of Broad Sound at latitude 22° S the maximum tidal range at the coast increases to ~9 m although it decreases both north and south. Middleton *et al.* (1984) suggest that this amplification of the tide in the vicinity of Broad Sound is due in part to the reef matrix offshore from the sound being particularly dense and acting as a barrier to the direct onshore penetration of the tide from the Coral Sea. Consequently, the tide in Broad Sound results from the confluence of the tidal wave propagating southeastwards along the lagoon with that propagating northwestwards through Capricorn Channel. Further, amplification results from a resonance effect within the Sound itself.

Tides in Keppel Bay, which is ~150 km to the southeast of Broad Sound, also have higher ranges than those along most of the GBR with daily tidal excursions of up to 5 m. Tides in the Mackay region (19.5 to 25° S) have been described by Pickard *et al.* (1977) as being dominantly semi-diurnal, with marked inequality between the high tides, but little at the low tides. These features are evident in the 20-day record of predicted water levels for Port Alma (southern Keppel Bay)

shown in Figure 3.4. The tidal range in Keppel Bay also undergoes a pronounced 14-day cycle of spring-neap tides. Figure 3.5 shows the daily tidal range for 2004 which illustrates this cycle. Spring tides have a range of as little as 4 m before mid-year and before year-end: these are the times of largest neap tidal ranges (~3 m). The times of maximum spring tidal range (king-tides) are near the ends of February and August. Neap tidal ranges are smallest near these times of the year (~1.5 m).

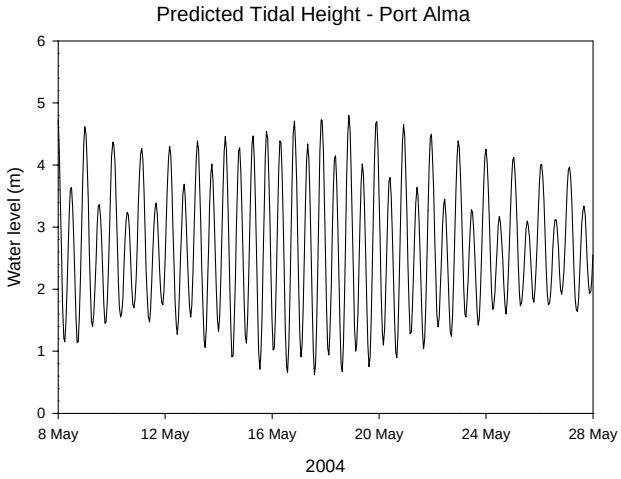

Figure 3.4: Predicted tidal heights at Port Alma.

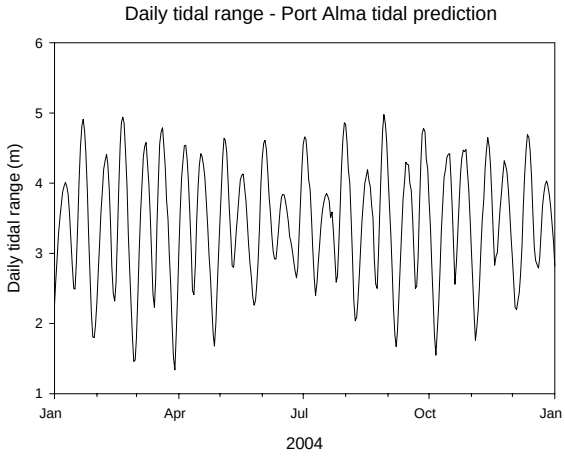

Figure 3.5: Daily tidal range in predicted tidal heights for Port Alma.

The tidal heights are due to the sum of a set of harmonic constituents which arise from the gravitational attractions from the sun and the moon variation of tidal range and from the hydrodynamic response of the ocean basins. Each constituent has a well-defined frequency and the modulation of the tidal range is due to the continuous variation in the relative phase of the main constituents. Tidal height variation tends to be large when the main constituents happen to be approximately in phase with one another and small when they are out of phase. The six main constituents for the tides in Keppel Bay (Port Alma) are listed in Table 3.1. Also listed is constituent SA which is the seasonal variation in water level. The spring-neap tidal cycle is mainly due to constituents M_2 and S_2 being in phase (spring tides) and out of phase (neap tides).

Table 3.1: The six largest tidal constituents at Port Alma. Also listed is constituent SA which is the seasonal water level variation.

Constituent	Name	Period (h)	Amplitude (m)
M_2	Principal lunar	12.42	1.44
S_2	Principal solar	12.00	0.54
N_2	Larger lunar elliptic	12.66	0.34
K_1	Luni-solar diurnal	23.93	0.30
O_1	Principal lunar diurnal	25.82	0.16
K_2	Luni-solar semi-diurnal	11.97	0.16
SA	Seasonal	365.25 days	0.11

Tides – currents

The large tidal range cause vigorous currents in Keppel Bay, in the tidal creeks, and in the Fitzroy Estuary. Although wind-driven currents can add to or subtract from tidal currents to make the total current strength stronger or weaker, the tidal currents are the principal agents causing short-term water motion and sediment resuspension within the Keppel Bay-Fitzroy Estuary system. Current meter measurements by Griffin *et al.* (1987) at two stations seaward of Curtis Island show that the tidal currents have a strong alongshore component and flood towards Broad Sound. The high tide lags the flood tide by 90° to 110° for diurnal components and by 60° to 80° for the semidiurnal components. Thus, the tide most closely resembles a standing wave with smaller progressive component propagating to the southeast for the diurnal components and towards the northwest for the semi-diurnal components. A pure standing wave occurs when the phase between height and current velocity is either 90° to 270°. The flow-

height relationship for the oscillatory flow into a closed basin would have the character of a standing wave; that is the flow speed into the basin is highest when the water level is near its average level and the rate of change of water level is largest.

During our survey in August 2004, we deployed an Acoustic Doppler Profiling Current meter (ADCP) at five locations in Keppel Bay and at one station in Casuarina Creek. These locations are shown in Figure 3.7 and listed in Table 3.2. Measurements were obtained at Timandra Buoy on two occasions (Timandra Buoy #1 and Timandra Buoy #2). The ADCP data were analysed to determine the principal axis of current variation for each station.

Table 3.2: ADCP deployments in August 2004. Also listed are the directions of the principal axis for the flooding tide and the fitted parameter, Ŭ.

Location	Station	Deployment duration (h)	Dominant direction axis (flood)	Amplitude factor ($x10^3$)
Flat Rock	A	20	234	1.15
Quartz Rock	B	21	189	0.66
Timandra Buoy #1	C	21	239	2.82
Halfway Timandra & Buoy 1	D	20	214	1.97
Timandra Buoy #2	E	10	241	2.97
Buoy 1	F	10	208	3.02
Casuarina Creek	G	23	269	3.19

For a pure standing wave, we might expect that the component of the current velocity in the direction of the principal axis of velocity variation to be proportional to the rate of change of water level. Thus, if v is flow velocity, h is water height and α is a constant that depends on position:

Equation 3.1

$$v = \alpha \frac{\mathrm{d}h}{\mathrm{d}t}$$

The ADCP depth-averaged current velocities were compared to velocities calculated using Equation 3.1 predicted water levels for Port Alma with Ŭas a fitted parameter (Table 3.1). Generally, the shape of measured velocity compared well to d*h*/d*t*. The major exception was the currents at Stn G in Casuarina Creek, which were noticeably flattened on their peaks compared to d*h*/d*t*. Presumably, this is a non-linear phenomenon. Figure 3.6 compares *v*

calculated from Equation 3.1 measurements along the principal axis at Stn C (Timandra Buoy #1) and for Stn G. The goodness of fit at the other stations lie between those for Stns C and G. The component of velocity orthogonal to the principal axis was small in magnitude compared to that along the principal axis demonstrating that the currents were dominantly co-linear during the time of measurement. Comparing phases between ADCP measurement and d*h*/d*t* showed a maximum phase difference of 25 minutes (for Stn G). Considering the possible error in this phase calculation, it would seem that currents are approximately in phase with d*h*/d*t*. Thus on the basis of this analysis, Keppel Bay acts like a filling box as far as the tides are concerned.

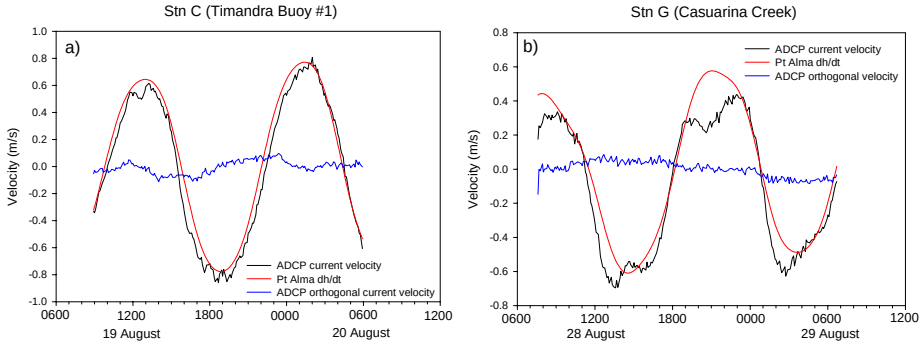

Figure 3.6: Comparison between measured ADCP current velocity and velocity calculated from derivative of Port Alma water level using Equation 3.1. Shown are the velocities along the principal axis of velocity variation and those orthogonal to this direction. Positive velocities are associated with the flooding tide; that is, the current is into Keppel Bay.

From the assumed relationship between water level change and current velocity, we can estimate current velocities at the ADCP sites throughout the year. Of course, this analysis does not account for possible wind-driven contributions to the current. Figure 3.7 shows the current vectors for the flooding tide at these sites. The amplitude of the vectors is the speed of the average estimated current over the year. Peak currents, which occur in late February and August, would range up to 2.5 times as large as these average currents. That is, peak currents at Stn G in Casuarina Creek, at Stn F (Buoy 1) and at Stns C and E (Timandra Buoy) would be expected to almost reach or exceed 1 ms^{-1}. The pattern of currents suggested by Figure 3.7, which is supported by numerical modelling of Keppel Bay currents, is for the strongest currents to occur in the southern part of the bay and towards the mouth of the Fitzroy Estuary.

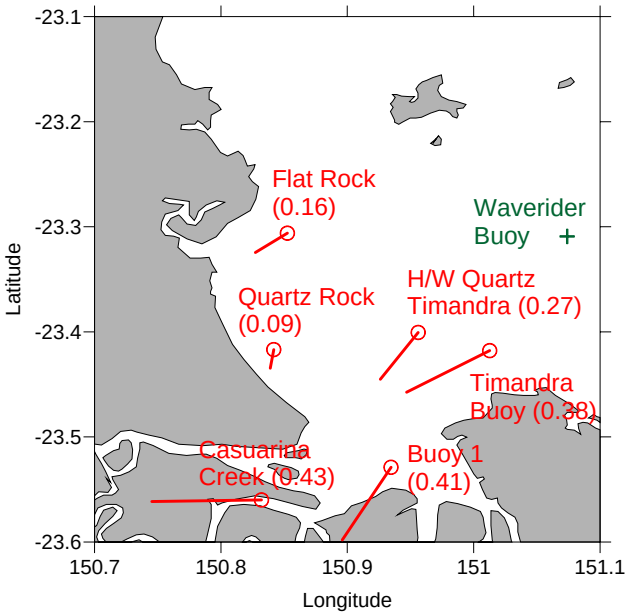

Figure 3.7: Calculated average tidal currents plotted for a flooding tide at the sites of the ADCP deployments. The numbers in brackets are the current amplitudes in m/s)

Waves

The shear stress of the flow over the bottom increases as approximately the square of the flow speed. When there is a mean current and waves together, the bottom stress increases as more than the sum of the stresses due to the waves and currents considered separately (Grant and Madsen, 1979). Thus, the presence of waves in a coastal environment can enhance considerably the ability of currents to mobilise sediments.

Wave height, direction and period are measured in Keppel Bay by a Datawell waverider buoy at a site 25 km from the coast east from Emu Park in 22 m of water depth (Figure 3.7). The largest waves measured at this site arrive from a generally easterly direction. The wave fetch is limited by reefs and shallow water for northeast and southeast directions, but waves from the east are able to propagate through Capricorn Channel from the deep sea (Piorewicz and Massel, 2001). High waves having significant heights greater than 2 m occur several times a year and have a duration of a few days (QEPA 2002, 2003, 2004) and are more likely to occur in the summer months (Figure 3.8). We can estimate what effect such waves will have on bottom currents in Keppel Bay. We consider a wave of 1.5 m height with a period of six seconds which is a moderately large wave for Keppel Bay, but not uncommon. We evaluate what happens to such a wave when it propagates from the location of the waverider buoy to a position 20 km to the west (close to Flat Rock in Figure 3.7). The water depth will be assumed to decrease at a constant rate from 22 m to 5 m over this distance.

If H_w is the waveheight, the energy density per unit area of wave is given by E = ¼ gH^2/8, where ¼ is water density and g is gravitational acceleration (Kinsman, 1965). The flux of wave energy per width of coast is $F = C_gE$ where C_g is the group velocity of the wave, which is the velocity of energy propagation. The group velocity depends on water depth and wave frequency, but the change in water depth causes a change in C_g of about 10% over the 20 km of wave run. If the wave energy flux towards the coast is considered to be constant, then such a variation in C_g will be associated with a 5% change in wave height.

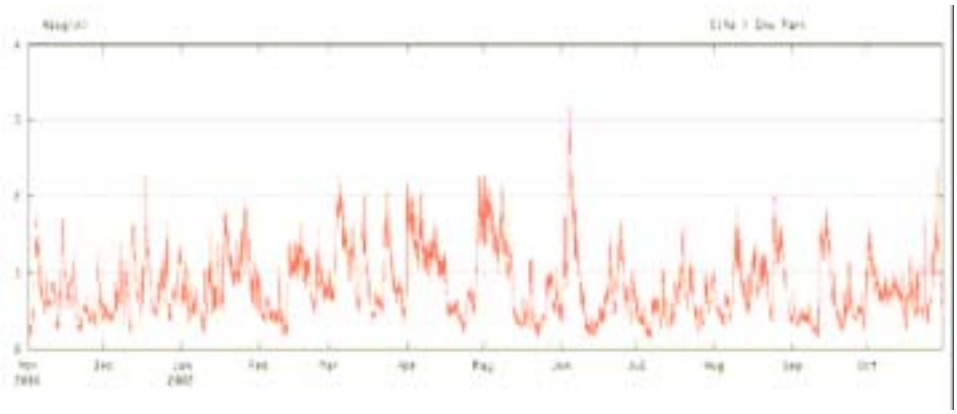

Figure 3.8: Time series of wave heights measured by waverider buoy off Emu Park (from QEPA, 2002).

Shoaling waves will be affected more by the bottom friction, which reduces the energy of the wave as it propagates into shallow water. Wave height tends to decrease as a consequence. Using a prescription of bottom friction presented by LeBlond and Mysak (1980), we can calculate how the energy and height of our wave would change as it propagates into western Keppel Bay (Figure 3.9). Also, shown is the estimated magnitude of the water motion due to the wave near the bottom.

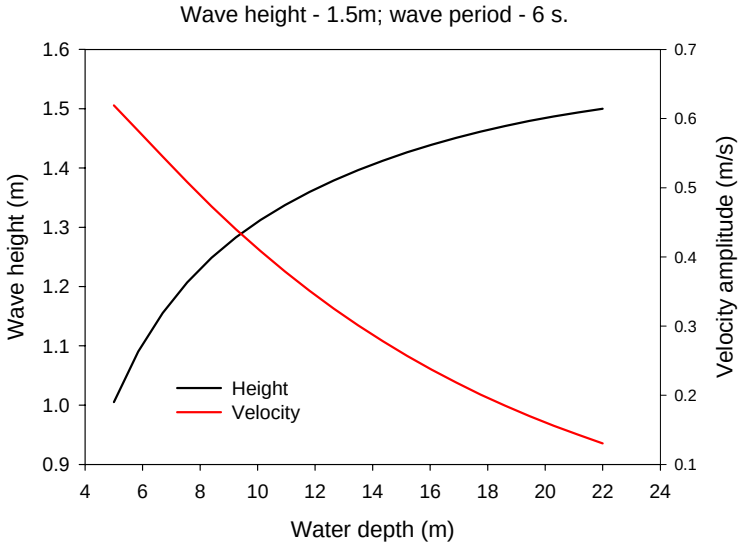

Figure 3.9: Modelled wave height and bottom current amplitude across Keppel Bay.

Note that even though the wave height decreases sharply as the wave propagates into shallow water, the bottom water velocity associated with the wave is predicted to increase in amplitude from less than 0.2 ms^{-1} to over 0.6 ms^{-1} near the coast. The latter current amplitude exceeds the estimated tidal current at Flat Rock even at its peak during spring tides. Currents of this size will later be shown to be active agents of resuspension in the channel approaches to the Fitzroy Estuary and superimposed on the tidal currents in the bay are likely to be particularly effective.

Salinity and temperature in Keppel Bay

Dry season

The field trips in September 2003 and August 2004 occurred during the dry season; flows down the Fitzroy River were low for at least the preceding five months (Figure 3.10). During the September 2003 trip, TS characteristics were measured over the bay at 58 sites over six days and measurements were obtained at 31 sites over nine days during the August 2004 trip.

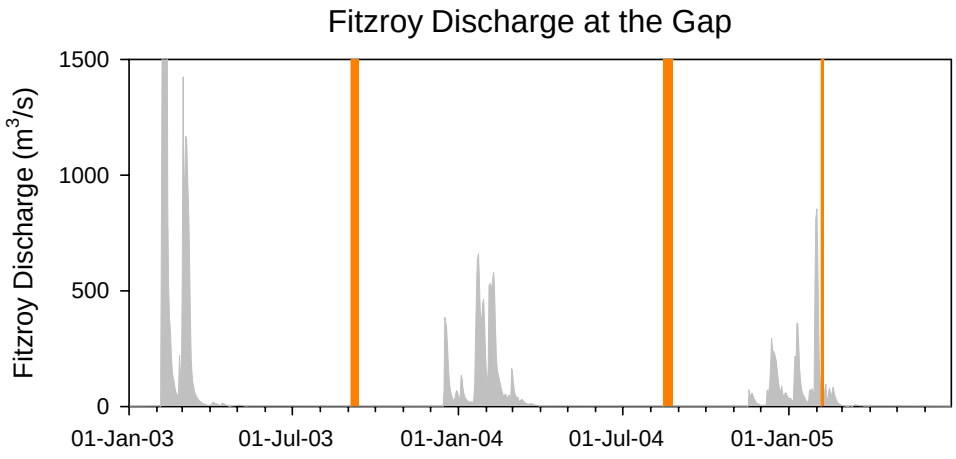

Figure 3.10: The time series of discharge of the Fitzroy River at the Gap showing the times of the three surveys in Keppel Bay (orange) during the study period.

The salinity distribution within Keppel Bay during the August 2004 survey is shown in Figure 3.11. The highest salinities were measured on the western side of the bay and in the mouth of the Fitzroy where salinities exceeded 37. Salinities ranged from 36.1 in the northeastern part of Keppel Bay to 37.5 towards the western end of Casuarina Creek. Salinities measured in September 2003 also mostly fell in the range 36–37, but salinities of up to 39 were measured near the western shore of Keppel Bay. Salinity stratification in the bay was fairly small with salinity tending to increase slightly from the surface to the bottom. The maximum difference between the salinity measured at the tops and bottoms of

the profiles was 0.18 measured at Stn 120 near the eastern side of the bay, but the median salinity difference was only 0.02.

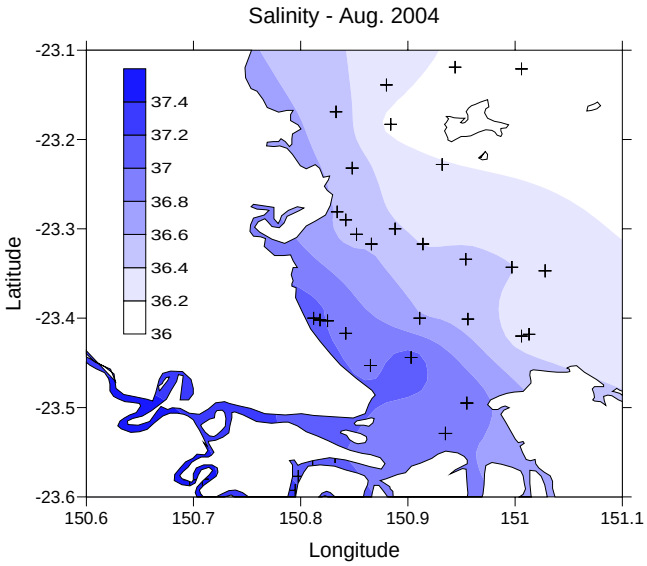

Figure 3.11: Salinity measured in Keppel Bay during the August 2004 survey. Salinity is depth-averaged.

The occurrence of the higher salinities near the coast during the dry winter-spring months is likely to be due to evaporation along the coast, in the tidal creeks, and in the Fitzroy Estuary. Not only does the effect of evaporation increase salinity more in shallow water than in deeper water due to the difference in the relative change in water volume when a fixed mass of water evaporates from the water column, but the water closest to the coast is likely to exchange less quickly with offshore water of lower salinity allowing the larger increases in salt concentration. Ridd *et al.* (submitted) have incorporated a model of offshore mixing with evaporation to explain the observed increase of salinity towards the coast in the central GBR.

Figure 3.11 shows that the difference in salinity between the inner and outer parts of Keppel Bay is ~0.5. The evaporation rate at Rockhampton is ~5 mm/day in August (Figure 3.2) and the rate over water is likely to be around 70% as large as this or four mm/day. We assume first that the difference in salinity is due to difference in water depth. A water column of five metres depth of salinity 36 evaporating at four mm/day will increase its salinity to 36.7 in 23 days, whereas a water column of 20 m depth will increase its salinity to 36.2 in the same time. Thus, a differential in salinity of 0.5 will occur between these two water columns, which are representative depths for the inner and outer parts of Keppel Bay in about 3 weeks. Alternatively, we will suppose that the differential in salinity is due

to limited exchange between the near coastal water mass (S_c = 36.5) with one which has a constant salinity further offshore (S_o = 36). In this case, the exchange time $T_e = H(S_c - S_o)/$ ŭS_o where ŭ is the evaporation rate. For an inshore depth of 5 m, T_e = 17 days The period of dry prior to the measurements was about five months, which is long enough that both mechanisms for enhancing nearshore salinity through evaporation could have been operative.

Profiles of salinity and temperature were measured repeatedly at seven stations (A-G) over ~12 h during the August 2004 cruise. The TS characteristics at these stations (averaged water column) are shown in Figure 3.12. Salinity at each station shows the overall variation across Keppel Bay that is illustrated in Figure 15. Highest salinities were observed at Stn B on the southwestern side of Keppel Bay and at Stn G in Casuarina Creek. Salinity variations of ~0.1–0.3 in range occur over the measurement periods due in large part to the movement of water masses past the measurement location with the tides. Measured temperatures also show temporal variation, but overall, temperatures at Stn B appear to be ~0.4°C lower than those at the other stations.

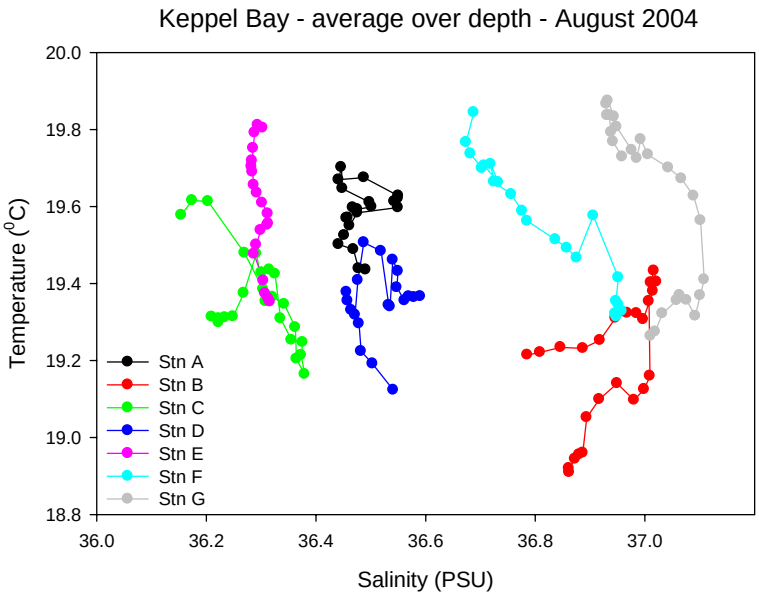

Figure 3.12: Measured TS characteristics at seven stations over ~12 hours during August 2004.

We examine further the nature of the temporal variations in temperature at these seven stations. Suppose that the increases and decreases in temperature are due to energy exchange across the water surface due to solar radiation, thermal emission, evaporation and heat conduction with the atmosphere. The solar radiation (R) on clear days (assumed) can be readily calculated from the time of day and the day of the year. The other energy input and loss terms are more

difficult to assess, but we shall assume that these are all constant during the day and that the net input of energy into the water column over 24 hours is zero. So, if L is the rate of energy loss, we set $L = \overline{R}$ where the overbar represents the 24-h average. The net energy loss is not likely to be constant during the day and will vary with wind speed and surface water temperature for example. Also, the net energy input over the day will not generally be zero and will be positive or negative depending on time of year and the passage of weather systems for example.

If T is average water temperature, H is water depth, ρ is water density, C_p is the specific heat of water, then assuming that changes in temperature with time are only due to energy exchange across the water surface, the equation that predicts the rate of change of T with time, t is:

Equation 3.2

$$\rho C_p H \frac{\partial T}{\partial t} = R - L$$

Starting with the measured temperature at the beginning of each measurement sequence, Equation 3.2 can be integrated to yield the expected variation in temperature due to solar heating.

The measured and 'modelled' results are shown for four of the stations are compared in Figure 3.13, the other stations showing similar levels of agreement. It is apparent that the simple model can explain the major part of the temperature variation at the measurement stations.

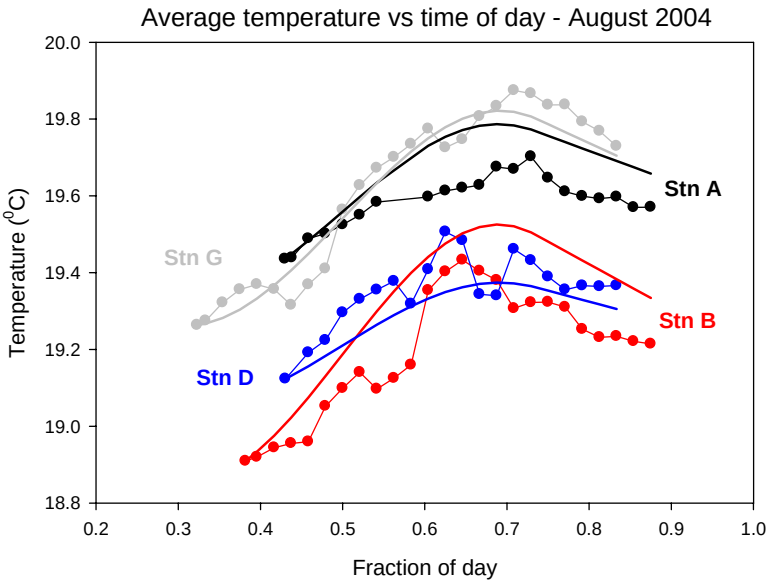

Figure 3.13: Average water column temperatures measured during the day at four sites. Also, shown is the modelled average temperature obtained through integration of Equation 3.2.

Wet season

In contrast to the September 2003 and August 2004 surveys, the February 2005 field trip followed a series of three modest flow events down the Fitzroy River (Figure 3.14). The total volume of water discharged during the period shown in Figure 3.14 was $9.2 \times 10^8 m^3$, which is almost four times the volume of the estuary ($\sim 2.5 \times 10^8 m^3$). Thus, one would expect that a significant volume of fresh water would have flowed through the estuary and into Keppel Bay. The median discharge of the Fitzroy between 1965 and the present is 87 $m^2 s^{-1}$. Although the average discharge in the period July 2002 to June 2003 was equal to the median discharge, flows in the following two years, 2003/2004 and 2004/2005 were 41 $m^3 s^{-1}$ and 38 $m^3 s^{-1}$, respectively which are closer to the 25%-ile discharge for the Fitzroy.

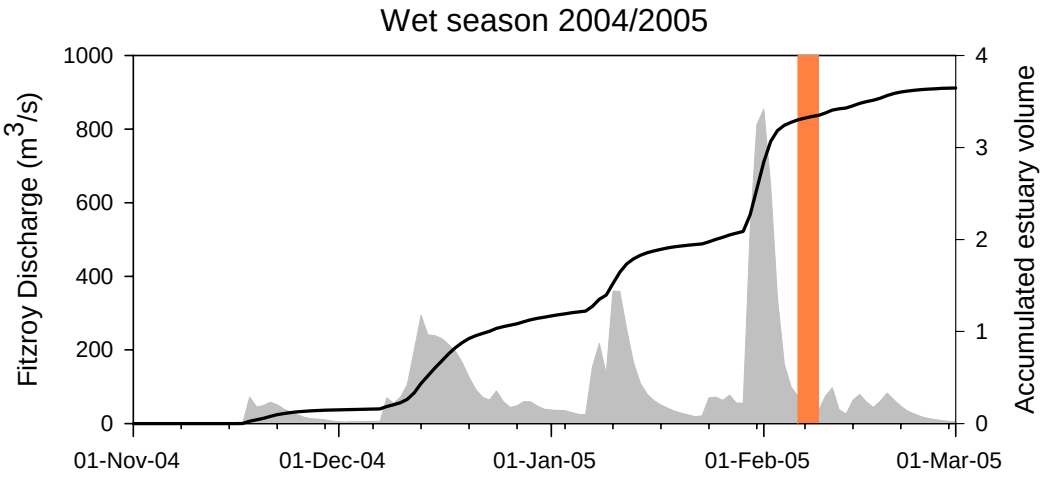

Figure 3.14: Fitzroy River (the Gap) discharge during the summer of 2004/2005. The grey infill shows the discharge, the black line is the accumulated inflow in terms of estuary volumes and the orange bar shows the time of the February 2005 field trip.

At the time of the survey in February 2005, Fitzroy discharges remained less than 100 $m^3 s^{-1}$ although sampling was undertaken about one week after the peak discharge of 854 $m^3 s^{-1}$ for the summer of 2004/2005 (Figure 3.14). This survey measured water properties at 25 sites over 4 days. Figure 3.15 shows the depth-averaged salinity measured over Keppel Bay during the survey.

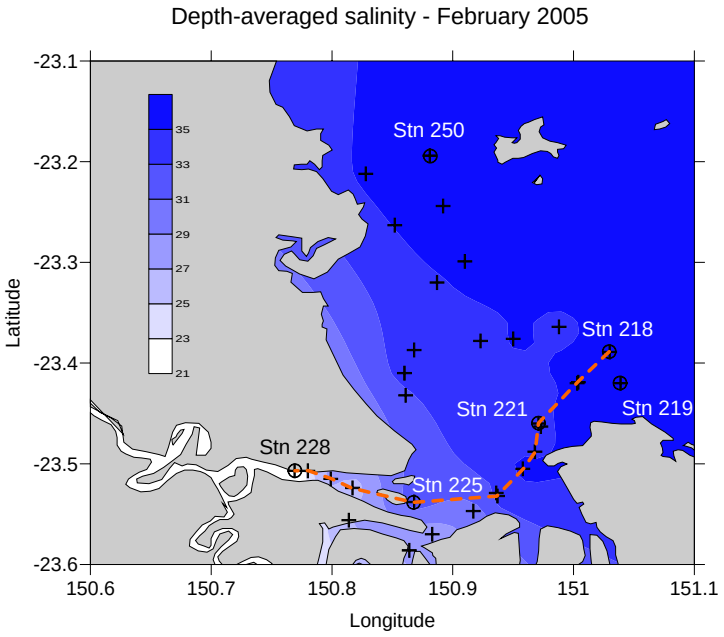

Figure 3.15: Depth-averaged salinity measured during the field campaign of February 2005.

In contrast to August 2004 (Figure 3.11), salinities were lowest near the coast and generally increased in an offshore direction away from the mouth of the Fitzroy Estuary due to the discharge from the river. Just as the high salinity water tended to penetrate northwards along the western side of Keppel Bay during August 2004, so to did the lower salinity water during February 2005. The highest salinities measured during the February 2005 survey were measured at Stn 219 (36.2) and at Stn 250 (36.1). These values are similar to the lowest salinities of 36.1, which were measured in the offshore parts of Keppel Bay during August 2004. These maximum salinities are higher than any of the salinities measured during an autumn cruise (May 1990) by Middleton *et al.* (1994) to the southern GBR lagoon including the Capricornia region. Their maximum salinities of ~35.6 appeared to be associated with the southward flowing EAC over the shelf break. Likewise, Pickard *et al.* (1977) report maximum monthly averaged salinities for the shoreward side of the GBR lagoon to be ~35.6±0.2 in February and August with a maximum of ~35.8±0.2 occurring in December. Of course, the occurrence of offshore gradients as observed in our Keppel Bay study would suggest that salinity comparisons will be affected by exactly where measurements are made.

The minimum salinity measured during the February 2005 survey was 14.9 at Stn 228 approximately 12 km up-estuary from the mouth of the Fitzroy Estuary. Salinity increased towards the mouth, which is consistent with salinity being mixed back up the estuary following the reduction in freshwater inflow (Webster *et al.*, 2004). The measurement at Stn 228 was obtained approximately 1 hour after high tide so that the more saline water from Keppel Bay was close its

maximum incursion into the estuary. At mid tide, one might expect the salinity at Stn 228 to be somewhat lower than that measured. Salinity profiles were also measured approximately 6 km up Casuarina Creek and 3 km up Raglan Creek at times close to low tide. These salinities were 27.0 and 26.9, respectively, which are about 75% of seawater (~36). At higher stages of the tide, these salinities would penetrate further into the creeks. In effect, the brackish flows from the Fitzroy Estuary reduce the salinities in the creeks also.

Figure 3.16 shows the measured salinity cross-section across the transect starting within the Fitzroy Estuary and running along the shipping channel out of the mouth towards the northeast (see Figure 3.15). The largest horizontal gradient is within the mouth region. Also, some vertical stratification is evident with surface salinity being ~1 less than that nearer the bottom.

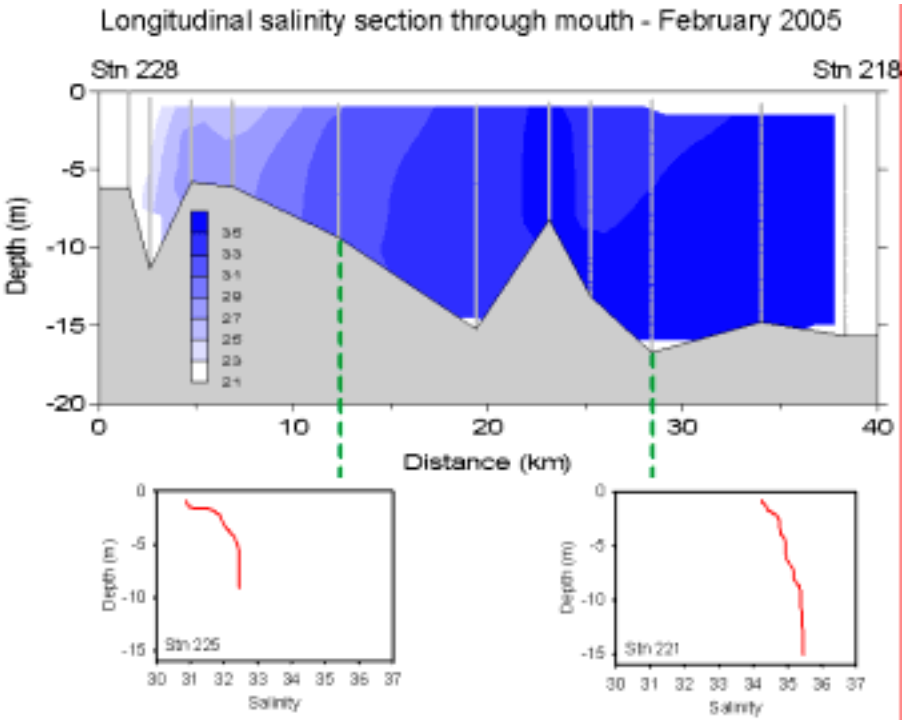

Figure 3.16: Longitudinal salinity section between Stn 228 and Stn 218 (see dashed line in Figure 3.15). The vertical grey lines show station locations. Salinity profiles are shown for Stn 225 and Stn 221.

From the salinity profile, *S(z)*, we calculate the effective freshwater content of the water column at each station. We shall assume that the seawater salinity during the February 2005 field campaign was equal to the highest measured; that is, S_{SW} = 36.2. Thus, the freshwater content expressed as a thickness, H_{FW}, can be calculated as:

Equation 3.3

$$H_{FW} = \int_{-H}^{0} \frac{S_{SW} - S}{S_{SW}} dz$$

If the water column were completely fresh, then the height of freshwater equals the water depth so $H_{FW} = H$. Conversely, if the salinity of the water column equalled seawater salinity, S_{SW}, then $H_{FW} = 0$. Figure 3.17 shows the contoured distribution of H_{FW} over Keppel Bay obtained from the February 2005 measurements.

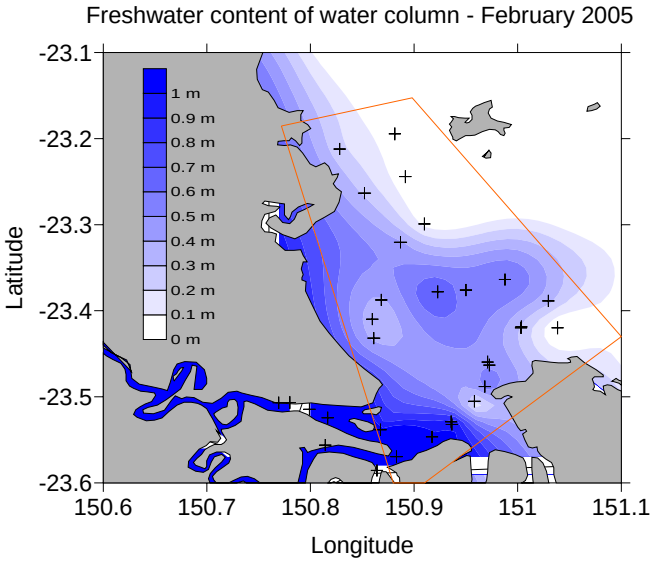

Figure 3.17: Estimated freshwater content of water column from February 2005 measurements. The orange polygon defines the area used for calculating total freshwater volume.

The volume of freshwater in Keppel Bay can be calculated by integrating the contoured freshwater heights over the area of the bay shown in Figure 3.17. This area is 800 km^2 and it contains an estimated $3.1 \times 10^8 m^3$ of fresh water which is approximately ⅓ of the $9.2 \times 10^8 m^3$ of fresh water discharged from the Fitzroy River in the summer of 2004/2005. Given that the Fitzroy Estuary itself is mainly fresh (volume ~$2.5 \times 10^8 m^3$), Keppel Bay and the estuary together contain 60% of the fresh water discharged that summer between them. There is an unknown but presumably substantial amount of fresh water mixed into Casuarina Creek, Raglan Creek, and into Connor Creek so it would appear that most of the summer freshwater discharge remained in the vicinity of the estuary and Keppel Bay. From the salinity distribution and from numerical modelling, the exchange time from the estuary has been estimated to be ~20 days. The apparent retention of fresh water in the region of the estuary mouth appears to be broadly consistent with such an exchange time given that the majority of the summer discharge took place within the month prior to the February 2005 measurements.

By comparison with the discharges in the summer of 2004/2005, the rains associated with Cyclone Joy caused the discharge of $18.5 \times 10^9 m^3$ from the Fitzroy River into Keppel Bay in January 1991. This discharge, equal to about 74

estuary volumes, was the third largest in the 20th century only being exceeded by floods in 1918 and 1954. Measurements made on the falling limb of the hydrograph showed near surface salinities of less than 10 up the western side of Keppel Bay and as far north as North Keppel Island (O'Neill *et al.*, 1992). Salinities near the bottom were mostly in excess of 30 demonstrating that the flood was propagating as a surface plume into Keppel Bay. Measurements made at the same locations a week later after the flows had subsided showed most surface salinities to have increased to 30 or more. It seems that up to the time of the first measurements, the wind was dominantly from the southeast causing the freshwater plume to spread northwards along the coast. Later, the wind direction switched to more northerly directions causing the plume to be blown southwards and eastwards impinging on the Capricorn-Bunker group of coral atolls. The near bottom salinities throughout Keppel Bay mostly increased slightly over those measured during the falling limb of the Fitzroy hydrograph suggesting that sea water of higher salinity was being advected into the region presumably from further north or from offshore.

The average water column water temperature during the February 2005 survey ranged between 28.4 and 30.9°C, the minimum measured at Stn 31 off Roslyn Bay and the maximum measured at Stn 24 in Raglan Creek. The measurement in Raglan Creek was obtained at ~1530 in the afternoon, a time when solar heating would have been close to its daily maximum. Temperature variations from the top to the bottom of the water column were small and averaged only 0.4°C. Time series of water properties were measured at Stn 26 only which is to the east of the mouth of the Fitzroy. Average water column temperature increased from ~29.3°C at ~0800 in the morning to ~30.4°C at 1700 in the afternoon. Water temperature at the same location in August 2004 increased by ~0.6°C over a similar time period even though the average solar daily radiation intensity was calculated to be 399 Wm^{-2} during both two sampling times. Some of the temperature variation during the February 2005 survey may have been due to advection of slightly warmer water from the tidal creeks or the Fitzroy during this time. The tide was falling during most of the sampling time and reached its lowest height ½ hour before the termination of sampling.

Regional oceanography

Currents

A major feature of the oceanography of the GBR coastal region is the occurrence of the East Australian Current (EAC). The EAC derives from the East South Equatorial Current which flow westwards across the Coral Sea and which bifurcates at latitude ~14°S (Burrage *et al.*, 1997). The southern flowing bifurcation becomes the EAC (Figure 3.18). The EAC flows southward and

mainly follows the shelf edge with a limited penetration into the GBR Lagoon. Hamon and Grieg (1972) have suggested that sea level rises by 1.7 m relative to geodetic between 30 and 11° S and it is the long-shelf pressure gradient associated with this sea level change, which drives the EAC.

Figure 3.18: Currents around Australia showing location of East Australian Current.

Measurements of currents in the Capricornia Region are limited. Woodhead (1970) released packets of drifters in September–October 1966. Although drifter paths crossed presumably due to temporal variation in the currents, a general pattern does emerge. Closer to the coast current directions are in the direction of the wind (or somewhat to the left of it), whereas further offshore current directions were more towards the southeast consistent with transport by the EAC which has penetrated to the inside of the reef.

Griffin *et al.* (1987) report on the results of an oceanographic study, which was undertaken in the region between Capricorn Channel and Fraser Island. Current meters and tide gauges were installed for a 6-month period starting in June 1983 at a location off Curtis Island and further out on the shelf close to its edge. The circulation near the shelf edge is complicated by the abrupt widening of the shelf from ~70 km to over 200 km at the Capricorn Channel (Figure 3.19). In particular, they suggest the presence of a large clockwise eddy to the southeast of Capricorn Channel, which is consistent with the track of a satellite buoy through the region. Evidence for the existence of clockwise circulation in this region also appears in measurements described by Middleton *et al.* (1994). It is not known how persistent this feature is in the region, but its presence also appears in satellite images described by Burrage *et al.* (1996). Kleypas and Burrage (1994) report on the analyses of a series of satellite thermal images in

the region. Some images show anti-cyclonic flow to occur in Capricorn Channel, whereas in other images flow turns westward into Capricorn Channel on the inside of the Swain Reef.

Griffin *et al.* (1987) suggest that sea level fluctuations were generally in balance with the longshore current. Over the continental slope, local winds were not a significant contributor to current variability. They postulate that this variability appears to have propagated from further south as Coastal Trapped Waves (CTWs), but that local wind stress contributed significantly over the shelf proper.

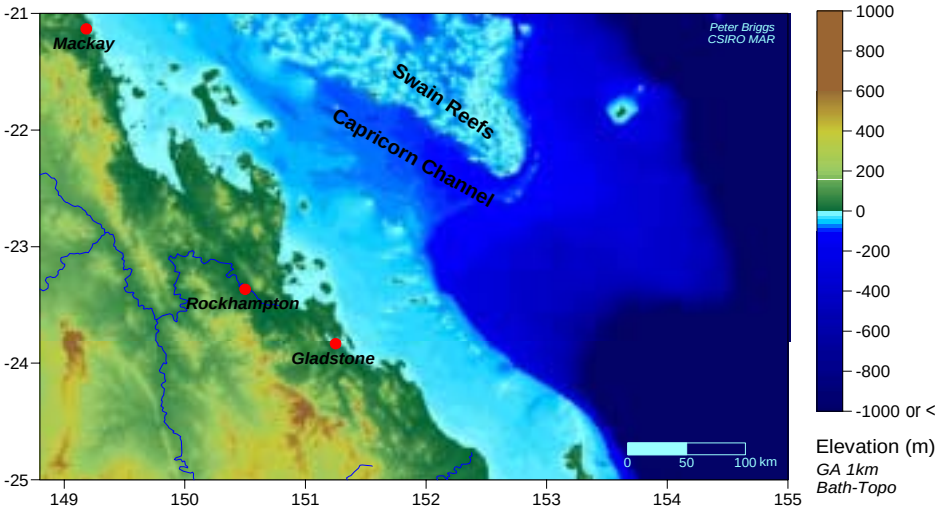

Figure 3.19: The bathymetry of the Capricorn section of the Great Barrier Reef. Map provided by Peter Briggs, CSIRO Marine and Atmospheric Research.

In order to estimate the prevailing direction of the currents along the coast near Keppel Bay, we reanalysed the data from the current meter off Curtis Island deployed in 1983. In particular, we examined how well wind stress could be used as a proxy for longshore current velocity here defined as the component in the direction 315°. The wind stress is a hindcast time series obtained from the National Centres for Environmental Prediction (NCEP) for a 200 km square centred on a location 60 km due east of Gladstone. If τ is the longshore component of the wind stress at time *t*, then we represent a proxy current velocity time series *v* as:

$$v(t) = A\tau(t - \delta) + V \qquad (1)$$

where *A* is a fitted amplitude factor, ŭ is a time lag, and *V* is an offset. The optimal values for the fitted parameters that minimised in a least squares sense the difference between proxy and measured currents were are $A = 1.09\ n^3N^{-1}s^{-1}$, ŭ = 21h and $V = 0.012\ ms^{-1}$. The fitting was carried out using time series that had been low-pass filtered to remove the tides. The comparison between proxy and measured current velocities shown in Figure 3.20 demonstrates that the proxy is

a good representation of the measured current velocity. Differences between may be due in part to CTWs propagating northwards past Fraser Island.

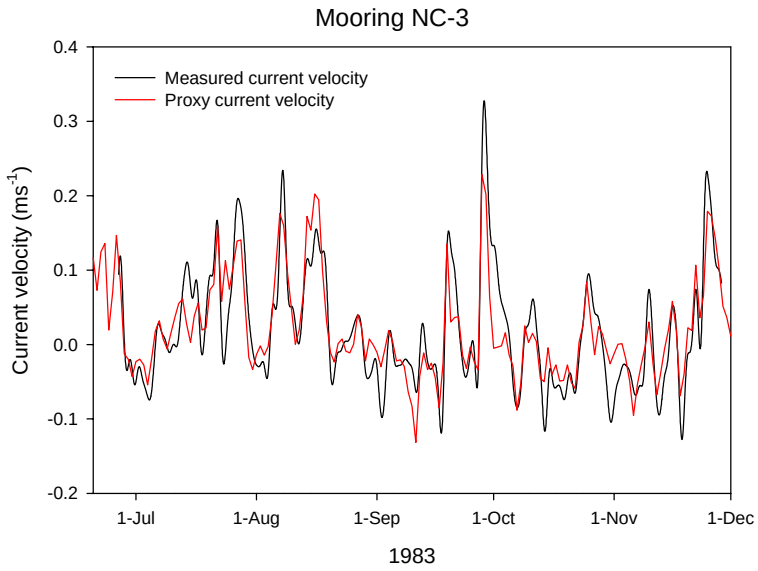

Figure 3.20: Comparison between proxy and measured currents July–November 1983. The measured currents have been low-pass filtered to remove the tidal variations.

Assuming that the proxy current velocity is a valid representation of the true current off Curtis Island, we can construct a time series of current velocities for the duration of the wind stress record 1982–2004. Figure 3.21 shows the current velocity averaged by month for this period. Monthly currents are most strongly towards the northwest in late summer and through the autumn falling to close to zero in spring. Note that this is really a reflection of the average longshore component of wind stress.

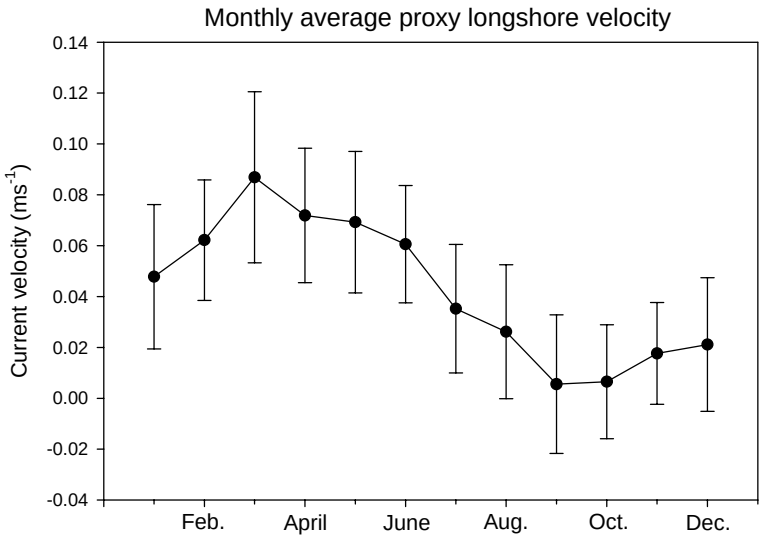

Figure 3.21: Proxy longshore current velocity averaged monthly for the period 1982–2004.

Sea level

On continental shelves, it is usual for the Coriolis force associated with a longshore wind-driven current to be balanced by an offshore pressure gradient. Positive longshore currents (northwestwards) should tend to occur with negative offshore pressure gradients; that is, with pressures (water levels) that decrease away from the coast. Figure 3.22 demonstrates that water levels at Port Alma do tend to be higher under conditions of southeast winds as one might expect. Both water levels and wind stresses undergo a similar pattern with highest water levels tending to occur in late summer. The average overall seasonal variation is captured by the SA tidal coefficient (see Table 3.1). Many of the features in the variability of the water levels are reflected in the wind stress also. This covariance is particularly striking in the summer of 2003.

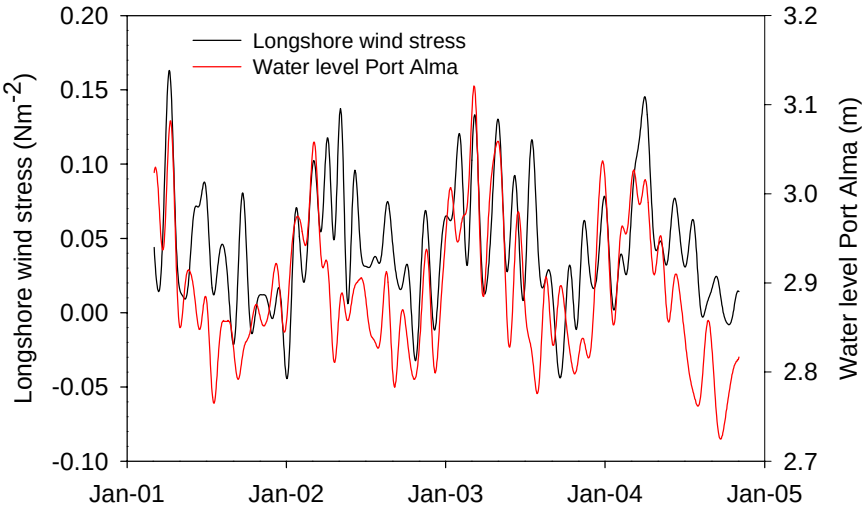

Figure 3.22: Longshore component of wind stress and measured water levels at Port Alma 2001–2004. The data have been filtered to remove variations at periods less than 30 days.

However, much of the water level variability is not reflected in the 'local' wind stress. It is probable that there are variations in the shelf break currents associated with the EAC and with northward propagating CTWs which are generated further south by wind events there. It has been noted by Griffin *et al.* (1987) that this variability is not well correlated with wind stress yet these currents would still impose a geostrophic adjustment to sea levels that would penetrate across the shelf. Using arrays of current meters and pressure gauges across the shelf near Townsville, Burrage *et al.* (1997) have shown that shelf and slope currents and cross-shelf water level differences are well correlated, and is better than the correlation with the local wind due to impact of remotely forced coastal trapped waves.

Fine-sediment dynamics

Introduction

The following chapter considers the spatial distribution of suspended sediments first. We show how it is related to the distribution of bottom sediments. Next, we show how total suspended sediment (TSS) concentration is related to measured turbidity. Continuously recording turbidity meters (nephelometers) were mounted on navigation buoys in the channel approaches to the Fitzroy Estuary on two occasions. The third section describes the temporal variability in measured turbidity (and inferred TSS concentration) observed in these measurements. From these measurements, we can estimate the fluxes of fine sediments past the measurement locations and compare these to delivery of fine sediments by the Fitzroy River. Finally, we develop a simple model of TSS concentration to explain major features of the observations.

Spatial distribution

Figure 4.1 shows measured TSM concentrations in g/m^3 measured over Keppel Bay during the September 2003 and August 2004 surveys. As will be discussed later, the inferred TSS concentrations are subject to considerable temporal variation due to active resuspension by the tidal currents and due to backwards and forwards motion of the water column past the measurement locations. Nevertheless, the measurements in both surveys and in the survey of February show a consistent pattern. TSS concentrations tend to be highest in the mouth of the Fitzroy and in a zone that extends northeastwards out from the mouth to the northern end of Curtis Island. Over most of the bay, TSM concentrations are less than 5 gm^{-3}, but in the mouth area and in Casuarina Creek they reached and exceeded 200 gm^{-3}. As both surveys were completed at least five months after significant discharge from the Fitzroy River (Figure 3.10), we postulate that the elevated TSM concentrations around the mouth are due to active resuspension of fine benthic sediments.

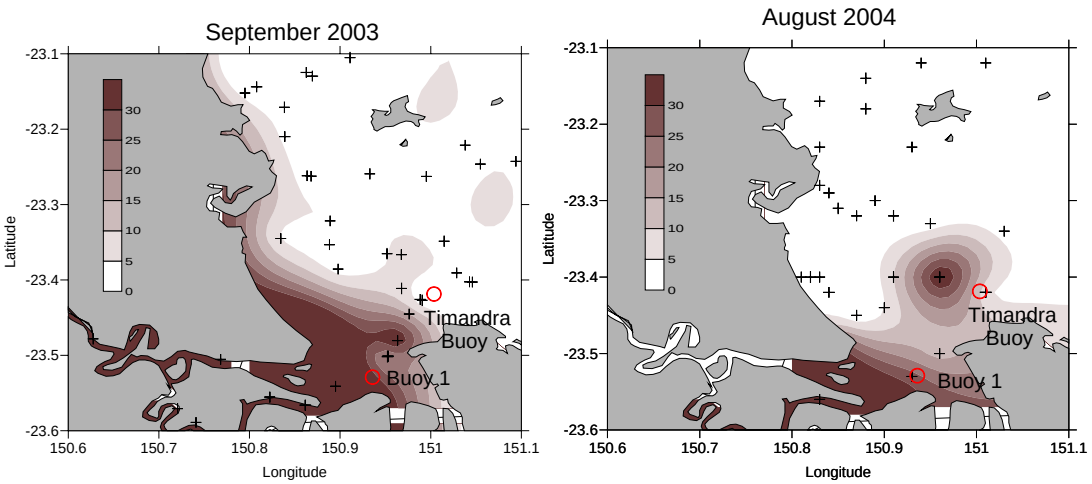

Figure 4.1: Contoured TSM concentrations in Keppel Bay during the September 2003 and August 2004 surveys. easurement locations are marked as +.

Figure 1.2 shows the distribution of muddy sediments across Keppel Bay. The highest percentages of mud (>50%) occur in the mouth of the Fitzroy Estuary and in a second node on the western side of Keppel Bay. High concentrations of TSM appear in the mouth of the estuary presumably due to the presence of high tidal currents there as well as sediments that have a high proportion of mud. We might postulate that even though the sediments on the western side of Keppel Bay have a high percentage of mud TSM concentrations are not particularly high there due to the smaller tidal currents than in the mouth (Figure 3.7:).

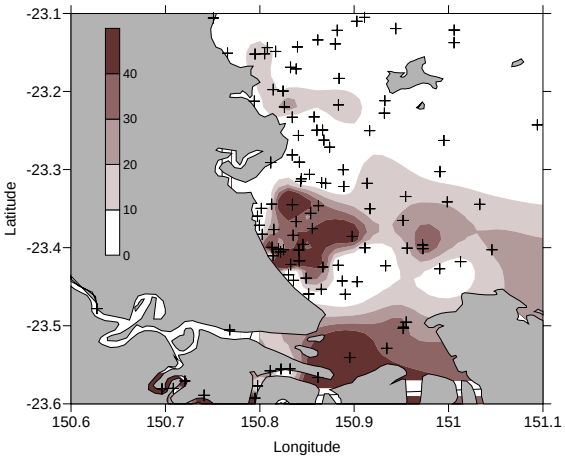

Figure 4.2: The percentage of mud in bottom sediments across Keppel Bay.

The tides during the September 2003 survey were mainly spring tides, whereas the tides during the time of the measurements in and around the mouth of the Fitzroy Estuary during the August 2004 survey were neap tides. As will be demonstrated later, tidal resuspension of sediments is strongly modulated by the spring-neap tidal cycle and this probably accounts for the generally higher TSM

concentrations in the mouth of the estuary in September 2003 compared to a year later.

Figure 4.3 shows a Landsat 7 satellite image for Keppel Bay obtained on 25 May 2003 at time when the tide was ebbing. The image shows turbid water near the estuary mouth and extending northeastwards in a pattern, which is broadly consistent with the TSM distribution shown in Figure 4.1. Also, note that the water along the western side of Keppel Bay appears to be more reflective (higher turbidity) than the water further offshore presumably a consequence of the muddy substrate. This image was obtained after the tidal current had been ebbing for four hours.

Figure 4.3: Landsat ETM+ image of Keppel Bay acquired 25/5/2003 9:41:58 AEST © Commonwealth of Australia)

Relationship between TSS concentration and turbidity

We demonstrate first that turbidity can be used as a surrogate for Total Suspended Sediments (TSS). Samples for Total Suspended Matter (TSM) analysis were collected and turbidity measured simultaneously at most of the stations on all three field surveys. Figure 4.4 shows the measured TSM plotted versus turbidity for the time series stations on the August 2004 cruise as well as for all the other stations. The results show that the relationship between TSM and turbidity is well represented over most of the measurement range by the line TSM = 0.65+1.13 × Turbidity where the units of TSM are gm^{-3} and the units of turbidity are NTU. The relative error in the predicted relationship is greatest for turbidity less than ~2 NTU where the scatter in the TSM measurements is ~$\pm 1 gm^{-3}$.

For larger turbidities, the relationship appears to apply across Keppel Bay and into Casuarina Creek implying a degree of uniformity of the physical properties of

the TSM. Further offshore in the zones of low turbidity, it may have been that a greater proportion of the suspended matter was not suspended sediment. Maximum chlorophyll concentrations are ~1 mgm^{-3} in Keppel Bay. If we assume that ratio of carbon mass in phytoplankton to chlorophyll mass is 50 and if that the carbon mass represents 50% of phytoplankton mass, then the maximum TSM concentration due to phytoplankton in Keppel Bay is ~±0.1 gm^{-3}. Thus, the deviation in measured TSM from the linear relationship does not appear to have been due to the presence of phytoplankton. Turbidity measurements are also sensitive to the presence of coloured dissolved organic matter (CDOM) in the water column. With dissolved organic carbon estimated as less than 2 gm^{-3} everywhere in the system, the effect of CDOM on the turbidity measurements is estimated to be less than 1% (Gippel, 1995). The turbidity measurement is most sensitive to particles having diameters between 0.5–10 µm (Gippel, 1989). We expected the peak sensitivity of the nephelometric instrument used for the measurements shown (McVan Instruments Analite NEP 260, 90° turbidity probe) to be ~1.7 µm (Gippel 1989). Some variations in the particle size distribution and particle characteristics between inshore offshore would also cause variation in the TSM-turbidity relationship. We conclude that at least for turbidities >2 NTU, that TSS concentrations can be estimated as: TSS ~0.65+1.13 × Turbidity.

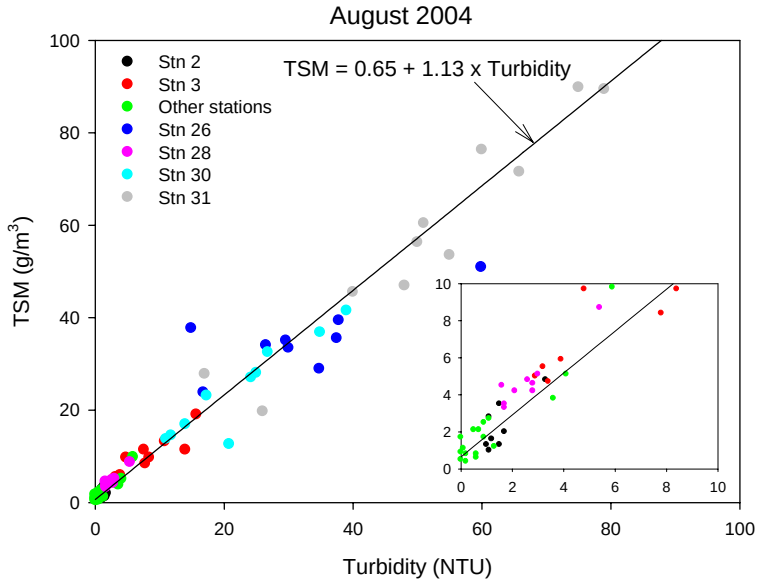

Figure 4.4: Relationship between measured TSM and measured turbidity across Keppel Bay and in Casuarina Creek in August 2004.

Figure 4.5 shows the TSM versus for the February 2005 survey, which was undertaken just after a flow event in the Fitzroy River. Over most of Keppel Bay, the TSM-turbidity relationship was consistent with that fitted to the August 2004 measurements. The largest deviations from this relationship (at least in relative

terms) mostly occurred at those stations where salinity was less than 30. These were stations up the Fitzroy Estuary and near its mouth. One might conclude that at these stations a significant amount of the turbidity was due to the turbidity associated with the river water whose particulate characteristics were different to some extent from those suspended from the bed of Keppel Bay.

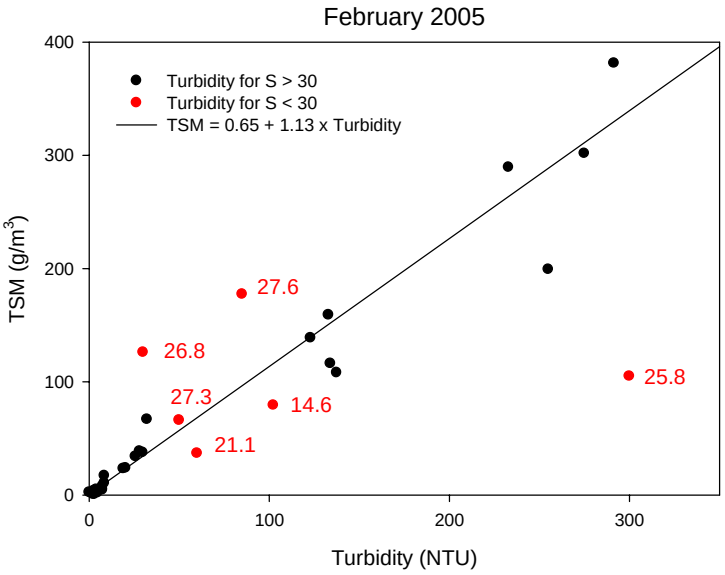

Figure 4.5: Relationship between measured TSM and measured turbidity across Keppel Bay and in Casuarina Creek in February 2005. Measurements for salinities less than 30 are shown in red. Numbers are salinities.

In the laboratory, the grain size of the suspended particulate material was measured directly by laser diffraction on collected water samples using a Malvern Mastersizer 2000. The laser diffraction measures particles as volume percentages in 34 logarithmically spaced bins, from 0.06–2000 µm. TSM within Casuarina Creek, the Fitzroy Estuary and just beyond the estuary mouth consisted mainly of silt-sized particles (>80%) with modal grain sizes ranging from 3.5 to 9.3 µm. Clay and colloid percentages were in the range from 5.1–15.3% and 0.9–4.3% respectively, and were highest in the river and lowest in the estuary mouth. Very fine sands were evident in most samples taken in Casuarina Creek and from beyond the estuary mouth. These are regions of high currents and very active resuspension of benthic sediments. We were unsuccessful in measuring sizes of the TSM at concentrations lower than 20 gm^{-3} due to the low obscuration values of these samples. Consequently, grain sizes of TSM could not be determined over most of Keppel Bay.

Time series of turbidity and TSS concentrations

Time series of turbidity were obtained at Buoy 1 and at Timandra Buoy (Figure 4.1). The first was a month-long record from Buoy 1 starting in mid-February

2004 and the other two were from Buoy 1 and Timandra Buoy starting in mid-August 2004. The second record from Buoy 1 had a duration of about two months and the Timandra record was approximately three weeks long. These measurements were obtained from nephelometers hung from the buoys at about 1 m depth. Thus, the first record was obtained at a time immediately following a period of discharge in the Fitzroy River (Figure 3.10), whereas the other two deployments occurred during the dry season.

Figure 4.6 shows the record from the second Buoy 1 deployment. Turbidity in this time series, and in the other two time series as well, undergoes a pronounced semi-diurnal variation whose amplitude varies over the 14-day spring-neap tidal cycle. A two-day section of this record (Figure 4.7) shows that the semi-diurnal fluctuations in turbidity have a phase such that the highest turbidity occurs 1–2 hours before low tide at Port Alma. Such a phase relationship is consistent with the majority of the semi-diurnal turbidity variation being due to the back and forward motion with the tide past the nephelometer of relatively low turbidity offshore water and high turbidity water found in the mouth of the Fitzroy Estuary and the tidal creeks (Figure 4.3). If this were the total explanation then high tide would have the lowest turbidity at Buoy 1 and low tide the highest. However, active resuspension of muddy bottom sediments would cause turbidity to increase in the water column when currents are strongest at mid-tide. This effect is a likely cause of the apparent phase shift between maximum turbidity and low tide.

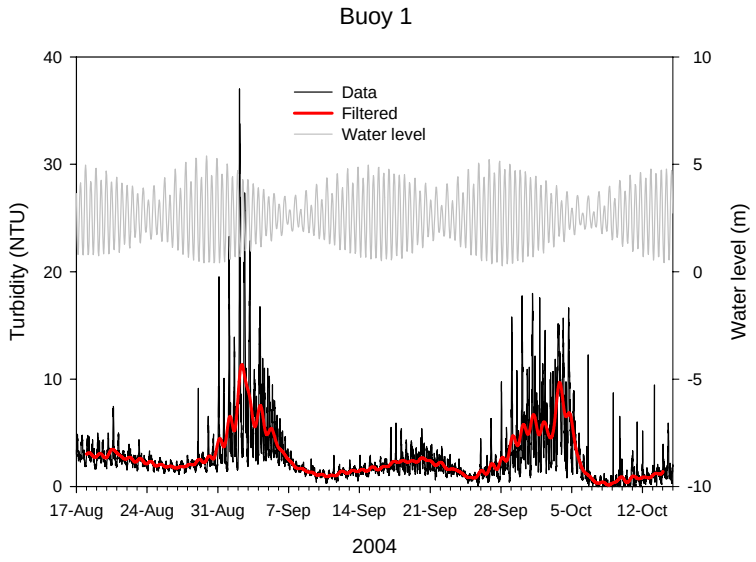

Figure 4.6: Time series of measured turbidities for the second nephelometer deployment at Buoy 1. Also shown are this time series low-pass filtered and the time series of predicted water levels at Port Alma.

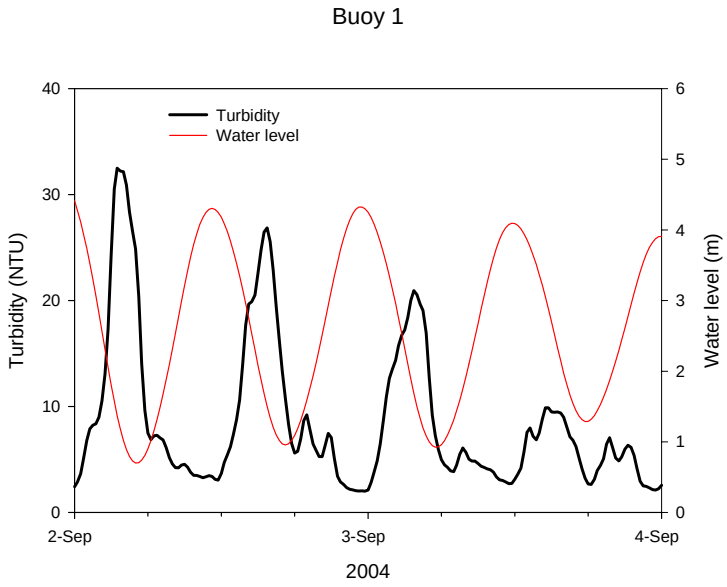

Figure 4.7: Time series of measured turbidities for the second nephelometer deployment at Buoy 1. Also shown is the time series of predicted water levels at Port Alma.

The turbidity data have been low-passed filtered to remove most of the variation at periods less than a day; the resulting time series are shown in Figure 4.6:. The daily range of turbidities and their low-pass filtered values are maxima ~3 days after the peak daily tidal variation during the spring tides. Tidal currents have their maximum amplitudes when the tidal range is largest. Hence, the horizontal excursion of water parcels over the tidal cycle and the resuspension rate of bed sediments are also largest during spring tides. A larger horizontal excursion would tend to cause a larger semi-diurnal variation in turbidity, but depending on the distribution of suspended sediment in the offshore direction the daily averaged turbidity could be larger or smaller other factors not considered. Conversely, resuspension rates typically increase with current speed so would always tend to cause higher suspended sediment concentrations around the time of spring tides. As sediment is suspended by tidal currents, it also settles out due to gravitation. If the variation in filtered concentrations were due to the relative effectiveness of resuspension for increasing TSS concentrations and settling for reducing them, then maximum concentrations would occur when TSS gain through resuspension balanced loss through settling. The settling loss rate equals the product of particle sinking speed and sediment concentration. The time of balance between resuspension and settling loss occurs after maximum resuspension rates.

Measurements made at Buoy 1 for a month-long period starting in mid-February 2004 show a similar pattern to that apparent in Figure 4.6. However, the February measurements show higher overall turbidity than those in August–

October later in the year. Turbidity averaged over two spring-neap cycles (28 days) was 5.9, whereas turbidity averaged over four spring-neap cycles (56 days) for the second nephelometer deployment was 2.8. Peak turbidity also differed by a factor of about two between the two deployments. Average daily tidal range for the two times was virtually identical being 3.40 m and 3.41 m respectively so the difference in turbidity was not likely to be due to stronger tidal currents during the first deployment. The February 2004 deployment did occur at a time, which followed flows in the Fitzroy River (Figure 3.10). Up to the end of the February deployment, the Fitzroy discharged ~$1.3 \times 10^9 m^3$ which is more than five estuary volumes. Even though turbidity reduced to less than 1 during the neap tide in late February, we might suppose that the availability of freshly deposited fine sediments from the river in the mouth area might lead to enhanced turbidity during the spring tides.

Turbidity measured at Timandra Buoy was substantially higher. Minimum turbidity was mostly greater than 5 and peak turbidity reached 100. Average turbidity over one spring-neap cycle was 25. Estimated tidal currents at Buoy 1 and Timandra Buoy are similar to one another so one might presume that the difference in turbidity at the two locations is due to a difference in the supply of fine sediment available for resuspension.

TSS flux

From the time series of predicted tidal heights at Port Alma and using the coefficients relating change in water level to tidal velocity (see section Tides – Currents), we can develop a time series of predicted current velocity at Buoy 1 and Timandra Buoy (v). Further, if we consider TSS concentration and turbidity to be directly proportional to one another using the relationship:

Equation 4.1 $$TSS = 1.13 \times \text{Turbidity}$$

then we obtain a time series for TSS. A time series of sediment flux at the buoys is then calculated as:

$$F_{TSS} = H \times v \times TSS$$

where H is water depth.

Figure 4.8 shows the time series of TSS fluxes calculated for Buoy 1 during the August 2004 deployment of the nephelometer. The positive and negative oscillations of the instantaneous flux are due to the flooding and ebbing tide. Also shown is the low-pass filtered flux, which effectively shows the net flux with the tidal oscillations removed. This filtered flux is only significant during the time of spring tides and is mostly negative indicating net sediment transport away from the mouth of the Fitzroy; that is, towards the northeast. The flux averaged over four spring-neap cycles is ī 3.8×10^{-3} $kgm^{-1}s^{-1}$ or ī 3.3×10^2 $kgm^{-1}d^{-1}$. In February 2004, the equivalent fluxes calculated over two spring-neap tidal cycles are ī 7.1×10^{-3} $kgm^{-1}s^{-1}$ or ī 6.1×10^2 $kgm^{-1}s^{-1}$. The fluxes at Timandra Buoy were averaged over one spring-neap cycle and are ī 4.6×10^{-2} $kgm^{-1}s^{-1}$ or

ī 4.0 × 10^3 $kgm^{-1}d^{-1}$. Thus, the estimated flux at Timandra Buoy is 6 and 12 times larger than the fluxes estimated at Buoy 1 in February and August 2004, respectively.

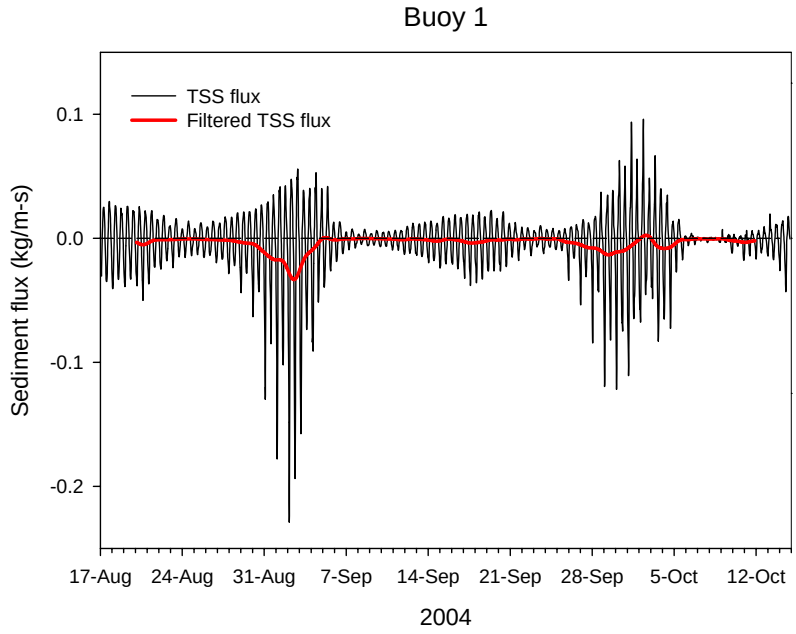

Figure 4.8: Estimated TSS fluxes at Buoy 1 for the deployment starting in August 2004. The red line is the flux low-pass filtered to remove the diurnal tidal fluctuations. A negative flux here is a flux away from the mouth of the Fitzroy; that is approximately towards the northeast.

Most of the water flowing in and out of the Fitzroy Estuary passes through a channel adjacent to Buoy 1 and Timandra Buoy is also adjacent to a channel through which much of the flow towards the mouth must pass. We can estimate the flux of sediment through these channels by considering their cross sectional area and assuming that the flow velocity and TSS concentrations are as described in the analysis just presented. At mid-tide the channel at Buoy 1 is estimated to have a width of ~2300 m and a mean depth of 9 m, whereas the width and depth of the channel adjacent to Timandra Buoy are estimated to be 1700 m and 15 m, respectively. Table 4.1 provides the estimated mass flux through each channel section in a year based on the nephelometry measurements.

Table 4.1: Mass fluxes estimated from nephelometry measurements.

Measurement site	Mass flux (kg/s)	Mass flux MT/yr)
Buoy 1 – Feb. '04	-15.8	0.50
Buoy 1 – Aug. '04	-7.6	0.24
Timandra – Aug. '04	-66.2	2.10

Limited data (Taylor and Jones, 2000) indicate high annual delivery of river sediments to the Fitzroy Estuary (~ 4 MT per year on average), but these loads vary very much from year to year partly due to interannual variations in discharge and partly to variation in the concentration of suspended sediment in the river flow.

A simple resuspension model

We propose a simple model for explaining the observed turbidity variations at Buoy 1 in August 2004. We consider a 1-dimensional balance between resuspension and settling of fine sediments. Thus, if C_{TSS} is considered to be low-pass filtered TSS concentration then the rate of change of concentration is taken to be:

Equation 4.2

$$\frac{\partial C_{TSS}}{\partial t} = H^{-1}(R - S)$$

where R and S are resuspension and settling rates of fine sediments per unit area of seabed, respectively and H is water depth. Sediment suspension rates are typically considered to be proportional to the amount by which the critical shear stress is exceeded raised to the power of 1.5 or more (e.g. van Rijn, 1993). The shear stress of the flow over the bottom increases as approximately the square of the flow speed. We will assume that resuspension takes place at a rate which is proportional to U the low-pass filtered flow magnitude. Thus, $R = \alpha U^{\beta}$ where α and β are constants to be determined. The settling rate is equal to the product of concentration and sinking speed of the sediment particles assumed to be uniform (W) so $S = WC_{TSS}$. Substituting into Equation 4.2, we obtain an equation for C_{TSS} as:

Equation 4.3

$$\frac{\partial C_{TSS}}{\partial t} = H^{-1}(\alpha U^{\beta} - WC_{TSS})$$

For specified α, β, and W, Equation 4.3 is integrated forward in time from an assumed initial condition that the measured and modelled TSS concentration are equal. Here, measured TSS concentration is that calculated using Equation 4.1. The parameters α, β, and W are determined by optimal fitting in a least squares sense between the modelled and the measured time series of TSS concentrations.

Figure 4.9 compares the measured time series of TSS concentrations with those modelled for constant W (black line). The simulation captures major features of the measurements but there are important differences. Although this simulation does show much of the observed phase lag between peak tidal currents and

measured peak sediment concentrations, the lag is a day or so too small in the simulation. Further, the reduction in TSS concentration from its peaks is significantly slower in the simulation than is observed.

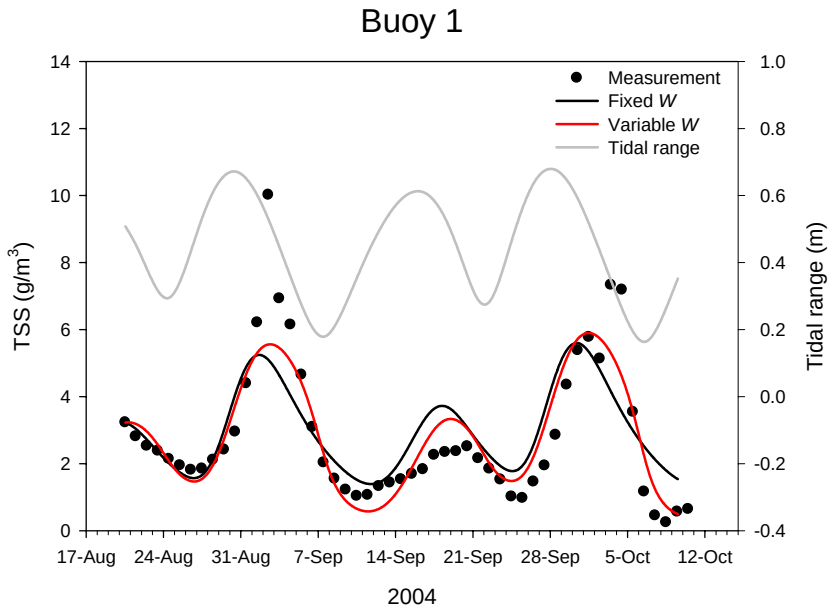

Figure 4.9: Comparison between measured and modelled low-pass filtered concentrations at Buoy 1. Simulations are shown for a constant W and for a W dependent on flow speed and particle concentration. Also, shown are the daily magnitudes of the tidal current.

We speculate that part of the disagreement between model and measurements is due to the impact of flocculation dynamics on particle settling rates. Flocculation is the process of particles aggregating due to electrostatic forces. There are basically three types of flocculation namely flocculation due to Brownian motion, differential settling and to fluid shear (Thomas *et al.* 1999). Flocculation due to fluid shear is likely to be the process that is most important in the Fitzroy Estuary and Keppel Bay. In shear flocculation, particles are continuously aggregating into flocs when they collide. At the same time, the flocs are being disrupted by fluid shear and by particle collisions. The mean size of flocs depends on the balance between particle aggregation and floc rupture which turn depends on the geochemical properties of the sediment, flow turbulence, and particle concentrations. In general, flocs tend to be larger with smaller turbulence levels (lower flow speeds) and with reduced TSS concentrations (Burban *et al.* 1989, Neumann, 2004).

Because the particles comprising flocs have spaces between them their density for a given floc diameter is usually considerably less than that of a particle grain of the same diameter. The sinking rate of a floc depends on its diameter as well as on its density. In the Fitzroy-Keppel Bay system the strength of the tidal flow

undergoes a pronounced spring-neap cycle which in turn implies that the floc size and its sinking rate also varies over this cycle. In our model, we account for this by specifying that *W* depends on tidal flow magnitude *U* as well as on TSS concentration C_{TSS}. Thus, we specify:

$$W = -\chi U^{\gamma} C_{TSS}^{\lambda}$$

where ɢ, ɔ, and ə are constants determined by fitting. In our analysis, we determine optimal values of ɔ and ə to be ɔ = ī 1.3 and ə = ī 0.3. The fit obtained with assuming *W* takes this form is also shown in Figure 4.9. Although the simulated peaks are not as high as those measured, the phase relationship with the measurements is well captured, as is the fall-off after peak concentration. The RMS differences between measurements and model are 1.34 NTU for the fit with constant *W* versus 0.98 NTU for the fit with variable *W*. The average value of *W* for the two simulations was 1.9 and 2.0 m/day for the constant and variable *W* respectively, whereas the respective values for the resuspension coefficient were also similar to each other being 4.7 and 4.9, respectively.

There are other factors that are likely to affect the turbidity at Buoy 1 most notably the wind. Winds give rise to waves, which can greatly enhance resuspension due to currents (Grant and Madsen, 1979). Further, wind-driven flows could affect the spatial distribution of the suspended sediment plume. No doubt, some of the differences between model and measurement are due to the wind. A visual examination of the wind records for the time of the turbidity measurements does not show any obvious reasons for the major discrepancies between the two time series. This modelling application analysis does suggest that fine sediment resuspension is a highly non-linear function of flow speed and that the average particle sinking rate is ~2 md^{-1}. The model with variable *W* suggests that flocculation may cause the sinking rate to vary between 0.5 md^{-1} and 7 md^{-1}. These are results obtained from measurements adjacent to the main channel where current speeds and TSS concentrations are high. In other parts of Keppel Bay, one might expect settling rates to be higher where current speeds and TSS concentrations are generally lower.

Surface water samples were collected from three sites during the August 2004 campaign and placed in a settling column. From the time taken for the column to clear a settling rate can be calculated. The three samples had calculated settling rates of 2, 3, and 3 md^{-1} which are consistent with the estimates obtained from the resuspension model.

The theoretical sinking rate for spherical particles of diameter *d* and density $ɟ_s$ is calculated by Stokes Law:

$$w = \frac{d^2(\rho_s - \rho)g}{18\mu}$$

where ɟ is the density of water, *g* is gravitational acceleration and μ = 0.008 $kgm^{-1}s^{-1}$ is the viscosity of water (Massey, 1980). If the nominal density of the particle is assumed to be that of mineral material ($ɟ_s$ ~2650 kgm^{-3}), then the range of sinking rates for the modal grain diameter range 3.5 to 9.3 μm is 0.12 to 0.84 md^{-1}. Only the highest of these rates falls within the range of sinking rates estimated by the resuspension model. Further, it is known that when flocs are formed as aggregates of particles, their effective density decreases due to the water-filled spaces within the floc. Neumann (2004) has shown that effective floc densities of Brisbane River flocs are much closer to 1150 kgm^{-3} than they are to 2650 kgm^{-3} which would result in much lower sinking rates calculated from Stokes Law. Although the effect of lower density is to cause sinking rates to decrease for a given floc size, this effect is compensated somewhat if water can flow through the floc as it settles (Vainshtein *et al.*, 2002). A major difficulty with measuring floc sizes in the laboratory on collected samples is that the floc sizes are likely to change once they are collected. Also, it is highly unlikely that the flocs would take the form of spheres. A selection of the samples collected in the Fitzroy was sonified prior to particle-size analysis to break up the flocs. Particle sizes determined for sonified samples were on average 30% smaller than those obtained from the corresponding unsonified samples.

Measurements of excess activity of the naturally occurring radionucleides ^{234}Th and ^{238}U on suspended particles in the water column, and in the surficial sediments provide independent estimates of the average particle life time in the water column, and the deposition rate of sediment at specific locations (Hancock and Ford 2004). Eight samples were collected at well-spaced sites in Keppel Bay in August 2004. The measured particle residence time ranged from 2.4 to 5.0 days with the longest residence time at Timandra Buoy. Taken together with an average water depth of 10 m these results imply a net particle settling velocity of between 2 and 3.3 md^{-1} which is in good agreement with the values inferred from both the settling experiments, and from the analysis of the moored turbidometer data reported above. The inferred particle deposition flux at three sites in the vicinity of Quartz Rock is in the range of 2–4 g m^{-2} d^{-1}. At two sites along the main channel running out to Timandra Buoy the measured deposition flux was approximately zero although the measurement uncertainty was of comparable size. As a deposition flux of about 60 g m^{-2} d^{-1} would be required to sustain the measured TSS concentrations and particle residence times this result is best interpreted as indicating a zone of net erosion, and thus confirms the identification of this region as a source of fine sediments in the dry season.

These sediments are exported offshore via the shipping channel running past Timandra Buoy.

We suggest that that there is evidence of particle properties changing as a consequence of flow and perhaps TSS concentrations. At TSS concentrations less than about 5 g/m^3, Figure 4.4 shows that the proportionality between TSS concentration and turbidity alters. In particular, a given turbidity is associated with a higher TSS concentration as TSS concentration decreases. This behaviour is consistent with the tendency of larger flocs to form under lower TSS concentrations and under lower flow conditions. For a given TSS concentration, it is well known that a larger number of small particles produces a higher turbidity than a smaller number of large particles. Oubelkheir *et al.* (in press) inferred particle properties from their inherent optical properties. Their measured back scattering efficiency can be used as a measure of particle size. They found that in the mouth of the Fitzroy, the behaviour of this optical property indicated the presence of larger particle sizes during times of strong tidal current. Oubelkheir *et al.* attribute this observation to the suspension of heavier particles by the strongest currents, which settle to the bottom quickly when the current speed drops.

The issue of particle sinking rates in environments where floc formation can occur is a difficult one and our measurements can't resolve what is really occurring. Douglas *et al.* (2005b) suggest that sediment delivered from the catchment is delivered as very fine clay particles (~1 µm diameter). These particles settle very slowly, but experiments by Douglas *et al.* (2005b) demonstrate that once salinity increases above ~1.5, flocculation occurs and settling rates are greatly increased. The propensity for floc formation depends on the geochemistry of the fundamental mineral particles as well as on the presence of organic coating which tend to hinder flocculation. These properties are site specific so that experiments on floc formation tend not to have universal applicability. Within the Fitzroy Estuary and Keppel Bay, we can expect floc formation and disruption to be a dynamic process depending on shear rates and sediment concentration. Floc size and form depends not only on the ambient conditions but also on the antecedent history of the flow and concentration conditions (Neumann, 2004). It is apparent though that particle settling rates have a profound influence on TSS concentrations and are certain to have a major impact on the transport of fine sediments away from the mouth of the Fitzroy Estuary.

Keppel Bay biogeochemistry

Introduction

This chapter deals with the biogeochemical functioning of Keppel Bay. It seeks to contribute understanding to the following questions outlined in the initial plan of the Fitzroy Contaminants Project (AC) in the Coastal CRC:

- How are sediments and nutrients transported through the Fitzroy Estuary and Keppel Bay to the Great Barrier Reef?
- What is the role of the Fitzroy Estuary and Keppel Bay – as regions for accumulating, transforming and redirecting contaminants from the catchment?
- What bio-physical processes are likely to be important for the dynamics of tropical macrotidal estuaries?

The chapter begins with a short discussion on the spatial distribution of modern Fitzroy River (MFR) sediments in Keppel Bay, and aspects of the geology and weathering of these sediments that influence distribution and reactivity of biogeochemically significant elements (i.e. C, N, P & Fe). Iron is highlighted as a surrogate for sediment surface area because it correlated closely with a limited suite of actual surface area measurements. Quantification of sediment nutrient concentrations and surface area relationships is a prerequisite for subsequent discussion on sediment P-pools and carbon and nutrient burial rates. It also lays the foundation for the second major sub-section on biogeochemical processes including loss of terrestrial organic matter (and nutrients) from particles when they meet the sea, the oxic and sub-oxic break-down of organic matter in Keppel Bay and nitrogen fixation and the role of iron. Included in the discussion on nitrogen fixation is a surprising result whereby this process was observed occurring under dark conditions. Water column nutrient dynamics are covered in the next sub-section in which the data from two dry season surveys and one wet season survey are conveyed in traditional mixing plots (nutrients vs. salinity) and maps. These diagrams (i.e. maps and mixing plots) are used to determine the regions in Keppel Bay where nutrients were behaving conservatively and non-conservatively, and where they were below detectable limits. In the final sub-section of this chapter, Keppel Bay is divided into three zones based on the outlined results: (i) the Zone of Maximum Resuspension (ZMR); (ii) the Blue Water Zone (BWZ); and the (iii) Coastal Transitional Zone (CTZ), and the features of each of these zones are discussed.

Bottom sediments: spatial distribution, geochemical character & nutrient accumulation

Spatial distribution of mud and sand

From a geologic perspective, the Fitzroy Estuary is in a mature stage of evolution because much the accommodation space for sediment is already full and mangrove areas are limited (Ryan *et al.*, 2004). As a consequence, the Fitzroy "Estuary" is evolving into a tide-dominated delta, and as such, much of the sediment that is delivered from the FRB is exported to Keppel Bay (Ryan *et al.*, 2004; Bostock *et al.*, 2005a) where it may enter the tidal creeks, or mix with the existing (relict) sediments. The Beach Protection Authority (Anonymous, 1979) and subsequently Ryan *et al.* (2005; in prep) used the feldspar and mud contents of Keppel Bay sediment to indicate the region of recent influence of the Modern Fitzroy River (MFR) in the sedimentation along the Capricorn Coast. The river-derived sediment is feldspathic (>10% feldspar) and has mud contents of >10% (see also Chapter 4). The chemical differentiation of these sediments from the quartzose relict sand sediments is evident on axis 1 of the PCA, and explains more than 50% of the variance in the sediment geochemistry data set (Figure 5.1a). Note that the mud percentage is positively correlated to axis 1 and inversely correlated to the quartz:feldspar ratio on this axis (Table 5.1; see also Ryan *et al.*, 2005). The MFR sediments have PCA axis 1 loadings of -10 to +4, and include muds and sandy-muds (MFR-M&sM), muddy sands (MFR-mS) and sands (MFR-S). These sediments occur in Casuarina Creek, and in two distinct lobes in Keppel Bay. The first (western) lobe follows the coast northwards and becomes thin and discontinuous to the north of Keppel Sands. The second (eastern) lobe extends in an east-ward direction from the estuary entrance toward Hummocky Island. The "relict sands" (*sensu* Anonymous, 1979) are found in the distal north-east of the study area (axis 1 PCA loadings >4). The Beach Protection Authority (Anonymous, 1979) sees the relict sands (REL-S) as a former sandy coastal plain that was drowned by rising sea levels in the early Holocene. The low feldspar and mud contents of the relict sands is thought to reflect the longevity of these sediments in the marine environment (Anonymous, 1979): feldspars are broken down into mud, which is subsequently winnowed out of the sediment by hydrodynamic sorting, while more resistant quartz is retained.

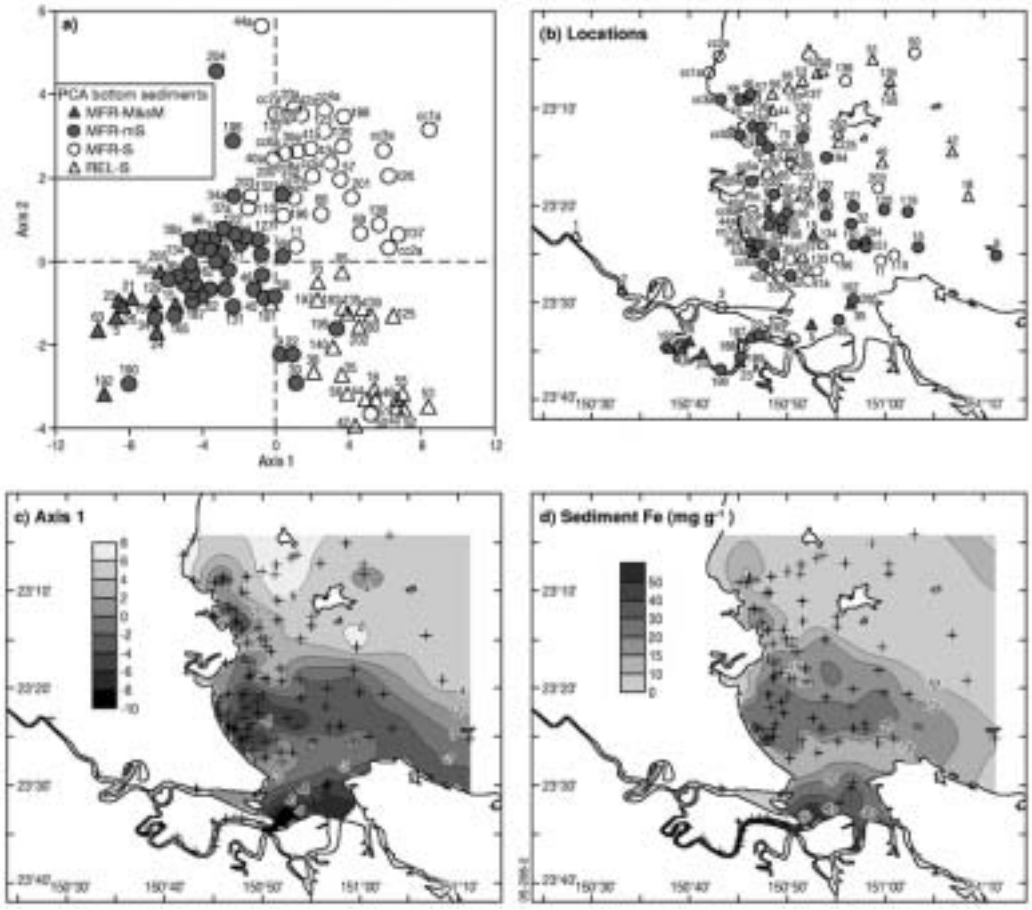

Figure 5.1: (a) Results of the PCA on bottom sediment geochemical constituents (axis 1 vs. axis 2) and grain sizes in the scheme of Folk (1970); (b) map show the locations of sediment samples used in the PCA and the grain sizes in the scheme of Folk (1970); (c) map showing the distribution of site scores for axis 1 of the bottom sediment PCA; and (d) map of bottom sediment iron concentrations.

Table 5.1: Factor coordinates of the variables on axes 1, 2, & 3 of the PCA. Axis 3 (calcium carbonate contents) is discussed in Ryan et al. (in prep).

Variables	Axis 1	Axis 2	Axis 3
Fe(tot)	-0.97	0.10	0.03
Al2O3:K2O	-0.97	0.07	-0.06
Al	-0.96	0.10	0.08
TP	-0.92	0.08	-0.02
TOC	-0.92	-0.17	0.16
CIA index	-0.92	0.09	0.14
Zn	-0.90	0.14	-0.01
TN	-0.90	-0.20	-0.13

Variables	Axis 1	Axis 2	Axis 3
FeIII	-0.89	-0.17	0.20
Mg	-0.89	0.05	-0.32
Na	-0.89	0.08	-0.06
%Mud	-0.88	-0.14	-0.04
S	-0.86	-0.27	0.02
K	-0.85	0.19	0.14
Ti	-0.85	0.19	-0.12
Cr	-0.84	0.07	0.01
Ni	-0.81	-0.13	0.21
Cu	-0.79	0.28	0.16
Kaolite minerals	-0.78	-0.14	0.15
TN:TP	-0.75	-0.33	-0.18
Cl	-0.72	-0.38	-0.06
FeII	-0.69	0.59	0.02
TP:TS	0.57	0.48	-0.02
%TOC-(TOC+TS+Fe(II))	-0.50	-0.58	0.17
Mn	-0.48	0.24	0.03
%S-(TOC+TS+Fe(II))	0.46	-0.51	-0.15
TS:FeII	-0.42	0.05	0.19
TOC:TN	-0.39	-0.05	0.57
FeII:FeIII	-0.26	0.72	0.03
%FeII-(TOC+TS+Fe(II))	0.25	0.83	-0.09
Fe(II):TOC	0.11	0.86	-0.13
Ca	-0.21	0.11	-0.89
Carbonate	-0.12	-0.01	-0.92
Greigite	0.11	-0.49	-0.50
TOC:TS	-0.07	0.24	0.03
TP:Fe	0.92	-0.12	-0.07
Si	0.87	0.04	0.32
Quartz	0.77	0.05	0.47
Quartz:feldspar	0.70	-0.32	0.15

Geological aspects and weathering

Keppel Bay sediments define three distinct arrays in Al_2O_3-K_2O-(CaO+Na_2O) space (Radke *et al.*, 2005c; Smith, in prep) that are sub parallel to the idealized basaltic and granitic weathering trends but which originate at a composition similar to that of the Upper Continental Crust (UCC). This general association reflects the large size of the Fitzroy River Basin and the integration of the weathering products of a large number of rock types to give a composition similar to that of a partially weathered average crust (c.f. UCC) for sediment that is deposited into Keppel Bay. As this average composition is weathered, this initially results in the loss of both Na and Ca, initially from feldspar and then from secondary clays and ultimately into formation of kaolinite and a suite of other minerals. Consequently, weathering is marked by a progressive increase in Al_2O_3:K_2O ratios in traditional Al_2O_3-K_2O-(CaO+Na_2O) trilinear diagrams (Radke *et al.*, 2005c; Smith in prep). Weathering products may also be size fractionated during transport and deposition with the finer mud and sandy-mud sediments becoming progressively kaolinite-, and probably illite-enriched. Importantly, weathering (and enrichment of fines due to hydrodynamic sorting) increases the average overall specific surface area of sediment, and enhances the secondary iron mineral concentrations due to the destruction of Fe-bearing primary minerals. These important points are illustrated with respect to some Keppel Bay data in Figure 5.2: Figure 5.2a shows that sediment surface area increases with the Al_2O3:K_2O ratio of muddy sediment (surface area = 88.3 * ln (Al_2O_3:K_2O) – 151.7); while Figure 5.2b shows that there is a linear increase in Fe concentrations with the surface area (i.e. 0.46 mg Fe m^2 sediment) of the muddy sediment.

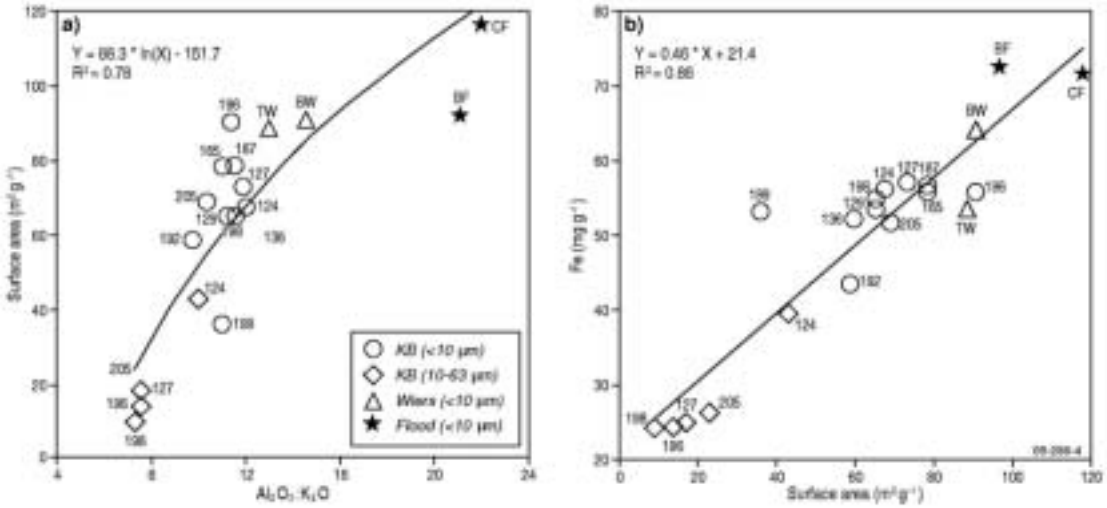

Figure 5.2: (a) Sediment surface areas vs. Al_2O_3:K_2O ratios of sediment; (b) Sediment Fe vs. surface area of sediment.

Nutrient & TOC-surface area relationships

Sediment nutrient (TP and TN) and TOC concentrations of Keppel Bay sediment correlate linearly with Fe concentrations (Figure 5.3abc), and therefore, probably, with the surface area of the sediment. The Fe, nutrients and also Al_2O_3:K_2O ratios have large negative loadings on axis 1 of the PCA (Table 5.1), which highlights the region of influence of modern Fitzroy River sediments in Keppel Bay (see also Ryan *et al.*, 2005). Consequently, the mapped distributions of these constituents look similar to that of the first principle component (see the Fe map for example in Figure 5.1d and the nutrient maps in Radke *et al.*, 2005c). The fact that TOC correlated with Fe (as a surrogate for surface area) is not surprising because sediment TOC concentrations normally co-vary with sediment surface areas in continental margin settings (see review by Hedges and Keil, 1995). This is because most sedimentary TOC is bound to the finest mineral grains, an association that reflects two mechanisms: (i) sorption onto mineral surfaces (i.e. the sorptive preservation hypothesis; see review in Hedges and Keil, 1995); and (ii) formation of organo-clay aggregates (Krull *et al.*, 2003). Aggregates are the main form of organic materials in marine sediments (Ransom, *et al.*, 1997), and nitrogen and amino-acid enriched organic matter preferentially enters into these organo-mineral associations (Aufdenkampe *et al.*, 2001). Likewise, iron oxides occur as coatings on mineral grains and are a major control on P concentrations (dissolved and solid-phase), and on the whole P cycle (see review in Haese, 2000).

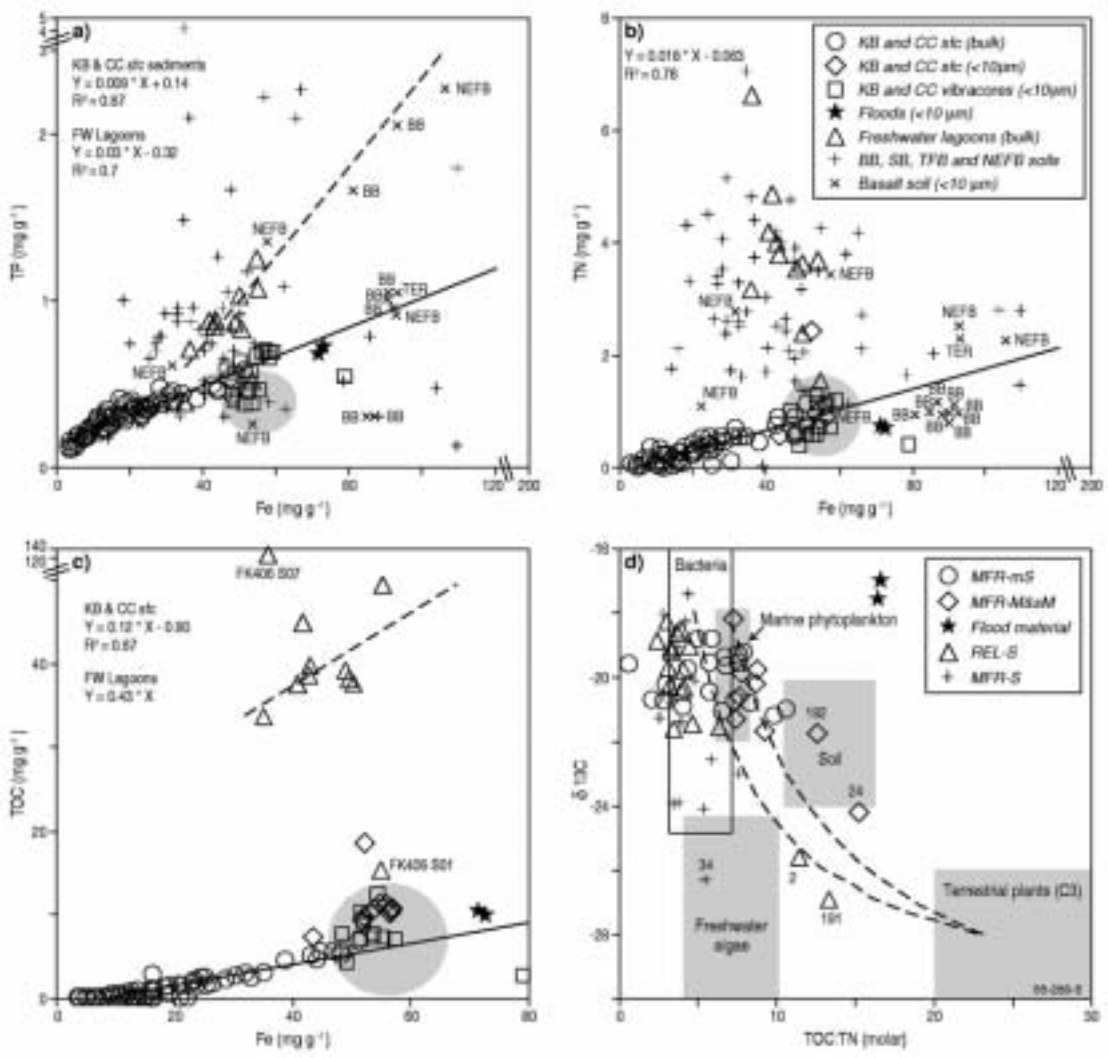

Figure 5.3: (a) TP vs. Fe; (b) TN vs. Fe; (c) TOC vs. Fe and (d) $\breve{u}^{13}C$ vs. TOC:TN. The shaded circles in a, b and c are the areas within which the down-core data from the floodplain cores plotted. Note that samples FK406_S07 and FK406_S01 were not included in the calculation of the regression equation through the floodplain samples in (c).

Sediment P-pools

Suspended sediment in Keppel Bay had TP concentrations that were similar to those of MFR mud and sandy-mud sediments (Figure 5.4a). This was expected because the suspended sediments were derived almost entirely from resuspension of bottom sediment during the time of the dry season surveys (Chapter 4). These mud and sandy-mud sediments stand out as having the highest proportions of biologically available P (Figure 5.4b) of the sediment classifications (30–45%), due mainly to larger concentrations of iron & aluminium bound P (Fe/Al-P; Radke *et al.*, 2005c). Note for example that there is a sharp increase in the amount of Fe/Al-P per iron surface area equivalent in the sediments with Fe concentrations greater than 20 mg g^{-1}, and a more robust

linear relationship than with the sandier sediments (i.e. Fe/Al-P = 0.003 * Fe (>20 mg g^{-1}) – 0.06 (R^2 = 0.95) compared to Fe/Al-P = 0.0005 * Fe (<20 mg g^{-1}) + 0.0004 (R^2 = 0.43); Figure 5.4c). The relict sand sediments had the lowest proportion of biologically available P of all sediment types in Keppel Bay (typically 19–27%), due to lower relative proportions of Fe/Al-P and higher relative proportions of residual-P (Figure 5.4b). The resistant P minerals that make up the residual-P pool may include rare earth phosphates such as xenotime and monazite. These minerals probably occur in the granitic terrain of the New England Fold Belt, and can contain as much as 25% phosphate by weight.

All sediment classifications had large proportions of biologically-unavailable Ca-bound P (medians >50%), and contained generally similar proportions of organic–P (i.e. medians in the 20–25% range; Radke *et al.*, 2005c). These P-pool constituents (Organic-P and Ca-P) correlated logarithmically with Fe (Ca-P (mg g^{-1}) = 0.072 * ln (Fe) - 0.057 (R^2 = 0.84)) and organic-P (mmol g^{-1}) = 0.033 * ln (Fe) - 0.032 (R^2 = 0.76)). As only 25% of sediment P was in the organic form, overall P concentrations were much higher than the Redfield ratio (Redfield *et al.*, 1963) in terms of TN:TP stoichiometric relationships (Figure 5.4d). It has yet to be established whether the Ca-P pool in Keppel Bay constitutes a major sink for P (i.e. it is formed from marine authigenic processes), or if a significant proportion of the Ca-P is of igneous origin and derived from catchment sources. Although Keppel Bay sediments are enriched in P relative to N compared to most non-basaltic catchment soils and floodplain sediments (i.e. the slope in Figure 5.4d has a TN:TP ratio of 5.3 compared to 7.7 ± 4.3 for the Bowen Basin (BB), Surat Basin (SB), Thompson Fold Belt (TFB) and New England Foldbelt (NEFB) soils and 10.2 ± 3.5 for the floodplain sediments but see also Tables 5.2 and 5.3) as would be expected if authigenic CFA precipitation were occurring, their TN:TP ratios were intermediate with respect to the basaltic soil samples (TN;TP = 5.0 ± 3.0; Figure 5.4d), and they were depleted in P compared to Fitzroy flood samples (TN:TP = 2.3). Using major and trace element geochemistry, Douglas *et al.* (2005a) demonstrated that suspended sediment in Fitzroy flood events is dominated by basaltic material (Tertiary basalts), and that this material is preferentially exported from the estuary to Keppel Bay. Similarly, Smith (in prep) has shown that the <10 µm fraction of Keppel Bay sediments is displaced to closer to the basalt weathering line in Al_2O_3-K_2O-(CaO+Na_2O) trilinear diagrams, than the majority of the bulk sediments.

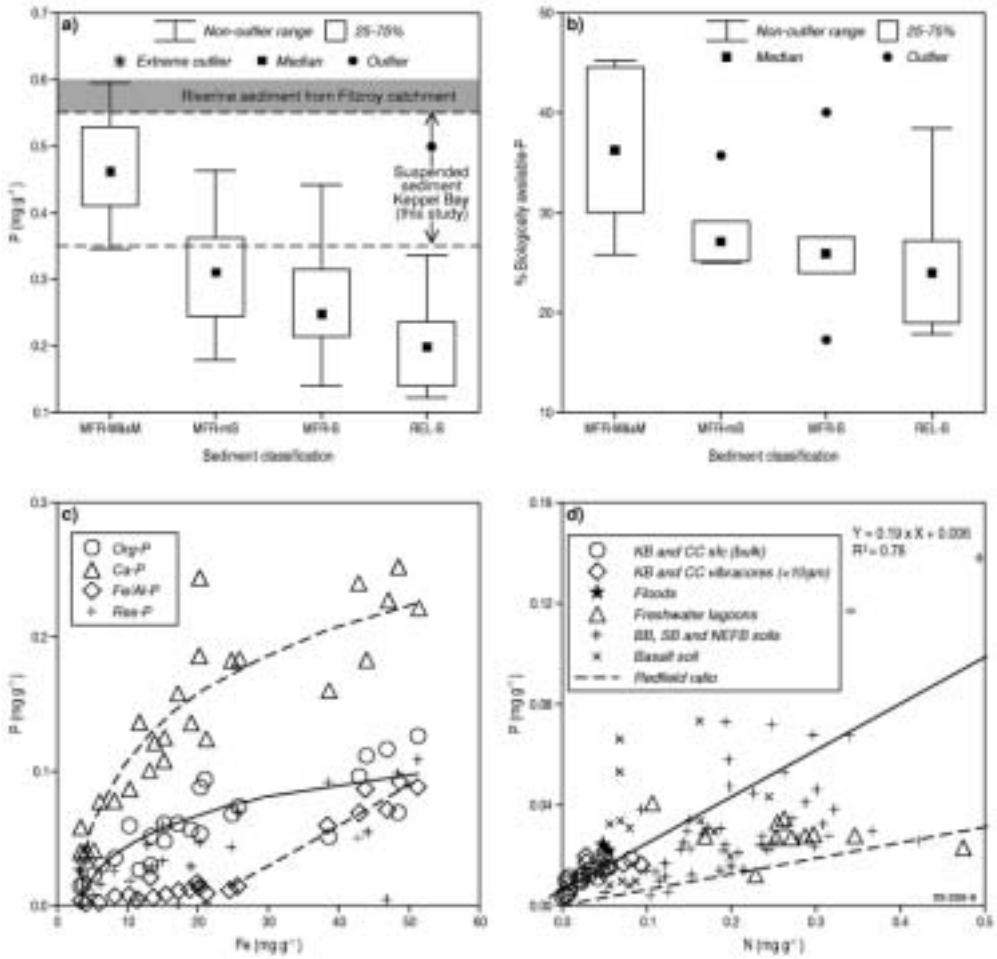

Figure 5.4: (a) Sediment P concentrations in each of MFR-M&sM, MFR-mS, MFR-S and REL-S in comparison to suspended sediment concentrations from both Keppel Bay and the Fitzroy catchment; (b) percentages of P in biologically available forms (i.e. organic-P + Fe/Al-bound P) in each of MFR-M&sM, MFR-mS, MFR-S and REL-S; (c) Organic P (Org-P), calcium-bound P (Ca-P), Fe and Al bound P (Fe/Al-P) and residual P (Res-P) vs. Fe in sediment; (d) Sediment P vs. sediment N concentrations.

The most important distinction between igneous- and marine authigenic fluorapatite is the presence within the apatite crystal lattice of carbonate derived from substitution with either phosphate of the fluoride, hence the name carbonate fluorapatite (CFA; Ruttenberg, 2005). Although CFA formation is widespread in the oceans and their margins, the mineral evades detection by direct mineral analysis (XRD or SEM). Instead, identification of CFA requires a sequential extraction method of a different sort than the one undertaken so far in this study (SEDEX; Ruttenberg, 2005), although 15 samples are currently undergoing analysis by this method.

Carbon and nutrient mass accumulation rates

Determination of the spatial extent and accumulation rates of sediment represents work in progress by the sedimentology team at Geoscience Australia. Preliminary reports on the subject have been completed by Ryan *et al.* (2005) and Bostock *et al.* (2005a), and a final report on the subject represents work in progress by Bostock *et al.*, in prep. In Table 5.2, the sediment accumulation rate and bulk density data reported by Bostock et al (2005a,b) for sediment cores were used to calculate carbon and nutrient mass accumulation rates for individual sites within Keppel Bay, the tidal creeks (Kamish Passage and Casuarina Creek) and the floodplain (Crescent and Frogmore Lagoons). As expected, modern nutrient accumulation rates were consistent with the sedimentation rate data (Bostock *et al.*, 2005ab; in prep), and were highest in the tidal creeks and floodplain sediments and lowest in Keppel Bay. This result is also consistent with the net estimated sediment flux at Stn F (this study; Chapter 4), which were towards the south-west in the direction of Casuarina Creek. In Table 5.3, we use estimates of sediment volumes accumulated over the last 7000 years rates in different regions within Keppel Bay and the Fitzroy floodplain (Bostock *et al.*, in prep), and the average surface sediment TOC, TN and TP concentrations (bulk sediment only) also from these regions, to estimate long-term nutrient and carbon burial rates. As with the specific site data (Table 5.2), carbon and nutrient accumulation rates were much lower in Keppel Bay than in the tidal creeks and floodplain sediments, where they accounted to 1.5% of total annual TOC burial, 3.6% of total annual N burial and about 10% of total annual P burial. However, these long-term accumulation rates probably over-estimate modern burial rates as sedimentation rates were almost certainly higher in the early to mid-Holocene when sea level was rising and there was more accommodation space for sediment (Bostock *et al.*, in prep). Similarly, Brooke *et al.*(in prep) have shown that there has been a general decline in the rate at which sediment has accumulated in beach ridges in Keppel Bay during over the last 1500 years, and that the decline was most marked during the last 230 years. Some alternative burial/export rates are presented in Table 5.4 in the next section.

Table 5.2: TOC and nutrient mass accumulation rates for sites in Keppel Bay. TN:TP ratios based on these data are also shown.

Core/Site	Approximate Age	Depth (m)	TOC (mg cm^2 yr^{-1})	TN (mg cm^2 yr^{-1})	TP (mg cm^2 yr^{-1})	TN:TP (molar)
Core VCO5; Site 200[a] Inner Keppel Bay	Mod.	0.0–0.02	6.9	1.3	0.2	6.6
Core VCO5; Site 200[a] Inner Keppel Bay	Mod–MH	0.4–0.43	0.9	0.1	0.0	2.7
Core VCO5; Site 200[a] Inner Keppel Bay	Mod–MH	1.0–1.03	0.5	0.0	0.0	1.8
Cire VC20; Site 205[a] Lower floodplain/estuary	LH	0.03–0.05	1.7	0.2	0.1	1.9
FK413A (Kamish Passage)[a] Lower floodplain/estuary	Mod	0.0–0.03	71.2	6.5	3.8	1.7
FK408A (Casuarina Creek)[a] Lower floodplain/estuary	Mod	0.35–0.36	41.8	3.9	2.7	1.5
FK407E (Frogmore Lagoon)[b] Upper floodplain	Mod	0.03–0.04	70.0	5.8	1.5	3.9
FK406E (Crescent Lagoon)[b] Upper floodplain	Mod	0.0–0.15	64.4	5.3	1.2	4.6

a. Sediment size fraction used in the calculation: (a) <10 µm; and (b) bulk sediments, however most of these sediment samples had mean grain sizes of <10 µm (Bostock *et al.*, 2005b).

b. Ages: Modern (Mod); mid-Holocene (MH) and late-Holocene (LH) (Bostock 2005a).

Table 5.3: Accumulation rates for regions in Keppel Bay and Fitzroy Estuary. TN:TP ratios based on these data are also shown.

Region	TOC (tonnes year-1)	TN (tonnes year-1)	TP (tonnes year-1)	N:P (molar)
Upper floodplain	25 093	2 320	537	9.6
Lower floodplain & estuary	15 755	2 207	1 789	2.7
Beaches & sand bars	262	93	160	1.3
Inner Keppel Bay	381	77	93	1.8
Total	41 491	4 697	2 579	

Biogeochemical processes

Fate of terrestrial organic matter

With few exceptions mud, sandy-mud and muddy-sand bottom sediments in Keppel Bay and Casuarina Creek had TOC:TN molar ratios and ŭ^{13}C signatures that suggested either a phytoplankton and/or bacterial origin for the organic matter (Bird *et al.*, 1995; Gagan *et al.*, 1987; Fukuda *et al.* 1998; Goni *et al.*, 2005). The lack of a strong terrestrial signature for organic matter in Casuarina Creek was initially surprising because abundant mangrove detritus was observed floating in this tidal creek. In addition, Ford *et al.* (2005a) identified soil organic carbon as the principal form of organic matter entering the Fitzroy Estuary, and the TOC, TN and TP concentrations of muddy sediments were within the range of carbon (13 ± 6 mg g^{-1}), nitrogen (0.9 ± 0.5 mg g^{-1}) and phosphorus (0.41 ± 0.25 mg g^{-1}) measurements made on soils from the Fitzroy catchment based on data compiled by Furnas (2003). Despite the above, evidence for a terrestrial organic carbon origin (plant or soil) were strong only in samples 24, 191 and 192 from Casuarina Creek, and in sample 2 from the Fitzroy River (Figure 5.3d). However, it has been frequently observed that a component of terrestrial organic matter (TOM) is replaced in deltas and estuaries by recently formed marine substances, suggesting that terrestrial particles undergo major transitions in surface characteristics, chemistry and microbiology when they meet the sea; after which protective sorption of organic matter may then again be possible (Hedges *et al.*, 1997; Keil *et al.*, 1997; Hedges and Keil, 1999). Even seemingly recalcitrant (highly degraded) organic substances can be de-sorbed from particles and re-mineralised, as has been shown in important Amazon delta studies (Aller *et al.*, 1996).

The organic carbon (and likewise TN) concentrations of Keppel Bay sediments is low compared to most estuarine systems, with TOC concentrations of 4.6 ± 1.7

mg g^{-1} (0.41 ± 0.23%; n = 11) in the mud and sandy-mud sediments decreasing to 0.45 ± 0.47 mg g-1 (0.07 ± 0.09%; n = 70) in the sands. Figure 5.3abc and Table 5.4 shows the amount of carbon and nutrients per Fe surface area equivalent of Keppel Bay sediments is also low compared to those of floodplain sediments (Crescent and Frogmore Lagoons) and soils from the Fitzroy catchment (see also Bostock *et al.*, 2005b).

The discrepancy between the carbon and nutrient concentrations of floodplain and Keppel Bay sediments may be due to several factors i.e. (i) higher biological productivity in the floodplain lagoons; (ii) different sources of sediment to the two environments; and/or (iii) to the mineralization of particulate TOM when the particles enter the marine environment. Although this matter cannot be resolved unequivocally, we highlight that the relationship between nutrients (TN and TP) and Fe in the modern (surface) billabong sediments is similar to that of the vast majority of soil samples from the BB, SB, TFB and NEFB (Figure 5.3ab); the regions that sourced most of sediment to the Fitzroy Estuary (Douglas *et al.*, 2005a) and floodplain (Kuhnen, 2004) in post-European times. Moreover, the organic matter in a sediment core from Crescent Lagoon has been dominated by soil organic matter (not freshwater algae) since shortly after European arrival (~1850), except for during a brief interval (1960-1980) that coincided with the extensive removal of Brigalow vegetation when a mainly terrestrial C3 vegetation signature was observed (Kuhnen, 2004). However, the TOC and nutrient concentrations from below the surface in the Crescent Lagoon core have a stoichiometry with Fe that is closer to that of the Keppel Bay sediments than the billabong surface sediments, even though these down-core billabong sediments were also mainly derived from the BB, SB, TFB and NEFB (Figure 5.3c; Kuhnen, 2004). Therefore, these down-core changes are probably caused by mineralization of the organic matter and the release of nutrients to pore-waters. Likewise, the lower concentrations of TOC and nutrients in Keppel Bay surface sediments compared to the floodplain sediments and (most) catchment soils is probably also due to mineralization of a substantial proportion of the TOM in the marine environment (see for example Keil *et al.*, 1997).

Table 5.4: Sediment TOC and nutrient concentrations per Fe surface area (SA) equivalent of marine sediments and terrestrial soils and sediments, and the net loss of nutrients and TOC from these particles in the marine environment. Estimated annual yields of C, N and P to the estuary (based on these data sets), and annual nutrient and TOC release rates from the particles.

Constituent	Terrestrial source (mg per Fe-SA equivalent)	Marine source (mg per Fe-SA equivalent)	Net loss (mg per Fe-SA equivalent)	Annual catchment yield (Kt yr-1)	Annual release rate (burial/export rate) (Kt yr-1)
TOC[a]	0.43	0.12	0.3 (69.8%)	29.2	19.5 (9.7)
TN[b]	0.06–0.1	0.018	0.042–0.082 (71.3–82.7%)	4.1–6.8	2.9–5.6 (1.2)
TP[a]	0.03	0.009	0.02 (66.7%)	2.0	1.4 (0.6)

a. Calculations are based on slopes of the regression lines through floodplain data in Figure 5.3abc.

b. The range shown represents the mean TN:Fe ratio minus the standard deviation and the mean TN:Fe ratio plus the standard deviation of the floodplain data in Figure 5.3b.

Based on the data presented in Figures 5.3abc and Table 5.4, there is a net loss of 69.8% of the TOC, 66.7% of the P and 71.3–82.7% of the N from the soil particles when they are in the marine environment. These estimates equate to yields of 29.2 Kt yr^{-1} C, 2.9-5.6 Kt yr^{-1} N and 2.0 Kt yr^{-1} P to Keppel Bay, and annual particle release rates of 19.5 Kt yr^{-1} C, 2.0 - 2.8 Kt yr^{-1} N and 1.4 Kt yr^{-1} P, based on extrapolation from the 1.7 Mt yr^{-1} annual sediment yield estimate (1990–2004) of Margvelashvili (personal communication; 29/11/05)[1], and assuming that this fine sediment has an Fe concentration of 40 mg g^{-1} (i.e. the average Fe concentration of the mud and sandy-mud sediments in Keppel Bay). Burial/export rates based on these calculations are roughly 25% of the long-term estimates presented in Table 5.2 and 5.3 (Table 5.4). As mentioned above, the $\check{u}^{13}C$ signatures and TOC:TN ratios of the Keppel Bay sediments (Figure 5.3d) indicate a mainly marine source for the organic matter, and therefore suggest that an apparent replacement of TOM by marine organic substances takes place when terrestrial particles enter seawater. It is also noteworthy, that TOC-Fe, TN-Fe and to a lesser extent TP-Fe stoichiometries changed little with sediment

[1] Loads were derived from a regression between TSS concentrations near the barrage and river flow: TSS = (0.5*River Flow +15)/1000), where TSS units are kg m^3, and units for river flow are m^3 s^{-1}.

burial, based on data from vibracores VCO5, VC13 and VC20 (Figure 5.3abc; Skene *et al.*, 2004; Bostock *et al.*, 2005a). This suggests that carbon and nutrient concentrations are maintained at near refractory values even in the surface sediment. We suggest that labile organic matter is liberated during frequent resuspension and deposition cycles, as the sediments pass through oxic, sub-oxic and anoxic environment in the water column and underlying sediments (Aller *et al.* 1986).

Carbon decomposition and trophic status

The importance of alternating oxic and sub-oxic processes facilitated by mixing in dynamic coastal environments was recognised in foundational work on Amazon Delta sediments (Aller *et al.*, 1986), and underscored in subsequent studies by Aller (1998) and Aller and Blair (2004). Those studies found that sediment mixing and re-working in energetic coastal environments produces an efficient decomposition system characterised by repetitive redox successions (oxic to sub-oxic, temporarily sulfidic), reoxidation and metabolite exchange. Bacteria, rather than macrofauna also often dominate benthic biomass in these energetic coastal sediments (Alongi 1995; Alongi and Robertson, 1995; Aller, 1998) and cannot be ruled out as an important contributor to the sediment organic matter pools of most Keppel Bay sediments, on the basis of TOC:TN ratios and $\check{u}^{13}C$ signatures in Figure 5.3d. A link has also been established between CFA formation and iron oxy-hydroxide reduction in sediment (Heggie *et al.*, 1990), and that Ca-bound P constitutes the largest P-pool in Keppel Bay (Figure 5.4c). There is also some additional evidence for alternating oxic and sub-oxic processes in the decomposition system in Keppel Bay sediments. First of all, in common with Amazon Delta sediments, muddy Keppel Bay sediments share low total sulfur concentrations (TS; <0.1%) and Fe concentrations in the range of 42.8–50.0 mg g^{-1} (0.77–0.9 mmol g^{-1}; Figure 5.1d). Secondly, ferrous iron (Fe^{2+} or FeII) is inversely related to TOC in the system TS-TOC-Fe(II) in Keppel Bay sediments (Figure 5.5b), and the FeII/(TS+TOC+Fe(II)) term and sediment FeII:FeIII and FeII:TOC ratios figured prominently on the second principle component (Table 5.1), which explained 11.1% of the variance in the sediment geochemical data. These parameters may be indicators of the prevalence of iron oxyhydroxide reduction because this sub-oxic reaction consumes carbon (i.e. CH_2O) and releases Fe^{2+} i.e.:

$$4Fe(OH)_3 + \mathbf{CH_2O} + 7H+ = \mathbf{4Fe^{2+}} + HCO_3^- + 10H_2O.$$

Samples with positive loadings on axis 2 of the PCA (Figure 5.5a), with corresponding high values for FeII:FeIII and FeII:TOC ratios (Figure 5.5cd) and FeII/(TS+TOC+Fe(II)), were found in the iron-rich MFR sand and muddy-sand sediments, and especially high values coincided with the western beach fringe

where high wave energy and sediment permeability may allow for extensive oxic diagnesis and regeneration of Fe (and Mn) oxides. Ryan *et al.* (2005) and Brooke *et al.* (2005) also identified the fine sand sediments in this region as being, by far, the best sorted in Keppel Bay. Thirdly, O_2:TCO_2 molar ratios were lower than 1:3 in all eight of the core incubations undertaken in Keppel Bay (Table 5.1), suggesting that more CO_2 was generated than could be accounted for by oxic mineralisation with complete nitrification (Radke *et al.*, 2005c).

The excess CO_2 flux that could not be explained by sediment oxygen uptake, accounted for 0–70% of the total CO_2 flux across the eight core incubations (Table 5.1). Interestingly, O_2 consumption by sediment was inversely proportional to sediment Si concentrations (indicative of higher relative sand and primary mineral contents; Figure 5.6a), while the excess CO_2 flux correlated linearly with sediment TS:FeII ratios (potentially indicative of a greater contribution to organic matter degradation by sulfate reduction; Figure 5.6b). By extrapolation of these calibrations to the whole of Keppel Bay[2] we derive an annual carbon decomposition rate of 10 100 tonnes per year under non-flood conditions, of which more than 50% is due to non-oxic processes (including iron- and sulfate reduction).

[2] These calculations represent integrations based on interpolations of measurements made at the different station locations using SURFER 7.

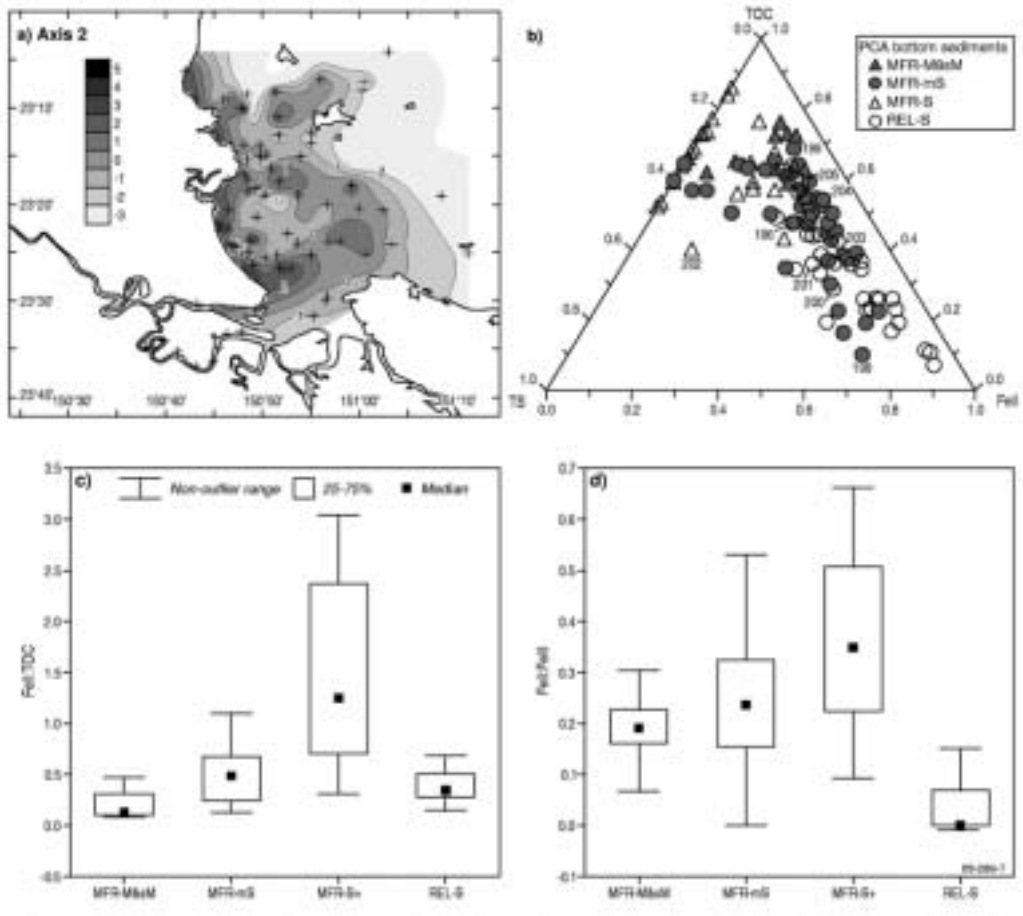

Figure 5.5: (a) Map showing the distribution of site scores for axis 2 of the bottom sediment PCA. (b) Trilinear diagrams showing the relative amounts of sulfur (TS), total organic carbon (TOC) and ferrous iron (FeII) for the different grain size classes in Keppel Bay; (c) FeII:TOC ratios against the different grain size classes and (d) and FeII:FeIII ratios against the different grain size classes.

Alongi and McKinnon (2005) found a near 1:1 relationship between the flux of carbon to the seabed (indicative of gross primary production) and organic carbon mineralisation rates in the coastal zone of the GBR shelf. If we assume the same relationship holds in Keppel Bay, then in the order of 10 000 tonnes of carbon are fixed annually under non-flood conditions. Based on the same criteria, we can also suggest that oligotrophic conditions prevailed throughout Keppel Bay during the August 2004 dry season (i.e. <48 mmol CO_2 m^{-2} d^{-1} in the classification scheme of Eyre and Ferguson (2002)).

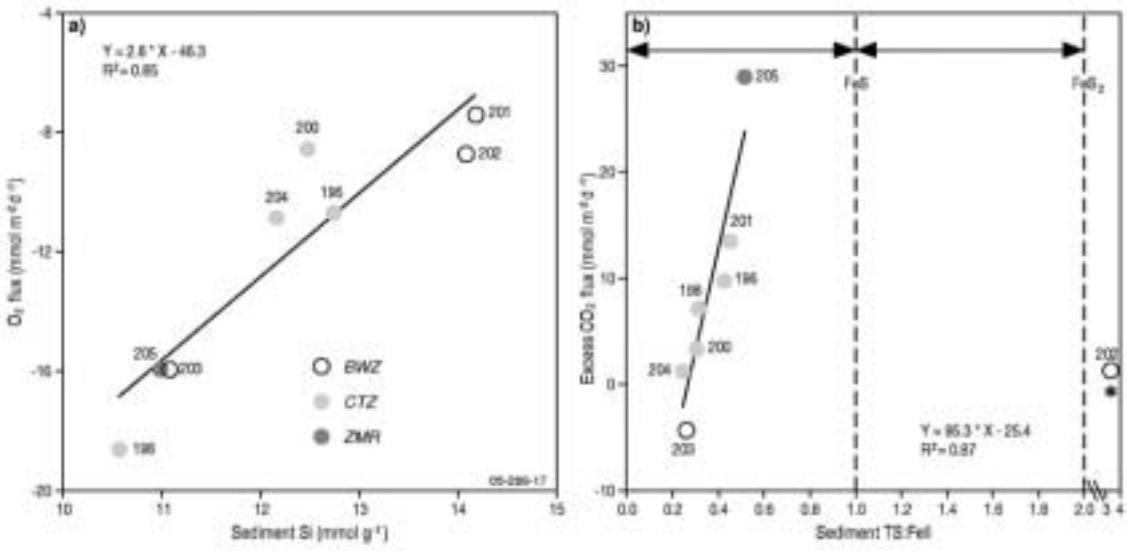

Figure 5.6: Sediment O_2 flux versus Si concentrations of sediment (note inverse O_2 scale); (b) Excess CO_2 flux vs. TS:FeII ratio of sediment. In both plots, negative fluxes imply uptake by sediment. Sample 202 was not included in the calibration equation in (b) because the FeII concentrations of these samples were very close to the error estimate for the FeII analyses.

*Table 5.5: Nutrient, O_2 and CO_2 flux determinations from the core incubation and bottle incubation experiments. Note negative fluxes imply uptake by sediment and positive fluxes imply release from sediment. *denotes measurements that were within the limits of analytical uncertainty.*

Core Inc sample #	O_2 flux (mmol/m^2/d)	CO_2 (mmol/m^2/d)	N as N_2 (mmol/m^2/d)	NH_4 Flux (mM/m^2/d)	FRP flux (mM/m^2/d)	NO_X flux (mM/m^2/d)	SiO_4 (mM/m^2/d)
196	-10.7	18.1	-1.2	-0.40	-0.02	0.2	0.2
198	-18.5	21.3	-2.0	-0.05	-0.01	0.0	0.1
200	-8.5	9.9	-0.4	-0.04	0.02	0.0	0.2*
201	-7.5	19.3	0.7	-0.45	-0.01	-0.1	0.5
202	-8.7	8.0	1.6	-0.94	-0.08	0.0	0.0*
203	-15.0	31.2	0.2	-0.12	0.01	0.0	0.4
204	-10.9	9.8	-0.9	N/A	N/A	N/A	N/A
205	-15.9	41.2	-3.5	N/A	N/A	N/A	N/A
Bottle Inc #	O_2 flux (μmol g^{-1}d^{-1})	DOP flux (μmol g^{-1}d^{-1})	DON flux (μmol g^{-1}d^{-1})	NH_4 flux (μmol g^{-1}d^{-1})	FRP flux (μmol g^{-1}d^{-1})	NO_X flux (μmol g^{-1}d^{-1})	SiO_4 (μmol g^{-1}d^{-1})
229	-640	-0.71	-14.1	14.1	-0.71	-3.9	0

Nitrogen fixation and the role of iron

An unexpected result from the August 2004 survey of Keppel Bay, was that a net uptake of N_2 (as well as NH_3) by sediment was observed in several of the core incubation experiments (Table 5.5). This result was surprising because this evidence for nitrogen-fixation was observed under dark conditions, and in situations where we would have anticipated net denitrification to be occurring; for example, in the resuspension zone (e.g. sample 205) where efficient nitrification was raised as a potential explanation for low NH_3 concentrations (Radke *et al.*, 2005c). A striking correlation between N_2-N fluxes and the ferric iron concentration of the underlying sediment was also observed (Figure 5.7a), and lends further support to the occurrence of nitrogen fixation under dark conditions. This is because nitrogen fixation is arguably the most iron-expensive process within phytoplankton because the two major sub-units of the nitrogenase enzyme collectively contain 32–36 iron atoms, and it now known that iron limits primary productivity in high-nutrient, low chlorophyll (HNLC) oceanic areas (Hutchins, 1995; Kustka *et al.*, 2002; Wilhelm, 1995). Evidently, several species of marine cyanobacteria (including *Synechococcus* spp.) can fix nitrogen in the dark, due to a temporal separation of nitrogen fixation and photosynthesis within a cell cycle (Mitsui *et al.*, 1986; Zehr *et al.*, 2000). As reviewed by Kustka *et al.* (2002): (i) night time N_2-fixing ability could allow for a more efficient use of cellular iron due to the potential for iron recycling associated within the diel cycle of degradation and synthesis of nitrogenase; and (ii) the temporal decoupling of N_2 and C fixation could reduce the redundancy of certain iron-containing catalysts.

It is worth mentioning that unicellular diazotrophic (N-fixing) bacteria, both heterotrophs (i.e. that feed on pre-formed carbon) and autotrophs, were recently discovered in the pelagic pico-phytoplankton and nano-phytoplankton in the subtropical North Pacific Ocean (Zehr *et al.*, 2001), and these organisms can fix nitrogen at very high rates (Montoya *et al.*, 2004). The heterotrophic diazotrophs also require an order of magnitude more iron than other heterotrophic species (Kustka *et al.*, 2002). The ability of heterotrophic bacteria to acquire from the N_2 pool the nitrogen they require to metabolise organic matter, would reduce competition with phytoplankton for scarce nitrogen under nitrogen-limiting conditions. Genetic sequences (nifH) indicative of a group of diazotrophs with phylogenetic affinities to N_2-fixing sulfate reducing bacteria have recently been found in nitrogen-rich sediments of Chesapeake Bay and the Neuse River (Burns *et al.*, 2002), and nitrogen-fixing microbial (gene) assemblages were also found to vary along a salinity gradient in the Neuse River Estuary (Affourit *et al.*, 2001). Clearly, nitrogen-fixing bacteria (heterotrophs and autotrophs) occupy a plethora of specialised niches allowing N-fixation to occur over a wide-range of environmental conditions. By extrapolation of the N_2 calibration to the whole of

Keppel Bay (Figure 5.7b) we arrive at annual “dark” nitrogen fixation rates of 5070 tonnes N per year and annual denitrification rates of 4120 tonnes N per year. These estimates, which approximately cancel each other, are of a similar magnitude to the catchment N inputs.

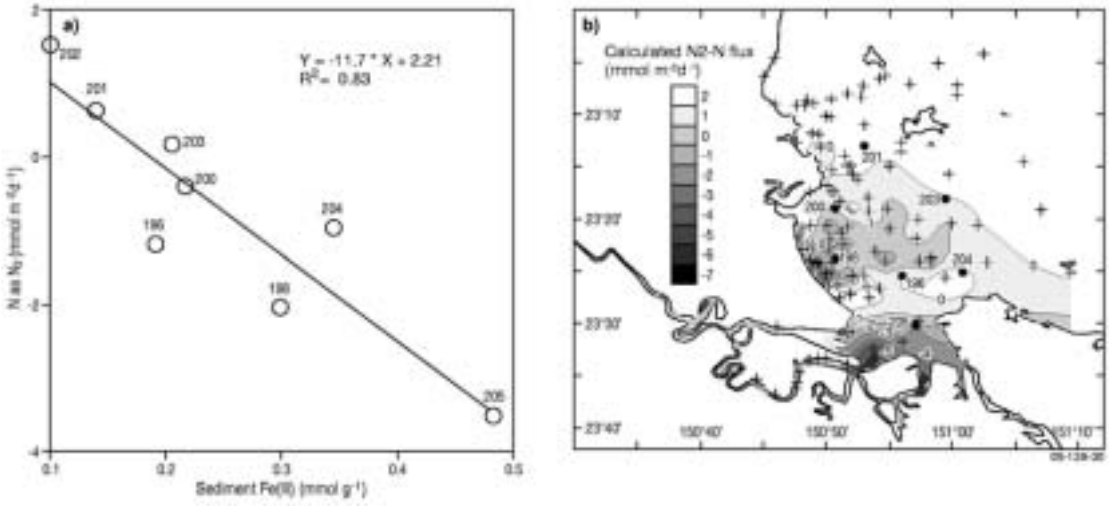

*Figure 5.7: (a) N_2 as N flux versus ferric iron (FeIII) concentrations of the underlying sediment (negative N_2 fluxes imply uptake by sediment); and (b) distribution of calculated N as N_2 fluxes in Keppel Bay based on the calibration in (a) i.e. N as N_2 = -11.7*FeIII +2.2.*

Water column nutrient dynamics: mixing diagrams, maps, nutrient-TSM relationships and pool sizes

Mixing diagrams, or property-salinity plots, provide useful information on nutrient inputs, sinks and degree of conservative behaviour in estuaries (Eyre, 2000; Devlin *et al.*, 2001; Devlin and Brodie, 2005). When changes in nutrient concentration are caused only by dilution associated with the mixing of freshwater with seawater, nutrients tend to conform to linear trendlines between end-members and are said to mix conservatively. Salinity is the conservative component of seawater, which typically has lower concentrations of nutrients than inflowing freshwater. The most distinguishing feature of the salinity distributions during the dry season surveys were the zones of elevated salinities in Casuarina Creek and along the shallow (<5 m) western shore of Long Beach (36.5 to 38.9 PSU; Chapter 3), where evaporation had the effect of concentrating dissolved salts (this is explained in more detail in Chapters 3 and 6). Elsewhere in Keppel Bay, salinity ranged from 36.1 to 36.4 PSUs. By comparison, during the wet season survey there was a clear gradient of increasing salinity away from the estuary and tidal creeks toward the bay (Chapter 3). The lowest salinity measured during this survey was 14.8 PSUs, in the Fitzroy River, not far from its

mouth. Maps showing the distribution of the various forms of nutrients during the dry season and wet season surveys are shown in Figures 5.8–5.11 and 5.15–5.16 respectively. Mixing plots for the dry season and wet season data sets (dissolved nutrients only) are presented in Figures 5.12 and 5.15 respectively.

Dry season water column nutrient dynamics

Reverse salinity gradients were apparent in the mixing diagrams of both dry season data sets (Figure 5.12); that is the highest nutrient concentrations were observed at the highest salinity levels. Although the slopes of nutrients with respect to salinity were basically the same between the two years, salinity levels were nearly 1 PSU higher in August 2004 than in September 2003. Whether this discrepancy is due to continued evaporation and a lack of freshwater input between September 2003 and August 2004 or to a calibration/instrument error is currently under investigation. There is some evidence that both data sets may be valid i.e.: (i) the mixing line for the September 2003 data could be extended through the annual mean data set (includes means and means ± SE) of Furnas and Brodie (1996) for southern GBR waters inclusive of inner and outer Pompey and Swains Reefs; and (ii) there was only a minor off-set (~0.2 PSU) between the YSI666 salinity data collected by Geoscience Australia and the Seabird salinity data collected by CSIRO Land & Water during August 2004.

During the dry season surveys, TP concentrations ranged from 0.4 to 0.14 mg L^{-1} in the Fitzroy Estuary and from 0.03 to 0.43 mg L^{-1} in Casuarina Creek, and were <0.02 mg L^{-1} over most of Keppel Bay (Radke *et al.*, 2005c). Similarly, TN concentrations were <0.2 mg L^{-1} over most of Keppel Bay, and were considerably higher in the Fitzroy Estuary (0.18 to 0.81 mg L^{-1}) and Casuarina Creek (0.17 to 0.73 mg L^{-1}) (Radke *et al.*, 2005c). Particulate nutrients and dissolved inorganic nutrients were also found at highest concentrations in the estuary (FigureS 5.8 and 5.9), near its mouth and in Casuarina Creek, and with the exception of silicate, were below detection over most of Keppel Bay (Figure 5.10). In comparison, dissolved organic nutrients were measured throughout most of the study area, but there was a seaward decrease in concentrations (Figures 5.11). Most of the NO_X, FRP and SiO_4 data within Casuarina Creek, and just beyond it, adhered to linear relationships suggesting that conservative dilution is an important control on the concentrations of these nutrients in the southwest region of Keppel Bay (Figure 5.12abcd). Elsewhere in Keppel Bay, the behaviour of these nutrients was either non-conservative or they were below detection limits, suggesting biological utilisation in both cases. A wider availability of iron (due to proximity to the catchment source) may account for the greater utilisation of nutrients in Keppel Bay proper compared to the representative GBR waters (Furnas and Brodie, 1996; but see also Devlin *et al.*, 2001). In

comparison, continual resuspension of the surface layer and high levels of TSM interfered with nutrient uptake by phytoplankton near the mouth of the estuary and within Casuarina Creek. As a consequence, a proportion of the dissolved nutrient load was exported from this region to greater Keppel Bay with the ebbing tide (see also Chapter 6), and there were strong numerical relationships between TSM in this high turbidity zone.

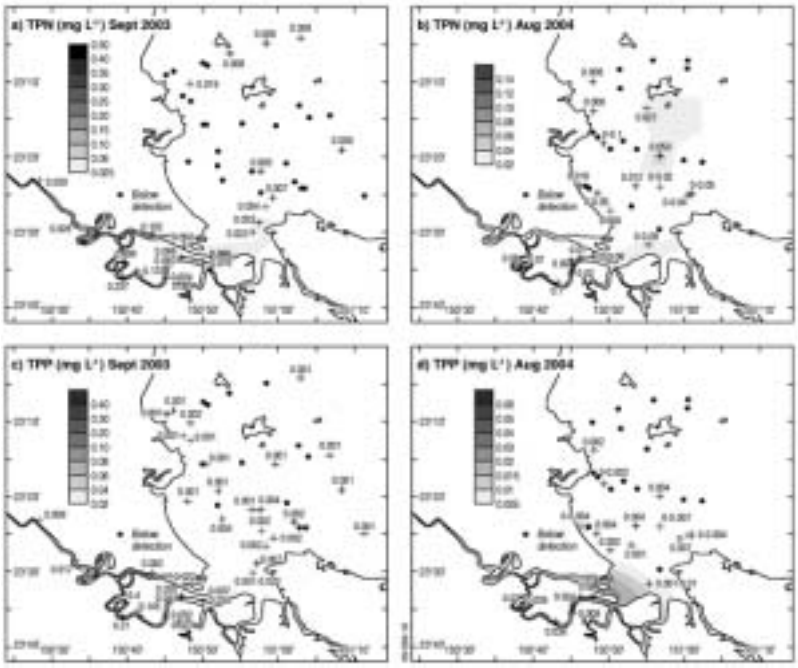

Figure 5.8: Maps showing the distributions of TPN (a & b) and TPP (c & d) during the dry season surveys.

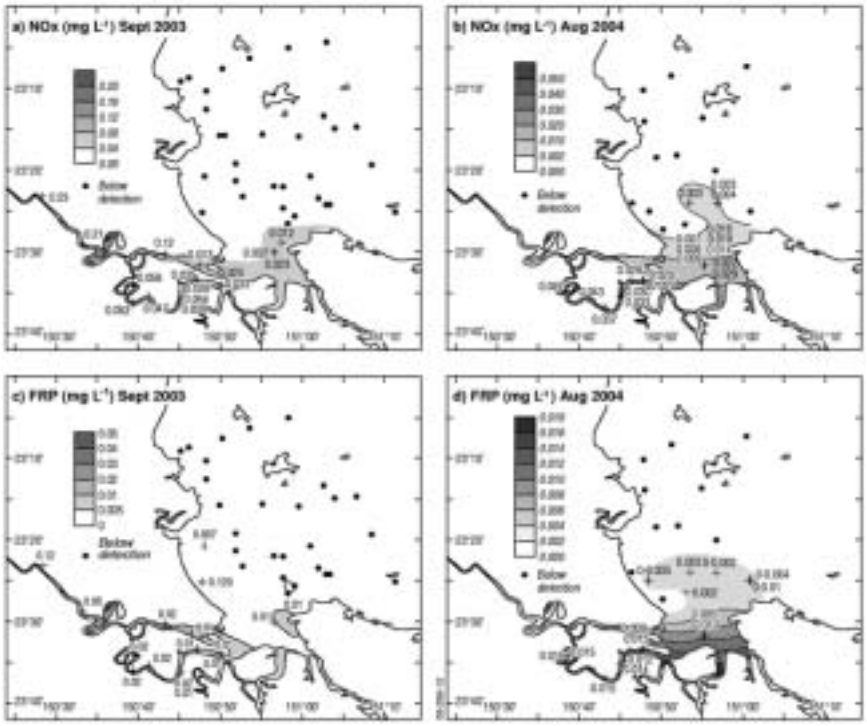

Figure 5.9: Maps showing the distributions of NO_X (a & b) and FRP (c & d) during the dry season surveys.

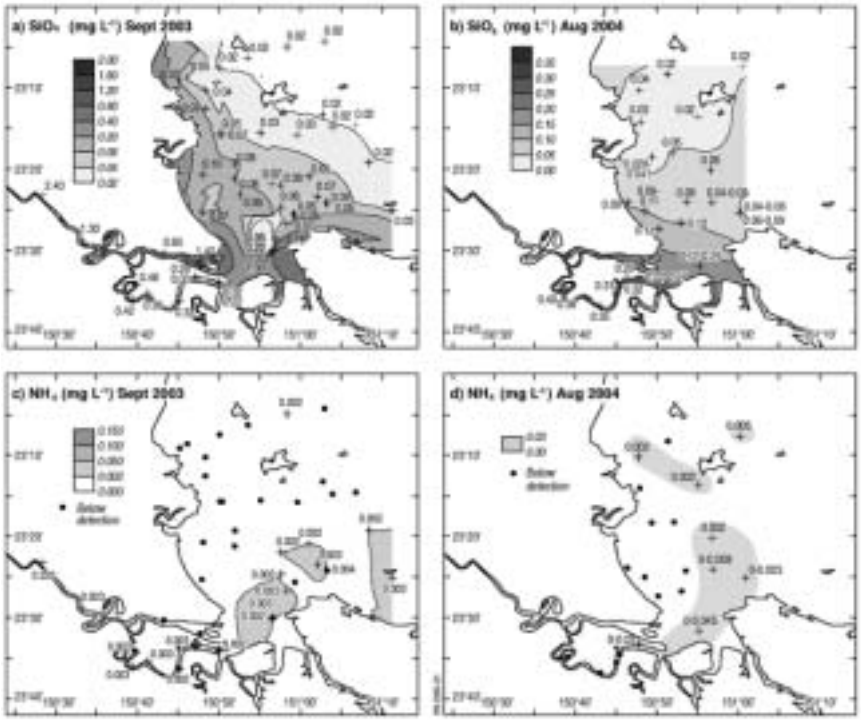

Figure 5.10: Maps showing the distributions of SiO_4 (a & b) and NH_4 (c & d) during the dry season surveys.

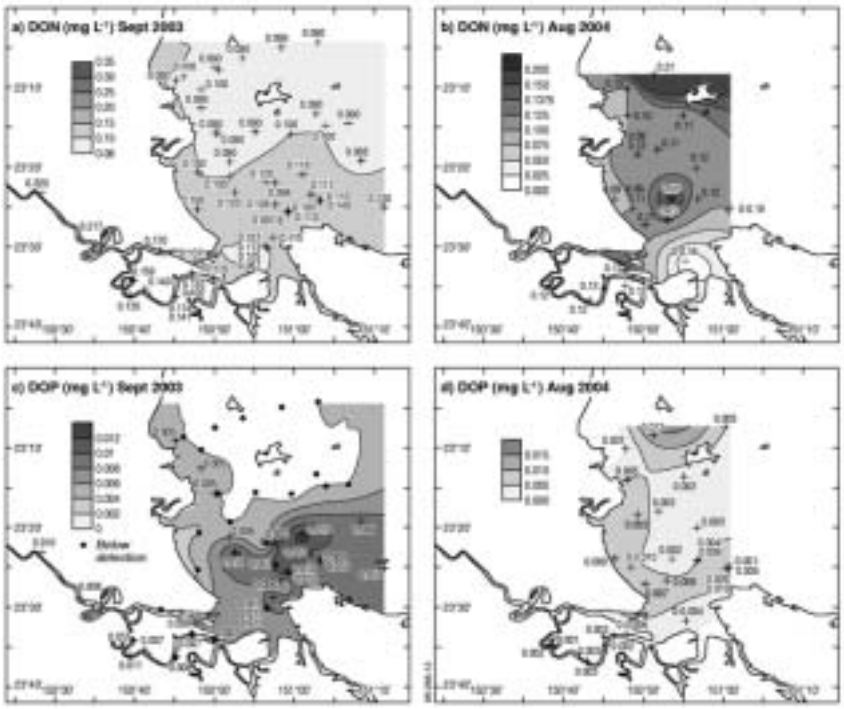

Figure 5.11: Maps showing the distributions of DON (a & b) and DOP (c & d) during the dry season surveys.

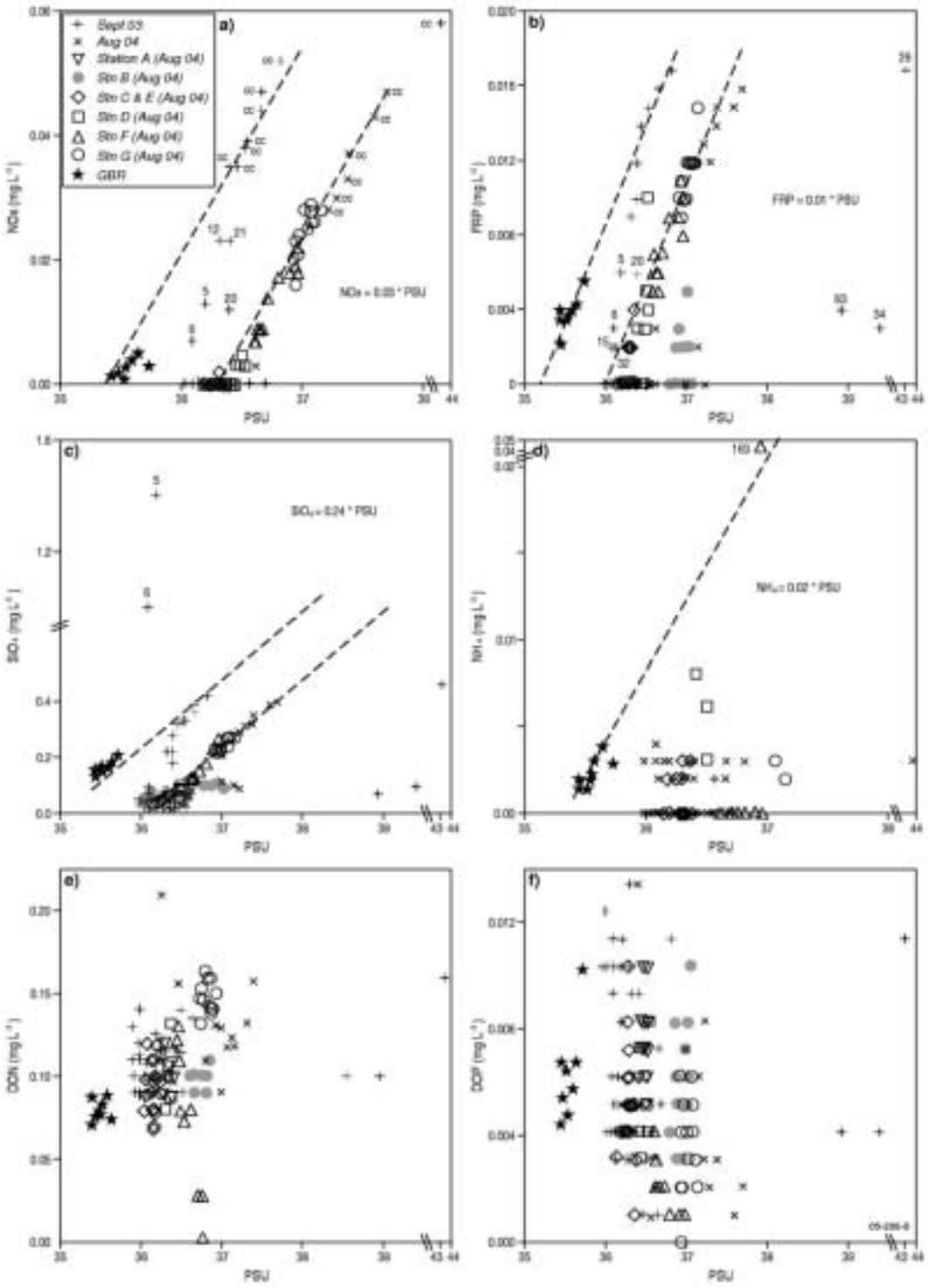

Figure 5.12: Mixing diagrams (nutrients vs. PSU) for the dry season data sets. Representative data for the inner and outer Pompey and Swains Reefs (includes means and means ± SE; Furnas and Brodie, 1996) are also shown.

NO_X correlated linearly to TSM in September 2003 (NO_X = 0.00025 * TSM + 0.007; Figure 5.13a), when higher turbidity levels were observed in Casuarina Creek. In comparison, the relationship between FRP and TSM could be

described with a logarithmic function of the form: FRP = 0.003 * ln TSM – 0.003 (R^2 = 0.89; Figure 5.13b). Indeed, the shape of the FRP vs. TSM relationship resembles a Langmuir isotherm for phosphorus adsorption which reflects the phosphate buffer mechanism of Froelich (1988), whereby the partially reversible adsorption of phosphate onto bottom and suspended sediment maintains phosphate concentrations in water columns, usually in a range from 0.019 to 0.043 mg L^{-1} for estuaries (see review of literature in Eyre, 1994). Under these dry season conditions, sources of dissolved nutrients include: (i) the sewage treatment plant and meatworks in the Fitzroy River; (ii) the diagenesis of phytoplankton, including those washed from the mud banks of the Fitzroy River and tidal creeks (Ford *et al.*, 2005b; Chapter 6); and (iii) the mineralisation of particulate organic matter (including soil/sediment particles) pumped into the creeks during flood tides or deposited in the estuary during flood events. These particulate nutrients dominated nutrient pools in the tidal creek and southwest Keppel Bay at the time of the dry season surveys, and their concentrations were linearly correlated with TSM, as expected (Figure 5.13cd). The concentrations of particulate (and dissolved inorganic) nutrients were higher in this region during September 2003 when the survey coincided with spring-tide conditions, than during August 2004 when the survey coincided with neap tide conditions (Chapter 2), due to the higher tidal velocities.

Interestingly, DON and DOP did not behave conservatively at any station, and in some cases these concentrations declined to below detectable limits (Figure 5.12ef). At Stn F, the station with the third highest photosynthetic N uptake (Chapter 7), DON concentrations decreased to below detection in Redfield stoichiometric proportion to chlorophyll production in the passing water mass (Figure 5.14b). Based on the above evidence, it is possible that phytoplankton were directly utilising components of the DON pool for their N nutrition (Berman and Bronk 2003; Zehr and Ward, 2002). DON comprises a variety of compounds that can differ markedly in terms of their bioavailabilities and molecular weights: from highly bio-available (low TOC:TN) compounds like urea and amino acids, to largely refractory (high TOC:TN) poly-phenolic compounds (McCarthy *et al.*, 1997; Seitzinger *et al.*, 2002; Berman and Bronk, 2003). As nitrogen loss from forests unaffected by humans is mainly via DON (Lewis *et al.*, 1999; Harris, 2001; Perakis and Hedin, 2002), it is not surprising that at least some algal species would evolve mechanisms for direct DON acquisition. Apparently, the affinity of algae for organic compounds is most pronounced in highly turbid environments where it may be comparable to that of heterotrophic bacteria (Berg *et al.*, 1997). In the context of Keppel Bay, potential sources of DON at the times of the surveys were leachates from mangrove detritus and soils, and exudates

from phytoplankton. Notably, Smith (2004) measured DON fluxes from intertidal mud-bank sediments to the Fitzroy River ranging from 0.02–0.41 mg m^{-2} d^{-1}.

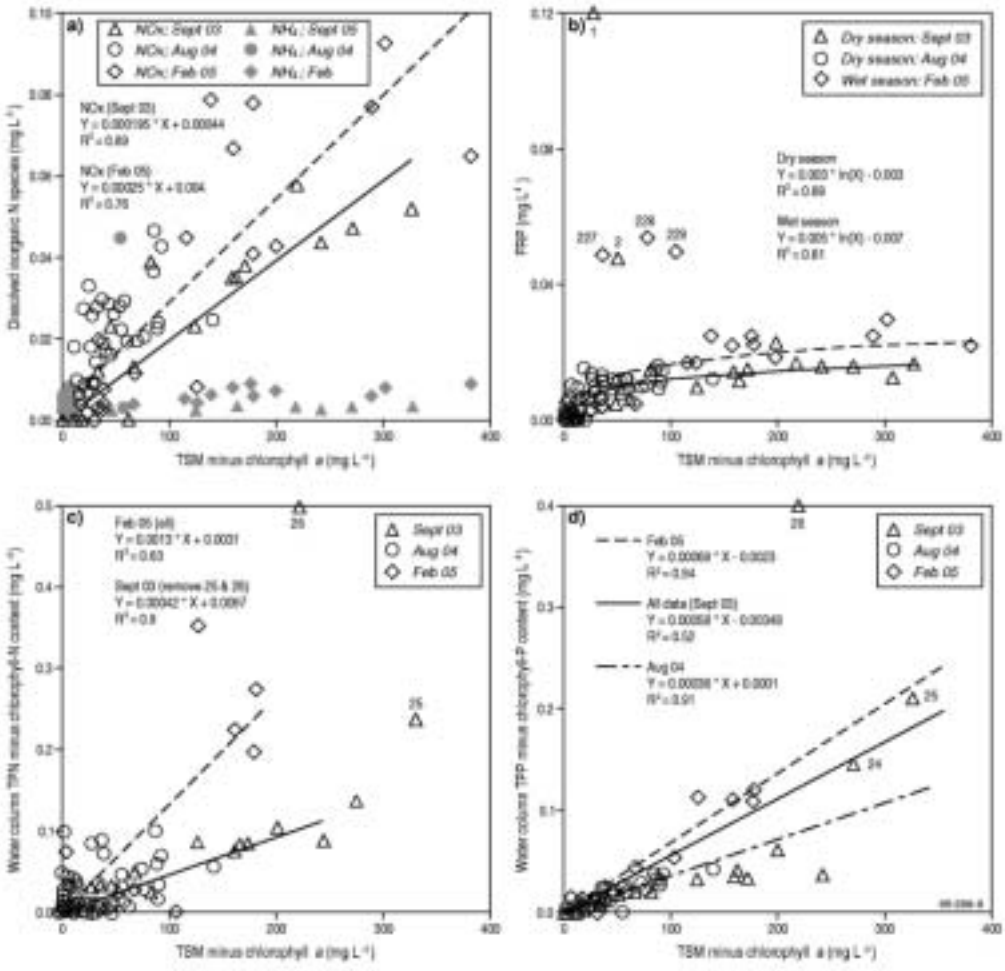

Figure 5.13: Cross plots of TSM vs.: (a) dissolved inorganic nitrogen species; (b) FRP; (c) TPN and (d) TPP for both dry and wet season surveys.

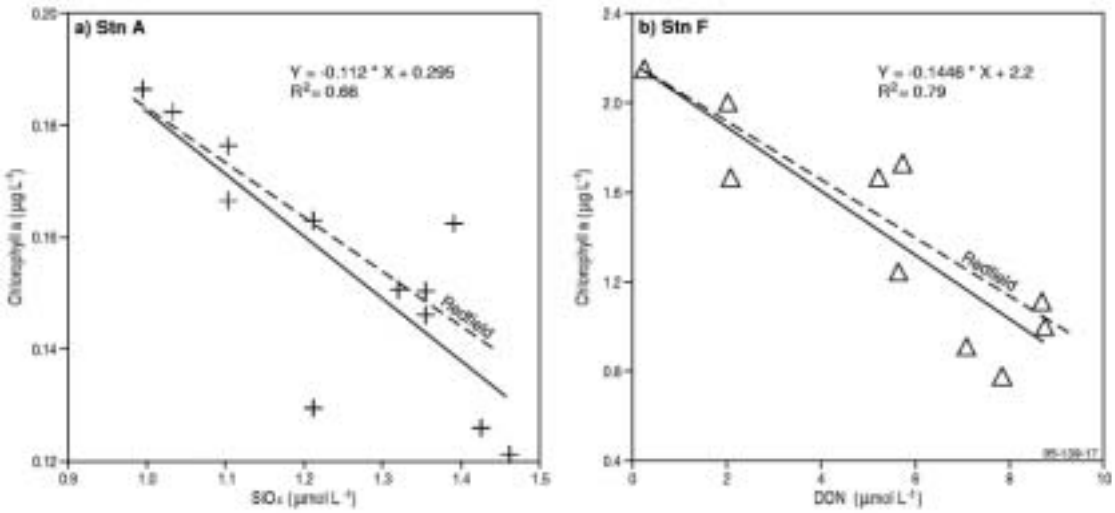

Figure 5.14: August 2004 chlorophyll a *versus (a) SiO_4 (Station A); and (b) DON (Station F).*

Wet season water column nutrient dynamics

Nutrient concentrations were generally higher during the wet season than the dry season (Figure 5.13). During the wet season survey, TP concentrations ranged from 0.075 to 0.094 mg L^{-1} in the Fitzroy Estuary and from 0.13 to 0.14 mg L^{-1} in the tidal creeks, and were <0.03 mg L^{-1} over most of Keppel Bay (Figure 5.15b). Similarly, TN concentrations were <0.3 mg L^{-1} over most of Keppel Bay, and were considerably higher in the Fitzroy Estuary (0.55 to 0.79 mg L^{-1}) and tidal creeks (0.72 to 0.73 mg L^{-1}) (Figure 5.15a). Particulate nutrients and dissolved inorganic nutrients were also found at highest concentrations in the estuary, near its mouth and in the tidal creeks, and with the exception of silicate, were below detection over most of Keppel Bay (Figure 5.15abcf and 5.16cd). In comparison, dissolved organic nutrients were measured throughout most of the study area, but there was a seaward decline in these concentrations (Figures 5.15ef).

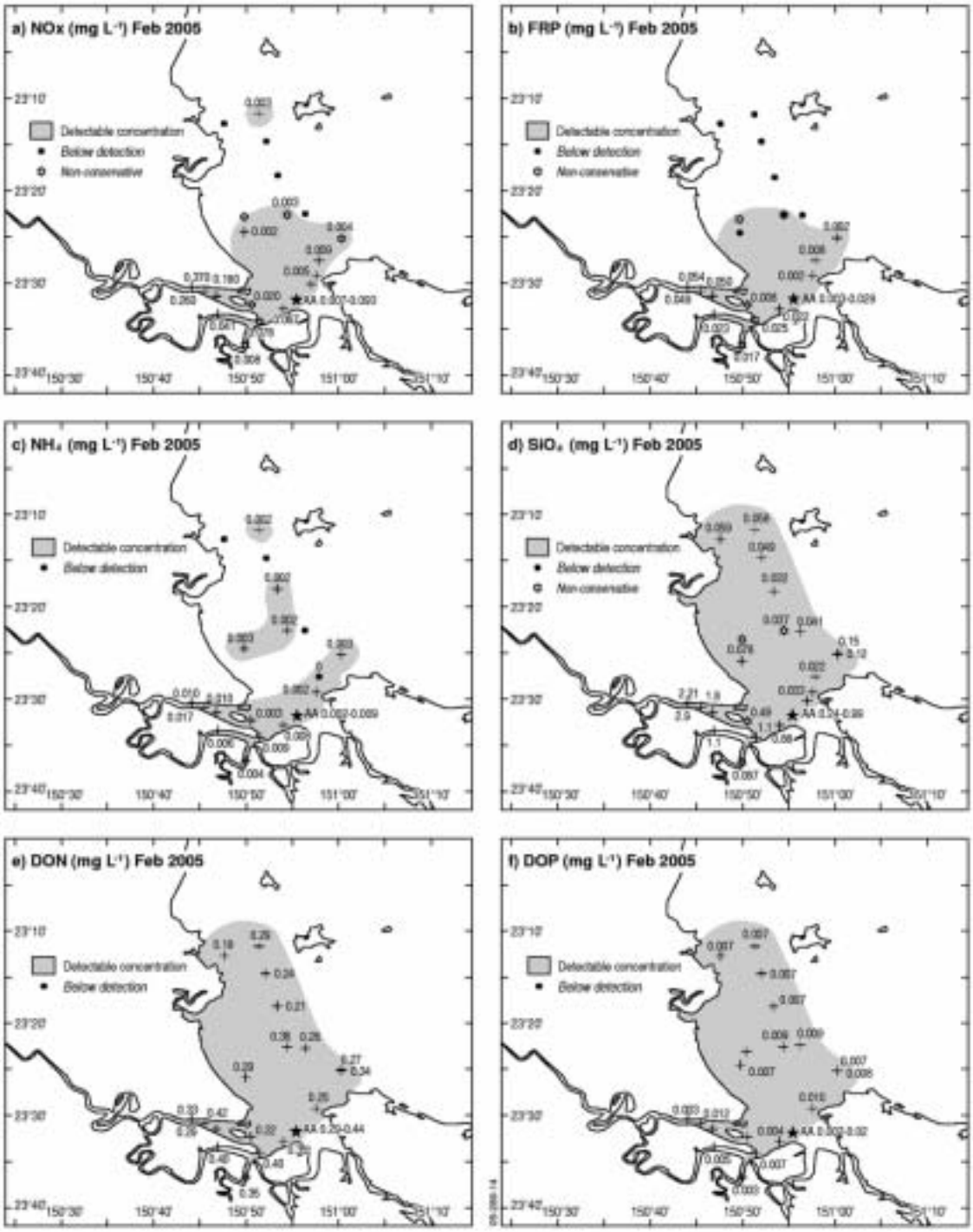

Figure 5.15: Maps showing the distributions of NO_X, FRP, NH_4, SiO_4, DON and DOP during the wet season survey.

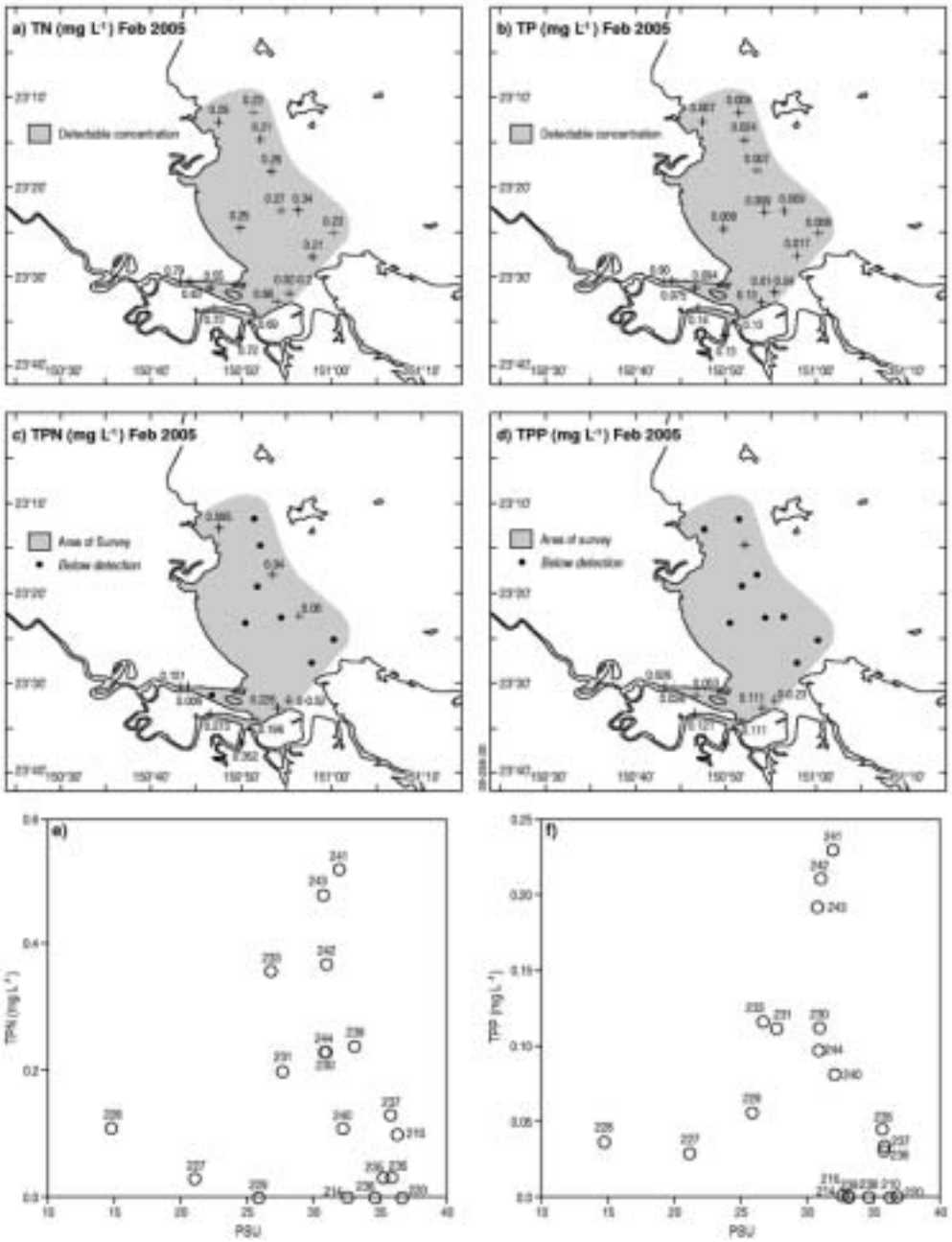

Figure 5.16: Maps showing the distributions of TN, TP, TPN and TPP during the wet season survey (a-d). Mixing diagrams of particulate nutrients vs. PSU are also shown in e & f.

K

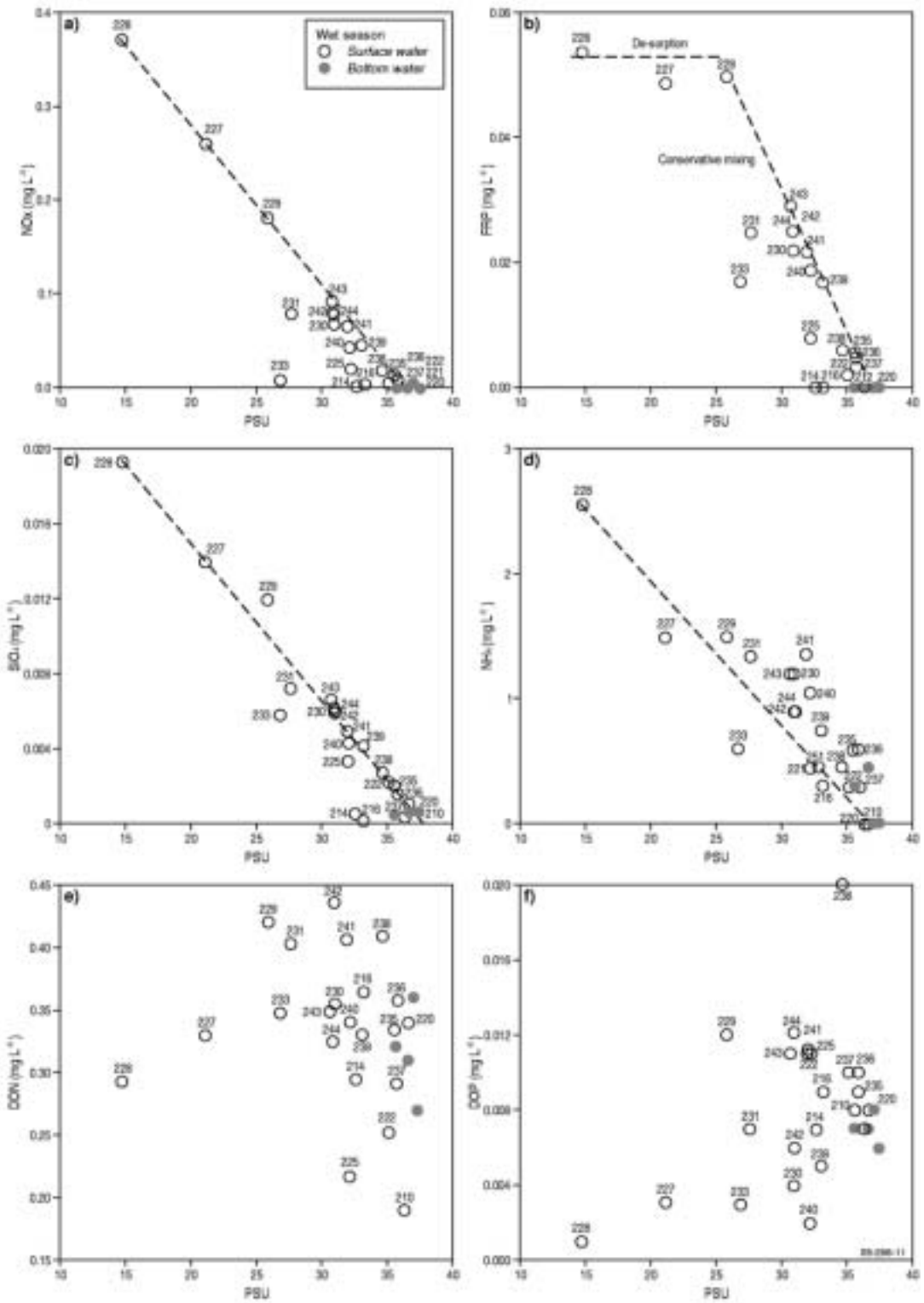

Figure 5.17: Mixing diagrams (dissolved nutrients vs. PSU) for the wet season data.

Mixing diagrams for the wet season survey differed from those of the dry season in the respect that normal salinity gradients were apparent in the data, with generally higher nutrient concentrations in the lower salinity waters (Figure 5.17). These low-salinity waters formed a distinct flood plume in the Fitzroy Estuary (Chapter 3), and were a source of NO_X, FRP, SiO_4 and NH_4 to Keppel Bay. TN entered Keppel Bay mainly as DON, NO_X and TPN with considerably lower concentrations of NH_4. The NO_X concentrations were higher at a given TSM level than during the dry seasons (Figure 5.13a), and together with SiO_4, adhered mainly to linear relationships with PSU suggesting that conservative dilution was an important control on the concentrations of these nutrients as they mixed outward into Keppel Bay (Figure 5.17ac). Non-conservative behaviour of NO_X and SiO_4 was evident in only a small number of samples and these were collected mainly near the mouths of the estuary and tidal creeks (Figure 5.17ac). DON concentrations in Keppel Bay were about twice as high as they were in the dry seasons, and the pattern with salinity was equally complex (see range of concentrations in Figure 5.17e compared to 5.12e). DON concentrations were constant with salinity in the Fitzroy Estuary between PSU levels of roughly 15 and 26, and were at the highest concentrations at sites 229, 231 and Stn AA (sites 238, 241 & 242) which were located at the mouth of estuary and tidal creeks in deltaic sediments (Figure 5.17e). The DON pattern with salinity can probably best be explained by decomposition of TPN in the deltaic region. On the basis of Figure 5.3abc it was estimated that ~70–80% of particle-bound N is released from terrestrial particles while in seawater (Table 5.4). It is also worth mentioning that an equivalent transfer of DON to NH_4 (1 mg g^{-1} day^{-1}; Table 5.5) was observed in the bottle incubation experiment undertaken on sample 229 collected in the mouth of the Fitzroy Estuary, and that studies have shown that heterotrophic bacteria can utilise DIN (including ammonia) and DON (especially dissolved free amino acids), while also simultaneously excreting NH_4 (Kirchman 2000; see also Palenik and Morel, 1990).

TP entered Keppel Bay in near equal concentrations of TPP and FRP, while DOP concentrations were generally low. However, while TPP concentrations increased with PSU in Keppel Bay near the mouth of the estuary and tidal creeks due to tidal resuspension (Figure 5.16f), FRP concentrations decreased with PSU over the same region (Figure 5.17b), and most often conservatively. The near constant FRP concentrations in the Fitzroy Estuary, at salinity levels from ~15 to 26 PSU suggests that FRP was liberated to the water column by desorption with the rise in pH that likely accompanied the mixing of flood waters into Keppel Bay. As with dry season situation, FRP concentrations increased logarithmically with TSM in Keppel Bay, albeit at slightly higher concentrations (Figure 5.13b).

Water column nutrient pool sizes

Estimated pool sizes of total, dissolved and particulate nutrients in the water column of Keppel Bay are presented in Table 5.6. These pool sizes were derived by integrating the interpolated data based on measurements (Figures 5.8–5.11 and 5.15–5.16) within the prescribed polygon area used to calculate freshwater volumes in Chapter 3. Interestingly, with the exception of DOP, TPN, SiO_4 and to a lesser extent the TP data, the measurements were remarkably consistent between the two dry season surveys. This suggests that, with respect to most nutrients, the observed conditions were generally representative for the end of the dry season. The smaller DOP pool and larger TPN in August 2004 compared to September 2003 may be due to higher rates of nitrogen fixation. However, the TPN data should be interpreted with caution due to potentially large errors. The February 2005 pool sizes confirm that nutrient concentrations were higher during the wet season, in the area of freshwater influence.

Table 5.6: Water column pool sizes of total, dissolved and particulate nutrients during the different surveys based on the integration of interpolated measurements (note that large error may be associated with the particulate nutrient concentrations)

Species	Sept 2003 (tonnes year^{-1})	Aug 2004 (tonnes year^{-1})	Feb 2005 (tonnes year^{-1})
TP	102	71	178
TPP*	33	28	130
DIP	13	12	25
DOP	59	32	64
TN	936	1117	2487
TPN*	77	218	452
DIN	27	30	101
DON	856	877	2210
SiO_4	1287	568	1212

Zonation of Keppel Bay based on biogeochemical data: a low-flow perspective

Based on the results of this study, Keppel Bay can be divided into three biogeochemical zones: (i) the Zone of Maximum Resuspension (ZMR); (ii) the Blue Water Zone (BWZ); and the (iii) Coastal Transitional Zone (CTZ). The discrimination of these zones was based on the nature of the underlying sediment, TSM levels and on behaviour of dissolved inorganic nutrients in the dry season mixing diagrams (Figure 5.18a). The phytoplankton size composition data of Oubelkheir (in prep), as inferred from HPLC analysis of particulate

pigments, was also taken in to account, and of all the water column variables in the data set, was found to correlate best with the percentage P in organic forms (i.e. %DOP-P; Figure 5.18bc). A more detailed account of the different pigments found and there inter-annual variability is provided in Chapter 7. The ZMR was defined on the basis of the conservative behaviour of nutrients (due to light limitation) and the predominance of mud and sand-mud bottom sediment derived from the modern Fitzroy River. It is located in southern Keppel Bay, near the mouth of the estuary and extending into the tidal creeks. The 40 mg L^{-1} TSM contour and the -6.0 contour from the bottom sediment PCA (Figure 5.18a) were used to define the seaward extent of this zone (Figure 5.18d). The BWZ is the region overlying mainly relict sand sediments (REL-S) where dissolved inorganic nutrient concentrations were never above detectable limits. The southern boundary of the zone is defined by a combination of the 2.5 mg L^{-1} TSM contour and the -2.0 contour on the bottom sediment PCA. As the name in implies, the CTZ is a transitional area, and it is found between the ZMR and BWZ end-members. Summary physical, biogeochemical and ecological data from the water column and bottom sediment of the different zones are provided in Table 5.7.

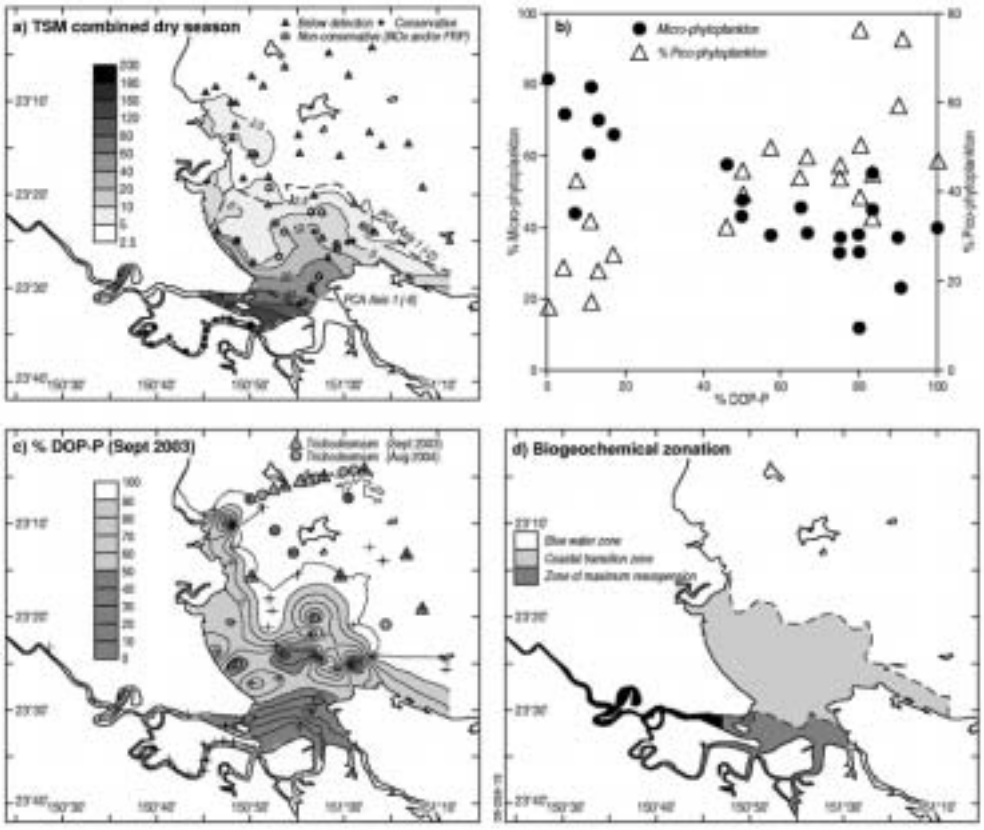

Figure 5.18: Some features used to differentiate Keppel Bay into three zones. (a) TSM map for Keppel Bay based on data from both dry season surveys with overlays of nutrient behaviour (conservative, non-conservative and below detection) as discriminated from the dry season mixing diagrams. The -2 and -6 contours from the sediment PCA diagram are also shown (Figure 5.1c). (b) %micro-phytoplankton and % pico-phytoplankton vs. the percentage of phosphorus in organic forms (September 2003 data only) and a map showing the percentage of phosphorus in organic forms in Keppel Bay also from September 2003 (c). (d) Zonation of Keppel Bay based on the combined TSM 2.5 and 40 mg L^{-1} contours and the -2 and -6 contours from the bottom sediment PCA.

Table 5.7: Some summary physical, biogeochemical and ecological characteristics of the water column and bottom sediments of the Zone of Maximum Resuspension, the Coastal Transitional Zone and the Blue Water Zone. BD refers to nutrients that were below detection (<0.002 mg L^{-1}).

Variable	**Zone of Maximum Resuspension**	**Coastal Transition Zone**	***Blue Water Zone***
Water Column Nutrients and TSM (medians; 25th-75th percentile range; minimum - maximum)			
Dissolved inorganic nutrient behaviour	conservative	non-conservative	*below detection*
Main limiting factor to primary production	Light	Nitrogen	*Phosphorus*
TSM (mg L^{-1})	56.3; 32.5–89.8; 13–326	4.4; 2.6–9.0; 0.8–45.6	*0.9; 0.6–1.7; 0.1–4.5*
TN (mg L^{-1})	0.2; 0.17–0.24; 0.1–0.73	0.12; 0.105–0.13; BD–0.19	*0.1; 0.09–0.12; 0.08–0.36*
TP (mg L^{-1})	0.037; 0.024–0.053; 0.01–0.43	0.009; 0.007–0.011; 0.004 –0.041	*0.006; 0.004–0.008; BD–0.015*
NO_X (mg L^{-1})	0.026; 0.018–0.035; 0.007–0.058	BD; BD; BD–0.023	*BD; BD;BD*
FRP (mg L^{-1})	0.012; 0.009–0.014; 0.005–0.17	BD; BD–0.003; BD–0.01	*BD; BD; BD*
NH_4 (mg L^{-1})	BD; BD; BD–0.045	BD; 0.0–0.002; 0.0–0.008	*BD; BD; BD–0.005*
%DOP	9.2; 4.4–13.2; 0–27	66.7; 50–80; 8.3–100	*87.5; 77.5–100.0; 22.5–100*
TN:TP (molar)	12; 10.3–14.9; 3.8–26.6	28.1 22.6–35.7; 10.3–57.6	*40.6; 31.2–49.8; 18.1–103.3*
Water Column Pigments (medians; 25th–75th percentile range; minimum–maximum)			
Chlorophyll *a* (µg L^{-1})	1.6; 1.4–1.9; 0.08–2.6	0.29; 0.18–0.61; 0.0 –2.3	*0.18; 0.15–0.23; 0.0–0.94*
%Pico-phytoplankton	22.5; 17.3–27.8; 14.5–42.6	44.6; 42.2–45.5; 32.1–50.2	*49.2; 44.3–58.7; 34.8–76.2*
%Micro-phytoplankton	71; 64.6–78.8; 44–81.4	44.0; 42.3–46.1; 37.7–57.8	*37.2; 32.9–38.1; 11.9–54.8*
%Nano-phytoplankton	5.6; 4.8–7.8; 3.5–13.4	11.9; 11.3–12.2; 10.1–13.3	*13; 5.2–18.3; 2.5–23.2*
Bottom Sediment Data (medians; 25th–75th percentile range; minimum–maximum)			
Major sediment group (this study)	MFR-M & sM	MFR-mS & S	REL-S
Major sediment class (Ryan *et al.*, in prep)	Class 3	Classes 2&4	Classes 1&5
%Mud	44.8; 12–73.4; 1.1–96.2	15.2; 2.3–33.6; 0.4–96.1	1.1; 0.3–4.3; 0.0–27.4
Fe (mg g^{-1})	33.8; 18.7–43.5; 8.4–48.3	18.6; 12.6–23.8; 8.8–51.2	8.5; 5.4–13.5; 3.4–22.8
Available P	0.18; 0.15–0.19; 0.11–0.12	0.07; 0.06–0.09; 0.03–0.21	0.03; 0.02–0.06; 0.01–0.07

Variable	Zone of Maximum Resuspension	Coastal Transition Zone	*Blue Water Zone*
(mg g^{-1})			
TN:TP (molar)	2.7; 1.9–3.0; 0.5–4.0	1.8; 1.0–2.5; 0.2–4.3	1.2; 1.0–1.6; 0.6–2.7
FeII:TOC (molar)	0.3; 0.2–0.3; 0.1–2.6	0.7; 0.5–1.5; 0.0–7.3	0.8; 0–1.3; 0.0–7.7

The Zone of Maximum Resuspension

Processes occurring in the Zone of Maximum Resuspension (ZMR) exert a fundamental control on nutrient cycling in coastal areas (Abril *et al.*, 2000; Goni *et al.*, 2005). This zone arises in Keppel Bay because of the large tidal currents; it was demonstrated in Chapter 4 that resuspension is a strong function of current speed. In other systems tidal asymmetries, gravitational circulation and stratification (see references in Goni *et al.*, 2005) all contribute. Resuspension and sediment entrainment on tidal time-scales caused elevated and highly variable TSM levels (i.e. the median was 56.3 mg L^{-1} and the 25th to 75th percentile ranges was 32.5–89.8 mg L^{-1}; Table 5.7), and the hydrodynamic sorting of particles based on different densities and settling velocities. The underlying sediments in the ZMR consisted of mud and sandy-mud in the classification scheme of Folk (1970), except in the highly-scoured tidal channels where muddy-sand sediments were found. The high Fe contents of these sediments (Table 5.7) provides an indication of the relatively higher surface area of these sediments compared to those of the CTZ and BWZ, and accounts for higher levels of available P (Table 5.7).

Particulate nutrients dominated nutrient pools in the ZMR of Keppel Bay at the time of the dry season surveys, and linear relationships were found between chlorophyll corrected TPN and TPP and TSM (Figures 5.13ab). The linear relationships are best explained by the resuspension of bottom sediment and bound nutrients by the strong tidal currents in the region. Dissolved inorganic nutrient concentrations were also highest in the ZMR (Table 5.7) because continual resuspension of the surface sediment layer and light limitations imposed by high levels of TSM prevented the full utilisation of dissolved nutrients by phytoplankton. Interestingly, inorganic N turnover times were highest in the ZMR (1–3 days based on modelled estimates; Chapter 7; F and G), yet chlorophyll *a* was found at its highest concentrations in this zone (Table 5.7). The phytoplankton community was strongly dominated by micro-phytoplankton based on the generalised pigment data of Oubelkheir in press (Table 5.7). At least some of this algal material was probably washed off the mud banks where a luxurious growth of diatoms was observed during the dry season. As mentioned previously, under dry season conditions, much of the dissolved nutrient in the

ZMR was probably derived from the from algal diagenesis, from the release of nutrients from sediments as they are alternately eroded during ebb and flood tides and then deposited again during slack tides and potentially from the sewage treatment plant and meatworks. As explained above, physical re-working and re-oxidation of the bottom sediment promotes the remineralisation of particulate organic matter and release of nutrients to the water column (see also Ullman and Sandstrom, 1987; Walker, 1981).

There is a reasonable amount of evidence that general turbulence in the ZMR produces an efficient decomposition system characterised by repetitive redox successions (oxic to sub-oxic, temporarily sulfidic), reoxidation and metabolite exchange. For example, the core incubation studies showed that, of the eight cores studied, the highest CO_2 fluxes were from the core taken from the ZMR (i.e. 41.2 mmol CO_2 m^{-2} d^{-1} in sample 205; Table 5.5). A CO_2 flux of this magnitude is indicative of oligotrophic conditions (<48 mmol CO_2 m^{-2} d^{-1}) in classification scheme of Eyre and Ferguson (2002). However, the core incubation experiments assume a static sediment-water interface and therefore probably underestimate the amount of organic matter degradation in this part of the estuary where episodic resuspension improves the opportunity for mixing between bacteria and labile organic matter in the sediment (Alongi and McKinnon, 2005). Moreover, the incubated core was collected from a site near the CTZ boundary (%mud = 69.0%) and therefore was not representative of the most organic-rich sediments in the ZMR (>95% mud). This is because the depo-centre of a 5m thick mud body was found at the junction of Raglan and Casuarina Creek, and pinches out over a kilometre in the direction of Keppel Bay (Ryan *et al.*, 2005). The ZMR core also had the largest excess CO_2 flux, with more than 70% of the CO_2 generated by organic matter diagenesis the result of non-oxic processes. As the sediment at this site also had the highest TS:FeII ratio, it is likely that sulfate reduction is more important in the ZMR than elsewhere in Keppel Bay. Indeed, the average TS:FeII ratio of sediments from Casuarina Creek is 1.8, which is close to the pyrite ratio of 2.

Ammonium is a product of non-oxic diagenesis and its concentrations were highest for Keppel Bay in the ZMR, and this was especially the case in the deltaic region, in a zone that extends from the mouth of Casuarina Creek along the narrow eastern channel and then broadens out in a deeper water area between Centre Bank and Timandra Bank. As with the tidal creeks (Chapter 6), this is an important region for fine sediment accumulation (Ryan et al, 2005) and organic matter degradation. However, the high particle concentrations, together with the high water temperatures and well-oxygenated waters probably bring about a rapid oxidation of most NH_4 produced, thus more NO_X than NH_4 is exported to Keppel Bay. The oxidation of NH_4 is called nitrification and this

process is often at its maximum in resuspension zones because nitrifying bacteria occur attached to sediment particles (Owens, 1986; Abril *et al.*, 2000).

The largest N_2 flux was also observed at the core incubation site in the ZMR, where the highest sediment ferric iron (FeIII) concentrations of the core incubations were measured. The negative sign of the N_2 flux probably implies net uptake by nitrogen fixing bacteria. Interestingly, Yoshida *et al.* (2002) showed that siderophores (FeIII specific ligands) produced by marine bacteria significantly increase dissolution rates and solubilities of ferric hydroxides in aeolian particles, and suggested that this transfer was an important step in the pathway of Fe into marine organisms. At present, we are not sure as to whether the N_2 uptake occurred in the water column or the bottom sediment of the core barrel.

The Blue Water Zone

The Blue Water Zone (BWZ) of Keppel Bay is defined as the region overlying mainly relict sand sediments (REL-S) sediments, where dissolved inorganic nutrient concentrations were always below detectable limits and where TSM levels in the overlying water were typically less than 2.5 mg L^{-1} (Figure 5.18a; Table 5.7). Consequently, the light climate is very good in this region (Secchi disk depths >3 m). Pico-phytoplankton (as inferred from HPLC analysis of particulate pigments) were also found to dominate phytoplankton assemblages (Figure 5.18b; Oubelkheir *et al.*, in prep) in this region, and DOP accounted for in the order of 85% of the water column phosphorus pool (Table 5.7). Nano-phytoplankton also increased in abundance over this region (Table 5.7), and slicks of the heterocystous cyanobacteria *Trichodesmium* were frequently observed (Figure 5.18c).

The increase in the abundance of cyanobacteria (including *Trichodesmium*) in the BWZ (Chapter 7) likely constitutes a domain shift in the terminology of Karl et al, (2001; but see also Karl *et al.*, 1995). The pico-cyanobacterial genera *Synechococcus* and *Prochlorococcus* usually dominate primary production and phytoplankton biomass in GBR waters (Furnas *et al.*, 2005), and diazotrophic *Trichodesmium* supply nitrogen to the GBR in amounts similar to the total amount entering from all the rivers in the GBRCA (Bell *et al.*, 1999). It is worth mentioning that community dynamics are expected to shift towards phosphorus limitation (or iron limitation Lenes *et al.*, 2001; Bell *et al.*, 2005) in the presence of such large amounts of fixed N (Karl *et al.*, 1995) because available P concentrations in bottom sediment were at their lowest in Keppel Bay in the BWZ. Indeed, the success of pico-phytoplankton (including *Trichodesmium* species found in GBR waters; Bell *et al.*, 2005) in nutrient depleted waters may in part rely on their ability to utilise numerous and sometimes novel organic P

and N sources including cyanates and phosphonates (Fuller *et al.*, 2005 and references therein), and in part on their uptake efficiencies (Donald *et al.*, 1997). It is also noteworthy that *Trichodesmium* can also excrete up to 50% of the nitrogen they fix in the form of DON (Glibert and Bronk, 1994), and the uptake of DOP and release of DON by *Trichodesmium* may account for the generally higher TN:TP ratios in this region (Table 5.7).

Interestingly, despite the abundant evidence for cyanobacteria-dominated phytoplankton communities in the BWZ, the three incubated cores from this zone all had positive benthic N_2 fluxes (sites 201–203; Table 5.5). The absence of a dark nitrogen-fixation signal in the BWZ may be due to the generally low Fe and P concentrations of the underlying sediment (Table 5.7), caused by the winnowing-out of the mud fraction (note low mud contents in Table 5.7). If the positive N2 fluxes are indicative of denitrification, then these denitrification rates are lower than most those previously measured in GBR waters (0.2–1.6 mmol N m^{-2} d^{-1} as compared to 1.3–13.7 mmol N m^{-2} d^{-1}; Alongi and McKinnon, 2005). Carbon dioxide fluxes in the BWZ ranged from 8 to 31.2 mmol m^{-2} d^{-1} at the three sites where they were measured (sites 201–203; Table 5.5), and thus were indicative of oligotrophic conditions (i.e. <48 mmol CO_2 m^{-2} d^{-1}) in the classification scheme of Eyre and Ferguson (2002). As with most GBR waters, the bulk of the phytoplankton N and P demand in the deeper waters of the BWZ is probably met by microbial recycling in the water column (Furnas *et al.*, 1995; Lourey *et al.*, 2001). Interestingly, N turnover times were at their fastest in the data set (<0.1 days) at Stn A, located in the BWZ, implying extreme nutrient limitation.

The Coastal Transitional Zone

The Coastal Transitional Zone (CTZ) represents the mixing zone between the ZMR and BWZ, and reflects the wide tidal excursion which prevents any clear cut boundary developing between the two end members. The transitional zone is perhaps best recognised by the distribution of turquoise coloured waters, and is roughly coincident with the distribution of predominantly MFR-mS sediments in Keppel Bay proper (Figure 5.1). For the purposes of this study, the CTZ is defined as the region in Keppel Bay where non-conservative nutrient behaviour was most commonly observed (Figure 5.18) Other defining characteristics of the CTZ include: (i) roughly equal proportions of micro-phytoplankton and pico-phytoplankton (Table 5.7; see also Oubelkheir *et al.*, in prep); (ii) intermediate percentages of P in organic forms (i.e. median = 66.7%; Table 5.7); and (iii) intermediate TSM concentrations (i.e. 25th to 75th percentile range was 2.6–9.0 mg L^{-1}). It is bounded by a combination of the 2.5 and 40 mg L^{-1} contours on the

combined dry-season TSM map (Figure 5.18a) and the -2 and -4 contours on the sediment PCA axis 1 map (Figure 5.1c and 5.18a).

The CTZ of Keppel Bay is the zone of maximum nutrient utilisation based on the data in Table 5.7. The average photosynthetic N uptake estimates from the CTZ are 0.017 g m^3 d^{-1} based on modelled data from 4 sites, compared to 0.15 g m^3 d^{-1} for the ZMR (two sites) and 0.14 g m^3 d^{-1} for the BWZ (one site). Our results are consistent with those of Devlin and Brodie (2005) in the respect that nutrient utilisation was most evident at TSM levels <10 mg L^{-1}. Alongi and McKinnon (2005) found a near 1:1 relationship between the flux of carbon to the seabed and organic carbon mineralisation rates in the coastal zone of the GBR shelf. If we assume the same relationship holds in Keppel Bay then carbon fluxes to the seafloor in the CTZ ranged from 9.8 to 21.3 mmol m^{-2} d^{-1} (sites 196, 198, 200 and 204; Table 5.5), and thus were indicative of oligotrophic conditions (i.e. <48 mmol CO_2 m^{-2} d^{-1}) in the classification scheme of Eyre and Ferguson (2002).

Based on the data in Table 5.7, there was no statistically significant difference between the percentages of micro-phytoplankton and pico-phytoplankton in the CTZ. The co-dominance of these two phytoplankton groups is likely maintained by fluctuations in general turbulence, P-concentrations and TN:TP ratios on tidal timescales (due to resuspension and advection). Diatoms tend to sink at relatively high rates, and therefore tend to flourish only in regions where they are actively resuspended by turbulence. In comparison, pico-phytoplankton are smaller and more buoyant so their losses due to sinking are much smaller and they can survive in regions of modest vertical mixing. It has also been frequently observed that large phytoplankton out-compete smaller species in areas of high nutrient supply (Donald *et al.*, 1997), while pico-phytoplankton (0.2–2 µm) biomass is usually highest in oligotrophic, and especially P-limited waters (Joint, 1986; Agawin *et al.*, 2004). Consistent with the results of our study (Table 5.7), Suttle and Harrison (1988) reported that the pico-cyanobacterium *Synechococcus* dominated over diatoms in laboratory cultures with high TN:TP ratios (TN:TP å 45), while diatoms dominated at lower TN:TP ratios. Similarly, Takamura and Nojiri (1994) found a positive correlation between micro-phytoplankton biomass and the TN:TP ratio of lake waters.

Non-oxic process accounted for 14.5–55.6% of the benthic carbon degradation in the CTZ, based on the excess CO_2 fluxes (Figure 5.6), and there is strong evidence for the occurrence of iron oxy-hydroxide reduction in the surface sediments. For example, axis 2 of the sediment PCA had particularly high loadings in the CTZ (Figure 5.5a), and this was especially the case along the western beach fringe where high wave energy and sediment permeability presumably allows for extensive regeneration of Mn and Fe oxides. As

mentioned previously, Ryan *et al.* (2005) and Brooke *et al.*, (2005) also identified these fine sands as being, by far, the best sorted sediments in Keppel Bay. The intermediate iron concentrations of CTZ sediments (Table 5.7) were probably not limiting to dark N_2 fixation because net uptake of N_2 was observed in all the core incubations from this zone (i.e. samples 196, 198, 200 and 204; Table 5.5).

Conclusions

The existence of strong spatial gradients in the distribution of geochemical constituents in the bottom of Keppel Bay was demonstrated through the use of Principle Components Analysis. Fe concentrations and the $Al2O_3$:K_2O ratios were the most strongly correlated to the first principle component, which identified the region of influence of modern Fitzroy River sediments in Keppel Bay. Fe concentrations and the Al_2O3:K_2O ratios were shown to correlate with the surface area of sediment in a limited suite of samples.

Keppel Bay sediments had large proportions of biologically-unavailable Ca-bound P (medians >50%). It is currently unresolved the extent to which this Ca-bound P is formed within Keppel Bay.

Useful predictive relationships were established between the Fe concentrations of the sediments (as a surrogate for surface area) and carbon and major nutrient concentrations. These relationships were used to derive annual fluxes of C, N & P to Keppel Bay, the annual release rates of these constituents from terrestrial particles and the annual burial rates of these constituents.

Nutrient mass accumulation rates were highest in the tidal creeks and floodplain sediments and lowest in Keppel Bay.

It was estimated that carbon deposition rates in Keppel Bay amounted to 10 100 tonnes C per year, of which more than 50% was due to non-oxic process. The evidence suggests that iron oxy-hydroxide reduction may be particularly important for organic matter degradation in Keppel Bay.

One of the more surprising results from this study was that N_2 uptake was observed under in the core incubation experiments, suggesting that nitrogen fixation was occurring under dark conditions. The N_2 flux from the sediment was inversely correlated to the ferric iron content (FeIII) of the sediment providing further evidence that nitrogen fixing organisms were utilising the N_2. By extrapolation of this calibration to the whole of Keppel it was found that dark nitrogen fixation rates were in the order of 5070 tonnes N per year, and annual denitrification rates were ~4120 tonnes N per year. These estimates, which approximately cancel each other, are of a similar magnitude to the inputs of N from the catchment.

Water column pool sizes for most nutrients were similar between the two dry season surveys, suggesting that these were representative conditions for the end of the dry season. Not unexpectedly, the pool sizes for most nutrients were larger under wet season conditions than dry season conditions.

Based on the results of this study, Keppel Bay can be divided into three biogeochemical zones: (i) the Zone of Maximum Resuspension (ZMR); (ii) the Blue Water Zone (BWZ); and the (iii) Coastal Transitional Zone (CTZ). The discrimination of these zones was based on the nature of the underlying sediment, TSM levels and on behaviour of dissolved inorganic nutrients (conservative, non-conservative, below detection) in the dry season mixing diagrams (Figure 5.12). Phytoplankton size composition data were also taken in to account, and of all the water column variables in the data set.

Tidal creek biogeochemistry

Introduction

Several large coastal creeks (Figure 6.1) enter Keppel Bay near the mouth of the Fitzroy Estuary. When designing the project it seemed possible that these creeks could make a substantial contribution to the nutrient processing capacity overall and thus play a major role in the biogeochemistry of the integrated system. This chapter outlines the physical characteristics of the major coastal creeks and compares them to the analogous properties of the Fitzroy Estuary. We then discuss the data sources and outline the experimental investigations, and go on to provide a description of the hydrology of the creeks. The temporal and spatial distribution of nutrients in the coastal creeks are described and we conclude this chapter with a quantitative analysis of the fluxes to/from Keppel Bay to the coastal creeks, and highlight important ecological characteristics of the creeks.

Physical characteristics of the major tidal creeks

The Fitzroy Estuary enters the south-western corner of Keppel Bay. In the same area, three major tidal creeks (Casuarina, Raglan (including its tributary, Inkerman Creek), and Connor Creek) enter Keppel Bay (Figure 6.1). The combined surface area and volume of these creeks is comparable to that Fitzroy Estuary (Table 6.1).

Figure 6.1: Location of the major tidal creeks in relation to the mouth of the Fitzroy Estuary.

Table 6.1: Areas and volumes of major tidal creeks entering Keppel Bay together with area and volume of Fitzroy estuary for comparison.

Creek name and region	Volume (1000 m^3)	Area (m^2)
Connor Creek and tributaries	120 708	13 062 889
Kamiesh Passage	7 459	768 000
Bobs Creek	4 883	640 000
Alligator Creek	1 144	320 000
Casuarina Creek	52 040	10 030 000
Raglan Creek (to junction with Inkerman Creek)	29 255	4 420 000
Raglan Creek (from junction with Inkerman Creek)	24 062	3 770 000
Inkerman Creek	6 368	2 555 000
Unnamed Creek (off Raglan ck)	2 557	555 000
TOTAL	248 476	36 120 889
Fitzroy (for comparison)	~250 000	~40 000 000

Further to the north, Coorooman and Cawarral Creeks enter Keppel Bay at Cawarral Bay, and Ross Creek enters at Yeppoon. These creeks are much smaller in area and volume than the major tidal creeks listed above and their net impact on nutrient dynamics in Keppel Bay was assumed small. They were not investigated further by the project.

In addition to the main stems of the tidal creeks, there are numerous “runners” - small mangrove-lined tidal creeks branching off from the main tidal creeks. These are more numerous than for the main stem of the Fitzroy hence the total area of the tidal creek surpasses that of the Fitzroy. The large intertidal area of these shallow small creeks offers greater scope for MPB production and enhanced exchanges between salt flats and creek.

The various creeks have quite different morphologies. While the Fitzroy, in its mid- reaches has fringing mangroves, these are lacking from Casuarina and Raglan Creeks where the creeks are quite steep-sided and mangrove growth is confined to the runners. In contrast, Connor Creek has much more gentle sloping sides and is lined by mangroves. The Fitzroy Estuary, Casuarina and Raglan Creek are of comparable depth while Connor Creek has almost twice the average depth of the Fitzroy. These geomorphological differences arise from (pers. com. Dave Ryan) the creeks being located in different regions which represent different stages of infilling of the Fitzroy delta and are discussed in greater detail in the Report from the geomorphological task of AC. (Ryan *et al*., 2005).

All the major tidal creeks have very small catchments and only Raglan Creek has a permanent source of freshwater. As the catchments are small, the inputs of sediments and nutrients from the catchments are correspondingly reduced compared to the Fitzroy estuary. In marked contrast to the Fitzroy estuary, freshwater is exchanged into the coastal creeks during flood events through the mouth as large flood events deliver large quantities of freshwater into the south western corner of Keppel Bay (there is evidence that under high flow conditions there is some upstream entry of freshwater into Casuarina Creek from the Fitzroy also, however the connectivity of the other tidal creeks across the Fitzroy flood plain during floods is not known). The exchange of freshwater into the Casuarina and Connor creeks driven by the macrotidal excursions creates a gradient where the salinity increases going upstream immediately after a flood event. Post flood, the freshwater in the mouth is rapidly replaced by maritime water from Keppel Bay. This changes the direction of the salinity gradient, with the fresher waters now located upstream. As the exchange process continues saltwater gradually makes its way upstream replacing the residual freshwater. As the exchange process is slow (time for exchange ~100 days), the winter rainfall is slight, and the evaporation rate considerable, the more distal parts of these coastal creeks become moderately hypersaline. This is an equilibrium state where the elevation of salinity due to evaporation is balanced by the inflow of salt water from Keppel Bay. The overall result is a salinity gradient from the head to the mouth.

Raglan Creek displays quite different longitudinal salinity behaviour. Because of the freshwater inflows at the head of the creek, and the exchanges at the mouth, immediately post flood, the maximum salinity is at the central region of creek. As the tidally-driven exchange of salt water from Keppel Bay sets in post flood, the salinity gradient evolves to a steady state with a gradient from the fresh head to the saline mouth. The vigorous macrotidal motion in all the major creeks ensures that they are well mixed vertically with minimum stratification.

Turbidity and suspended solids concentration is high in Casuarina and Raglan Creeks due to tidal resuspension and the shallow depth (~5 m) of the creeks. The range was 150 to 300 NTU at the surface and up to 600 NTU just above the bottom indicating strong resuspension/settling within the creeks. TSS increases on going up stream. In contrast, Connor Creek is much deeper (average depth ~ 10 m) and the tidal prism is a much smaller fraction of the total volume. The lower TSS concentration in Connor Creek relative to Casuarina Creek is consistent with a simple analysis of the tidal flows, which shows that the mean tidal velocity is inversely related to the water depth. Accordingly, tidal velocities in Connor Creek are less, and resuspension is considerably reduced, thus both turbidity and TSS are generally much lower and decrease on going upstream

(minimum 20 NTU, maximum 100 NTU at surface; minimum 20 NTU, maximum 150 NTU at bottom). Secchi depth increases on going upstream in Connor Creek also. Average chlorophyll *a* concentrations in Connor Creek are twice those in Casuarina creek.

Dissolved Oxygen concentrations in Casuarina creek decreased from 7.0 mg l^{-1} near the mouth to 6.7 mg l^{-1} at the most upstream station indicating net oxygen consumption in the water column/sediment system. A similar gradient i.e. decreasing on going upstream, existed in Connor Creek with the DO levels somewhat reduced (6.50 to 6.0 mg l^{-1}) in comparison to Casuarina creek.

Biogeochemical aspects of tidal creeks

Both particulate and dissolved nutrient concentrations were measured at multiple stations along the length of Casuarina Creek in August 2003 and August 2004, and at an additional 24 hour mooring near the mouth of the creek (for details see: Draft milestone Report AC32, Ford *et al.* 2005b). With the generous collaboration of the Queensland EPA, a series of stations along both Casuarina and Connor Creeks were occupied in August/September 2004. Dissolved and particulate nutrient samples were collected. This data was augmented by chemical and physical data collected by the Queensland EPA at monthly intervals in Casuarina, Raglan, and Inkerman Creeks over a 2-year period July 1998 to June 1990.

There is a clear dichotomy between Casuarina, Raglan and Inkerman Creeks on the one hand, and Connor Creek on the other and they will be discussed separately. While in first group of creeks interpretation of the Total Nitrogen (TN) and Total Phosphorus (TP) data is partially confounded by the tidally driven resuspension of sediment reflecting purely local effects rather than the overall biogeochemical performance, a statistical analysis of the data shows that there is a significant (at either 0.01 or 0.05 level) difference between the upstream and downstream concentrations for each creek and species. The downstream concentration is lower than the upstream concentration. The dissolved nutrients (FRP and NO_X) both show clear concentration gradients decreasing towards the seaward end along the length of each of these creeks. As the concentrations of all these species are lower in Keppel Bay, these results imply that there is a flux of these species from the tidal creeks to Keppel Bay. Thus, these creeks serve as sources of dissolved inorganic (i.e. bioavailable) P, N, and dSi to Keppel Bay.

The available data on the spatial variation in nutrient concentrations in Connor Creek is much more limited consisting of one cruise in August 2004. Caution should be exercised in extending these results to the whole of the dry season. The results show a clear gradient of NO_X and FRP decreasing towards the head of the estuary, In contrast, the dSi concentration gradient is in the reverse

direction decreasing towards the mouth. Thus, Connor creek acts as a sink of NO_X and FRP while acting as a source of dSi to Keppel Bay.

As noted in the discussion of the experimental results, for much of the dry season Casuarina, Raglan, and Connor Creeks all have increasing salinities moving upstream. In our conceptual model, we attribute this to evaporative losses from the creeks. These losses are balanced by the inflow of seawater of lower salinity from Keppel Bay. The higher salt concentration upstream is dissipated downstream by tidally driven dispersion. If we make the reasonable assumption (this is addressed in Ford *et al.* 2005b) that the system has achieved steady state, then we can apply the analysis of Smith and Atkinson (1983) to calculate the fluxes of dissolved nutrients into/out of the various coastal creeks. Briefly, the method requires that the system be at steady state with upstream evaporative salt concentration balanced by downstream dispersion. Then the source sink strength (B_Y) of a non-conserved species Y is given by:

Equation 6.1 $$B_\gamma = E \times (S_0 \times \mathrm{d}Y / \mathrm{d}S) - Y_0$$

Where *E* is the net water loss (i.e. evaporation minus rainfall, stream flow, and groundwater inputs. In this analysis, we neglect these water inputs. S_0 is the salinity at the seaward boundary of the system; Y_0 is the concentration of the non-conserved species at the seaward boundary; and d*Y*/d*S* is the concentration gradient of species *Y* with respect to salinity.

The flux B_γ is the sum of all processes affecting the concentration of *Y*, excluding advection and mixing with ocean water. Note that by using the concentration gradient with respect to salinity (d*Y*/d*S*) rather than the spatial gradient (d*Y*/d*x*, where *x* is distance along the creek) this analysis obviates the need to take account of tidal displacement effects arising from measurements made at different stages of the tidal cycle.

As the first stage of the application of this analysis, we have replotted the longitudinal concentration for data for Casuarina and Connor Creek (Figure 6.2 and Figure 6.3) against salinity. Note especially that the directions of the gradients for DIN and DIP (but not dSi) are of opposite sign for Casuarina and Connor Creek.

In addition, we have applied the same analysis to the nutrient concentration and salinity data from the 24-hour mooring at the mouth of Casuarina Creek. This is essentially of the same character as the longitudinal profiles of salinity and concentration. The only difference In this case the boat is stationary while the water moves past it, while in the longitudinal profiles the boat is moving relative to both the water and to the bank.

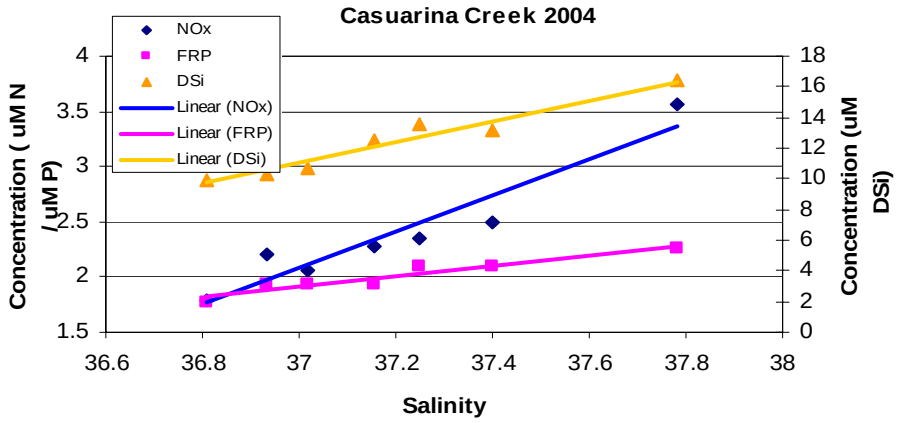

Figure 6.2: Dissolved nutrient concentrations as function of Salinity in Casuarina Creek, EPA Cruise August 2004. Note that FRP concentration has been multiplied by 5 to make gradient discernible.

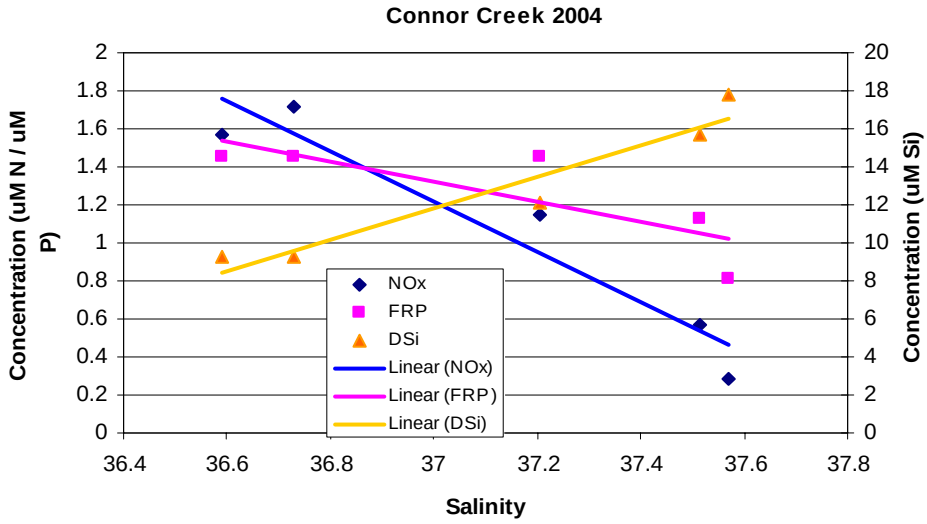

Figure 6.3: Dissolved nutrient concentrations as function of Salinity in Connor Creek, EPA Cruise August 2004. Note that FRP concentration has been multiplied by 5 to make gradient discernible and that gradients for NO_X and FRP are opposite to those in Casuarina Creek (Figure 6.2 above).

Using Equation 6.1 and the best fit lines for the various nutrient species shown in Figure 6.2 and Figure 6.3 we have calculated the net fluxes of different species into Keppel Bay together with the annual loads based on a 300-day dry season. The results are shown in Table 6.2. In addition, DO concentration in both systems shows a clear decrease on going up stream. The gradient is approximately linear with salinity and we have applied the same technique to calculate the net dissolved flux of dissolved oxygen into the system. This is also shown in Table 6.2.

Table 6.2: Calculated fluxes and loads (based on a 300-day dry season) of dissolved nutrients INTO Keppel Bay from Casuarina and Connor Creeks. Note that a negative sign indicates a flux from Keppel Bay into the tidal creek.

CREEK	SPECIES			
	DSi	NO_x	FRP	DO
Casuarina				
Flux (mM m^{-2} d^{-1})	1.58	0.37	0.02	-0.73
Load (kgMole)	4770	1132	61	-2180
Connor				
Flux (mM m^{-2} d^{-1})	1.86	-0.32	-0.03	-2.55
Load (kgMole)	7300	-1241	-98	-7700

The results of the quantitative approach are consistent with the fluxes inferred from the longitudinal concentration profiles for the dissolved nutrients. While both creeks are sources inputs of DSi to Keppel Bay, Casuarina and Connor Creeks function in different ways. The areal fluxes are comparable for the two systems but are of a different sign and the overall effect is that they partially cancel each other out. The other two creeks (Inkerman and Raglan) have similar characteristics to Casuarina Creek and the overall effect of the complex of coastal creeks is to be a source of nutrients to Keppel Bay. Other species such as DOC do not show any detectable variation with salinity within the creeks, which leads to the conclusion that their net rate of transformation within the creeks is slow on the time scale of exchange between the Creek and Keppel Bay proper. It is note worthy that the N:P for the dissolved fluxes of nutrients from Casuarina Creek is 18.5:1 while the comparable ratio into Connor Creek is 12.7:1. Both these ratios are quite close to the Redfield ratio for marine phytoplankton (N:P =16:1). This suggests that Casuarina Creek is the site of diagenesis of predominantly fresh phytoplankton; while Connor Creek takes up dissolved inorganic nutrients from Keppel Bay and converts them into phytoplankton at the normal stoichiometric ratio.

Ecological significance of tidal creeks

The complex of coastal creeks in the vicinity of the Fitzroy mouth is somewhat unusual in the juxtaposition of a number of large creeks to a macrotidal estuary which has very large episodic freshwater flows relative to the combined volume of the main stem of the estuary and the coastal creeks. As the qualitative analysis of the EPA data shows, fresh water is pushed into the mouths of coastal creeks at times of major flood flow. The salinity declines markedly and the lower

reaches of the creeks become brackish to fresh with the distance of penetration of the brackish water determined by the hydrodynamics of the particular creek, and the meteorological and tidal conditions. This upstream salinity decrease will persist longer than the less than full seawater salinity conditions at the mouth because of the finite exchange time between the creeks and Keppel Bay proper. The creeks thus provide an environment for species, especially the larval and juvenile forms, adapted to less than full seawater salinity conditions. The apparent unique character of Raglan Creek, where, due to the continuous freshwater inflow, an especially wide range of salinities exists over the whole seasonal cycle, makes the conservation of this creek especially important.

The coastal creeks are also subject to freshwater inflows from heavy rainfall in their relatively small local catchments. This has the effect of flushing the coastal creeks from the distal end and changing what is, after the prolonged dry season, a hypersaline environment to a brackish or fully fresh environment. This again provides a more hospitable environment for salt sensitive species. The changes in salinity at the mouth and distal ends of each creek are driven by different processes and do not necessarily coincide.

Primary production

Introduction

This chapter deals only with pelagic (suspended in the water column) phytoplankton. Benthic phytoplankton and microphytobenthos of the intertidal area of the Fitzroy estuary and tidal creeks are covered in Milestone Report AC 64 (Revill *et al*. 2005). One of the key elements in the overarching Fitzroy Agricultural Contaminants project was to investigate the scope for using remote sensing to provide a synoptic view of key biogeochemical characteristics such as chlorophyll *a*, CDOM, TSS, optical depth and turbidity. This chapter, describing the primarily field-based part of the project, has a clear nexus with the remote sensing initiative and shares observations and results with this work as a contribution to the field comparison and validation of remote sensing inferences. Some of these data are discussed here. The detailed summary of the remote sensing results is to appear later (Brando *et al.*, 2006 in prep.).

Primary production is the formation by photosynthesis of organic matter (combined carbon, nitrogen, phosphorus, silica, and other elements) from inorganic species such as carbon dioxide, ammonia and oxides of nitrogen, and phosphate. Because primary production unconditionally requires both dissolved inorganic nutrients and solar energy, the process integrates biogeochemical processes controlling the availability of the essential inorganic nutrients with the physical processes which, through mixing, sediment resuspension and turbulence, control the spatial distribution of phytoplankton in the water column and the amount of light available to them. While primary production by phytoplankton is always associated with the production of O_2, O_2 production does not necessarily imply production of new cells and nutrient uptake. Under conditions of good illumination and low nutrients, much of the light energy adsorbed by the cell is channelled into producing organic substances such as carbohydrates, while change in cell numbers does not occur.

Photosynthetic organisms (and their by-products) are the initial stages of all food webs. Phytoplankton are the food source of higher organisms such as zooplankton, metazoans etc, which are eaten, in turn, by fish and other predators further up the foodchain. Since the progress of matter and energy up the food chain is inherently inefficient, a lot of phytoplankton is required to ultimately produce a small quantity of fish. Thus, primary production can be considered to be the principal determinant of the overall biological productivity of a region such as Keppel Bay.

Phytoplankton have a very wide range of species-specific characteristics in terms of their optimum growth rate. In some coastal systems, the conditions of

light, temperature, and nutrient availability are especially favourable to a particular phytoplankton species, which grows rapidly until all the available nutrients are consumed or it reduces its own supply of light by forming dense surface concentrations. They are known as “blooms” and are often considered to be a nuisance because their uninviting colours (red, brown, green, grey), unpleasant odours, and, in some cases, the presence of toxins, inhibit recreational activities in coastal waters. Wind-driven accumulation can contribute to the formation of high surface concentrations also.

In tropical waters, pelagic phytoplankton of the *Trichodesmium* spp. are the dominant bloom forming species. *Trichodesmium* belong to a group of organisms called cyanobacteria, which share a capacity to fix nitrogen from the atmosphere (Carpenter and Capone, 1992; Capone *et al*., 1997). They are thus freed of the constraint of nitrogen limitation, the usual growth limiting nutrient to phytoplankton under marine conditions (phosphorus- another key nutrient is relatively more abundant in the tropical coastal seas and oceans). This characteristic makes *Trichodesmium* a significant contributor to the nitrogen budget of tropical (deep) oceanic waters (Karl *et al.*, 1997; Dore *et al.*, 2002). The nitrogen fixed by *Trichodesmium* spp. subsequently enters the oceanic food chains when other organisms ingest them, and also through the excretion of DON, and the mineralization of fixed nitrogen to dissolved inorganic nitrogen by microbial degradation of dead *Trichodesmium* cells both in the water column, and as they settle to the sea floor.

The role of *Trichodesmium* in tropical (shallow) coastal systems has been less thoroughly investigated. *Trichodesmium* blooms are especially troublesome to beach communities north of the mouth of the Fitzroy Estuary, as the wind-driven concentrations of cells form red, green, and grey scums on the near shore waters and beaches. These scums can smell very unpleasantly and the toxins released by the cells can cause skin irritations. Because of the concentration of *Trichodesmium* in the scum and the nutrients contained within the cells, *Trichodesmium* delivery to the beach is a form of nutrient subsidy to the intertidal animal community, as well as providing a sustained slow release source of dissolved nutrients, especially inorganic and organic nitrogen back into the coastal waters as the dead material decays.

Because of its apparent abundance in summer it is necessary to take account of the quantity of *Trichodesmium* and its nutrient (especially of biologically available nitrogen species) content in constructing nutrient budgets for Keppel Bay and comparing the relative significance of nutrient inputs from the Fitzroy catchment *vis-à-vis in situ* nitrogen fixation. We have adopted as a working hypothesis that the atmospheric nitrogen fixed by *Trichodesmium* becomes an additional input of

new nutrient for the Keppel Bay biogeochemical system. A subsidiary question is whether the *Trichodesmium* populations in Keppel Bay are produced *in situ,* or are advected to the beach from further off shore. The answer to this question determines if other nutrients principally iron and phosphorus associated with *Trichodesmium* spp. are imported also, or derived from purely local sources. These issues are discussed in the biogeochemical Chapter (5).

Spatial and seasonal distribution of phytoplankton

Figure 7.1 shows the spatial distribution of chlorophyll *a* concentration based on a 10-year average of monthly observations by GBRMPA (Anon. 2005). The key points to note are the spatial gradients, where the highest concentration in both summer and winter occurs in close proximity to the mouth of the Fitzroy Estuary, and the decreasing concentration moving both northwards (River mouth–Pelican Island) and eastwards (River mouth–Hummocky Island–mid Channel). The high chlorophyll *a* concentrations at Wreck Point probably reflect its proximity to the shore and exposure to higher ambient nutrient concentrations derived from terrestrial sources coupled with shallow and relatively clear water.

Summer chlorophyll *a* concentrations are approximately double the average winter concentrations. Detailed analysis of the data shows that the appearance of *Trichodesmium* spp., usually in August, contributes, in part, to the increase in summer over winter concentrations, but a significant part of the increase is due to the growth in abundance of smaller (<10 µm) species. The appearance of *Trichodesmium* is episodic and contributes to the high variance in the average concentrations during the summer months.

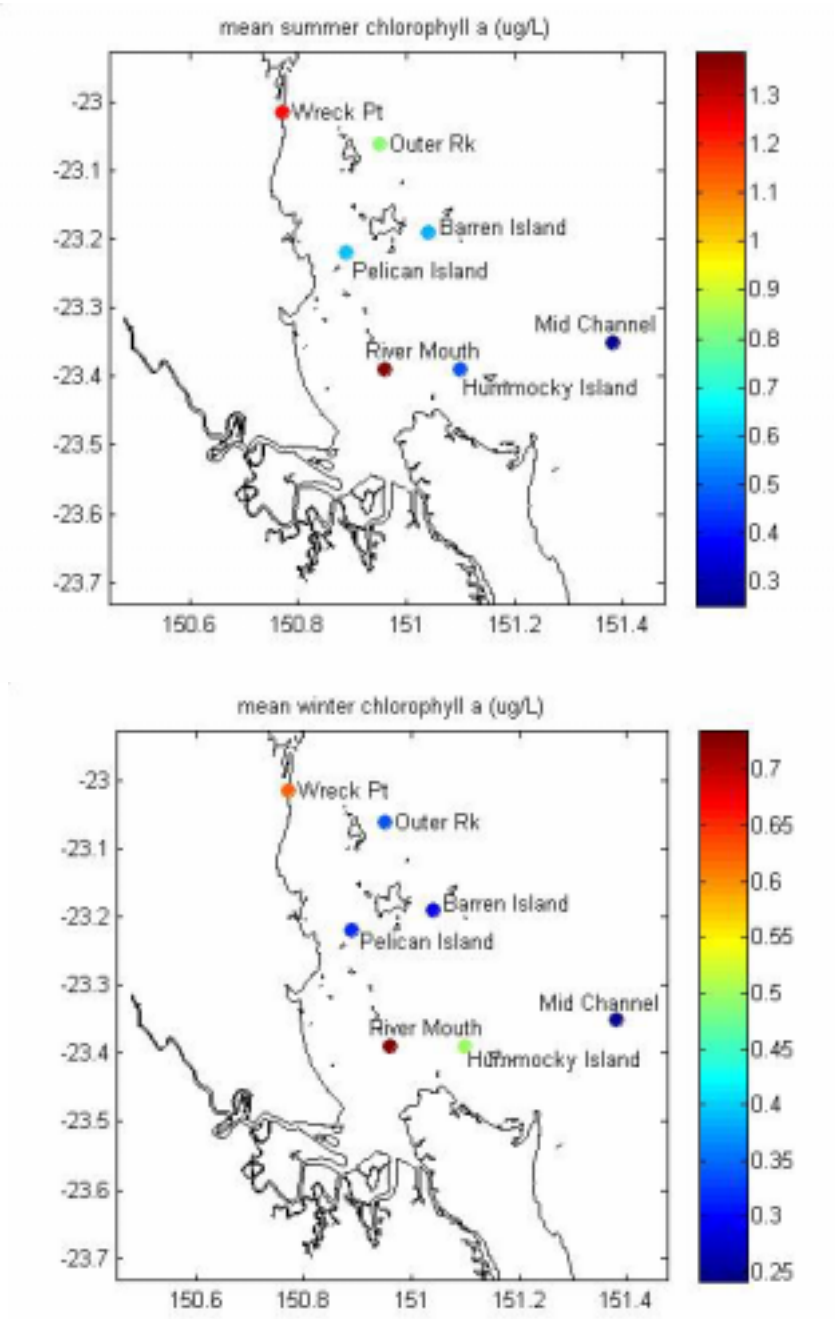

Figure 7.1: Average concentration of Chlorophyll a *(including* Trichodesmium *spp. and greater than 10 µm species) (data: Anon. 2005). Note especially the differences in the colour scale (µgL^{-1} Chl a) between summer and winter.*

The chlorophyll *a* concentration data gathered during the Coastal CRC field trips (August 2003, August 2004, and February 2005) are generally consistent with the patterns revealed by historic data. Since the latter data draw on a much greater number of spatial observations (though less precise individual determinations of chlorophyll *a* concentration) they define more clearly the spatial distribution (Figure 7.2). The enhanced summer vs. winter production can be clearly seen by comparing the August 2003 and September 2004

observations with the February 2005 results. In addition, the results show a higher concentration of chlorophyll *a* some distance off shore in the spring and summer cruises reflecting the landward advection of *Trichodesmium* from further off shore.

Despite these seasonal differences, the zone of higher chlorophyll *a* concentration in the vicinity of the mouth of the Fitzroy Estuary, with concentration declining both northward and seaward is clear. Looked at on this synoptic scale, the lower concentrations between Rosslyn Bay and Great Keppel Island support the view that the Wreck Point site is heavily influenced by very near shore phenomena. These results suggest that despite the high turbidity and limited light climate in the water column, pelagic phytoplankton can grow successfully in the estuary mouth environment. Detailed analysis of the diurnal changes in the dissolved oxygen concentration at sites throughout Keppel Bay (see later) supports this proposition. These observations suggest that there are two distinct zones separated by a transition zone for primary production: an estuary mouth area where primary production is limited by the available light; and a second more marine environment further offshore where primary production is limited by the supply of inorganic nutrients. These zones coincide approximately with the zones defined by the water column biogeochemical characteristics, and the sediment composition and particle size discussed in Chapter 5.In addition to this local primary production there is an input of *Trichodesmium spp* advected in from much further offshore (for evidence see later this Chapter). This material represents another external input (in addition to local nitrogen fixation and atmospheric inputs) to Keppel Bay in addition to the inputs from the catchment and thus needs to be considered in developing nutrient budgets for Keppel Bay.

What is doing the primary production?

As part of the remote sensing investigations, the pigment composition of filterable pelagic primary production was examined by High Performance Liquid Chromatography. The various pigments provide insights into the taxonomic structure of the pelagic phytoplankton community.

Table 7.1 (after Vidussi *et al.*, 2000, Vidussi *et al.*, 2002) shows the relationship between pigment, taxa, and the inferred phytoplankton size. In addition, the pigment composition through its connection with the various phytoplankton functional groups may be used to characterise the phytoplankton size distribution (Claustre, 1994). Inferences regarding the size of the cyanobacteria based on the presence of zeaxanthin need to be treated with caution in the presence of *Trichodesmium* spp. While the individual *Trichodesmium* cell size is <10 µm it exists in the form of multi-cellular filaments and thus almost pure samples of this

species (such as those gathered at Stations 38 S and 50 S - locations are given in Radke *et al*.2005) collected by skimming off particles about 200 µm long from the surface may be classified as very small particles.

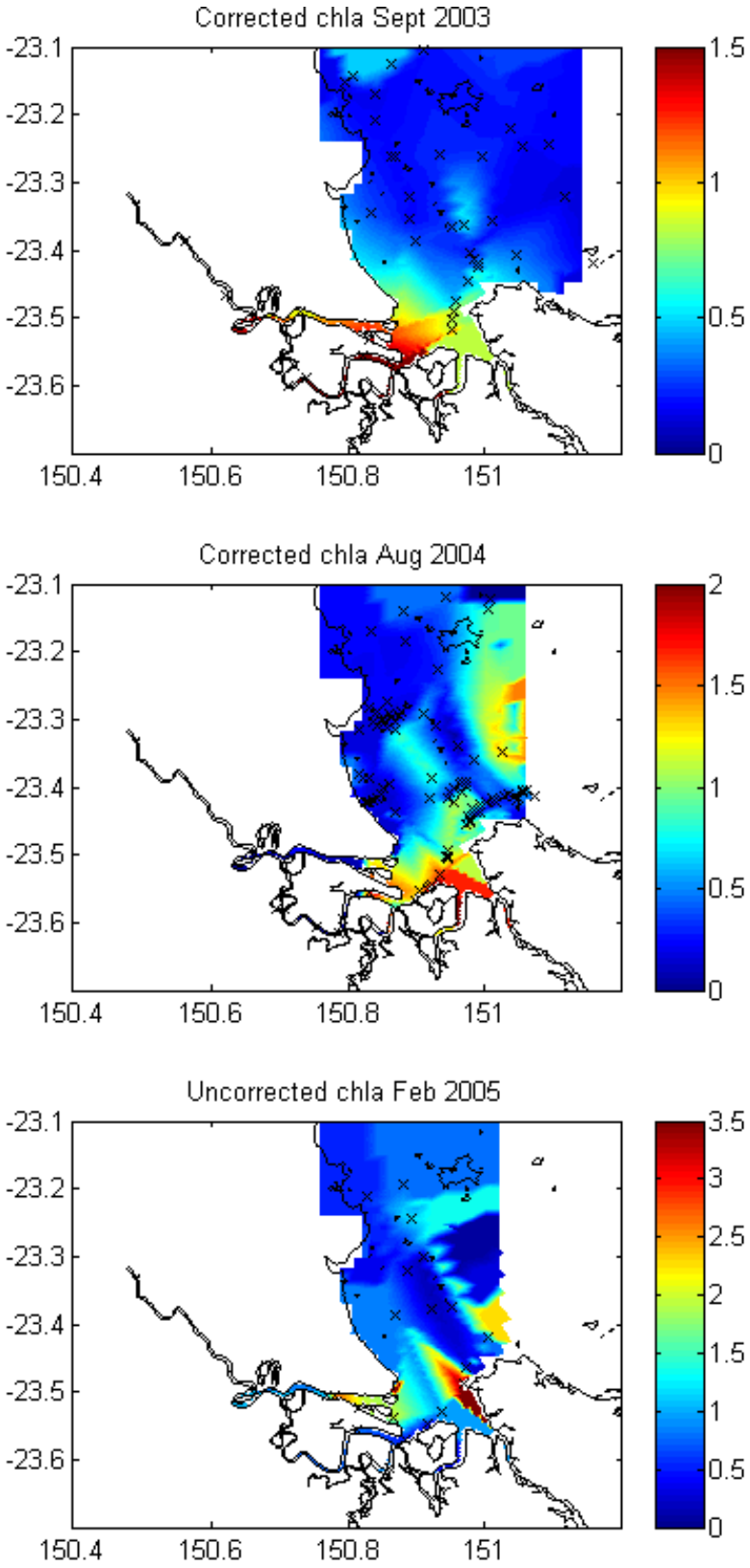

Figure 7.2: Chlorophyll a *concentration in Keppel Bay during CRC cruises. Corrected/uncorrected indicates that the station positions have been adjusted for tidal motion.*

Table 7.1: Taxonomic pigments and relationship to size class, based on data assembled in Vidussi et al. (2000), and Vidussi et al. (2001) and the classification scheme of Claustre (1994).

Pigment	Abbreviation	Taxonomic significance	Size µm
Zeaxanthin	Zea	Cyanobacteria and prochlorophytes	<2
Chlorophyll *b* and divinyl chlorophyll *b*	Chl *b*	Green flagellates and prochlorophytes	<2
19'hexanoyloxyfucoxanthin	Hex-fuco	Chromophytes nanoflagellates	2–20
Alloxanthin	Allo	cryptophytes	2–20
Fucoxanthin	Fuco	Diatoms	>20
Peridinin	Perid	dinoflagellates	>20

The pigment composition shows that a taxonomically diverse community exists at most of the sites despite the differences in total chlorophyll *a* reflecting the biomass of phytoplankton at each site (note that the pigment concentration has been normalized with respect to the total chlorophyll *a* concentration). The principal groups (and the key diagnostic pigment) present (Figure 7.3) are diatoms (Fuco), cyanobacteria (Zea), chromophyte nanoflagellates (hex-fuco), with less frequent occurrences of green flagellates (Chl-b).The diatoms appear to be concentrated in the high turbidity zones near the river mouth and in the inshore areas to the north, while the cyanobacteria are more offshore in the clearer but nutrient depleted waters. No divinylchlorophyll was detected ruling out the presence of significant concentrations of prochlorophytes. Cryptophytes (Allo) occurred at several sites. It is noteworthy that relative proportions of cyanobacteria in February 2005 are considerably reduced relative to their abundance in either August 2003 or September 2004. We hypothesise that these different seasonal species distributions arise due to differing meteorological conditions which prevail. Early 2005 was marked by uncharacteristic strong winds from the south to south west (cool water areas not conducive to *Trichodesmium* growth (Stal *et al.*, 2002)), while in the spring of the two preceding years, winds were more from the north to north east – blowing from warmer waters known to favour *Trichodesmium.* The elevated abundance of diatoms reflects the general capacity of this group to grow under relatively low light conditions, which would arise from the elevated wind-driven resuspension. The implications of the spatial differences in the relative abundance of the different taxonomic groups are still being explored.

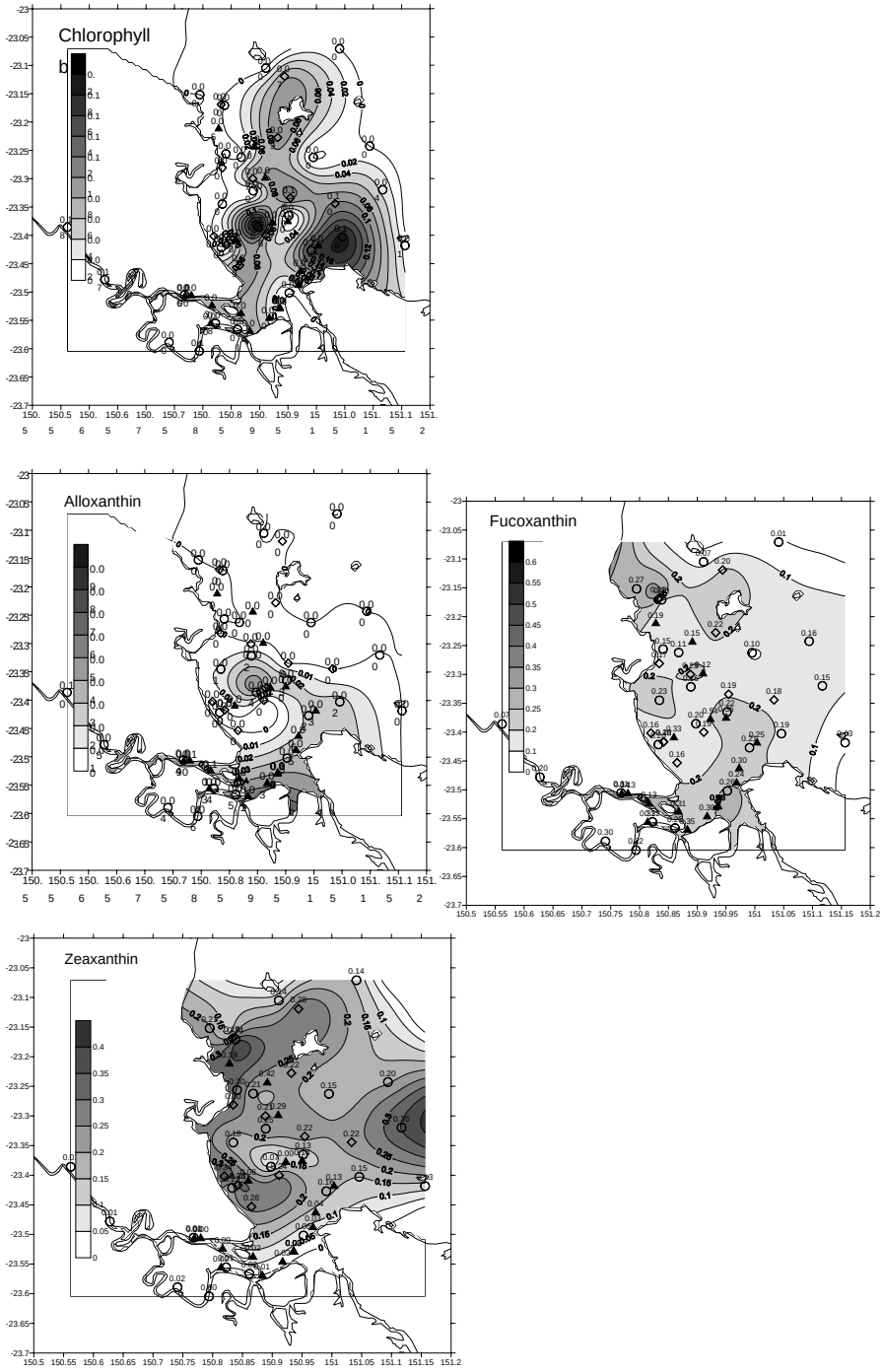

Figure 7.3: Spatial distribution of the relative pigment concentration (normalized to chlorophyll a *concentration) in Keppel Bay.*

Trichodesmium deliveries to the coastal zone

As noted earlier, in summer months the Keppel Bay coastline receives large amounts of *Trichodesmium*. The isotopic ratios: ŭ^{15}N = -0.9$^{0}/_{00}$ and ŭ^{13}C = -14.9$^{0}/_{00}$ are consistent with offshore production using atmospheric nitrogen (average ŭ^{15}N = - 0.4$^{0}/_{00}$; range -0.7 to -0.25$^{0}/_{00}$. ŭ^{13}C= -12.9$^{0}/_{00}$; range -15.2 to -

11.9 $^{0}/_{00}$) (Carpenter *et al.*, 1997). The concentrations of dissolved and particulate nutrients in the littoral *Trichodesmium* (Table 7.2) are all orders of magnitude higher than the values measured within Keppel Bay although they vary widely, reflecting the heterogeneity of the material and the local effects of winds and waves. Thus, the advected material is highly significant nutrient input at the local scale.

Table 7.2: Organic carbon and nutrient concentrations in surface samples of Trichodesmium concentrations collected near the shore line September 2005. Stations are in vicinity of Yeppoon and detailed locations is given in Ford et al. (2005b).

Station	TOC (mg l^{-1})	TN(mg l^{-1})	TP(mg l^{-1})
1	95	-	-
2	200	60	1.4
3	410	135	3
4	8900	2850	60
5	480	120	2.9

Scaling up these concentrations on the basis of a coast line length 20 km and a 100 m wide *Trichodesmium* littoral stretch gives a standing biomass of 20 to 1000 tonnes TOC; 12 to 500 tonnes TN; and 0.2 to 6.6 tonnes of TP. If we assume that the turnover time for this material is comparable to that of the water in Keppel Bay (~20 days) (see Chapter 3) then the amounts of nutrients especially N and P delivered by wind driven advection from off-shore are considerably less than the annual inputs from the Fitzroy Estuary. They are, however, a significant input into Keppel Bay during low flow conditions. Thus, the *Trichodesmium* is a relatively minor contributor to the dry season budget

Dissolved oxygen

Profiles of dissolved oxygen were measured across Keppel Bay and in the mouth of the Fitzroy Estuary during the survey of August 2004. The variation in dissolved concentration between the top and bottom of the water column was mostly less than 1 mgL^{-1} suggesting that the water column was fairly well mixed with respect to oxygen. Depth-averaged concentrations over the study area varied between a minimum of 6.9 mgL^{-1}measured near the mouth of Casuarina Creek (Stn G) to a maximum of 7.3 mgL^{-1} measured on the western side of Keppel Bay at Stn B. Measured oxygen concentrations lay between 94% and 99% of saturation.

The measured oxygen concentrations at the 7 stations that were repeatedly sampled over ~12 h showed a tendency to increase over the day (Figure 7.5). We investigate whether this increase can be explained as being due to photosynthesis in the water column by phytoplankton in an analysis that parallels that undertaken for temperature in Chapter 3.

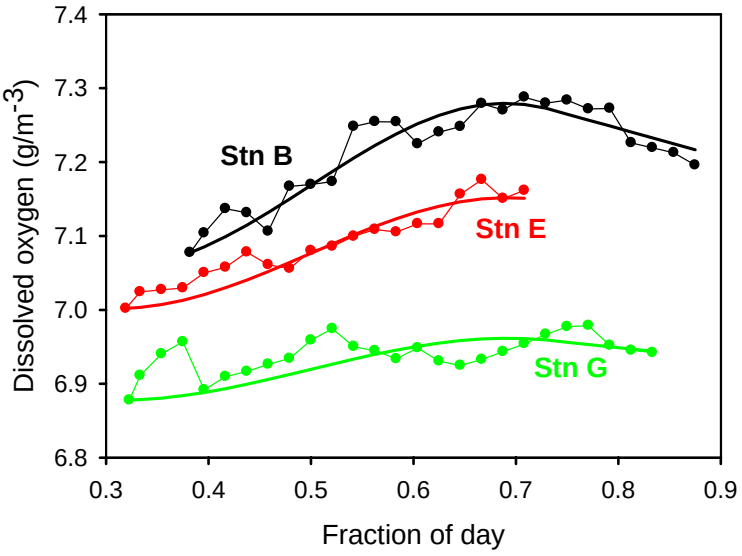

Figure 7.5: Average water column oxygen concentration measured during the day at 3 of the 7 time series sites.

The average rate of change of oxygen concentration in the water column due to photosynthesis can be expressed as:

Equation 7.1

$$\frac{dO}{dt} = \theta(\alpha C\bar{I} - L)$$

where O is oxygen concentration in mgm^3, t is time, ď is the ratio of oxygen production to carbon fixation during photosynthesis, Ŭ is the photosynthetic efficiency, C is the chlorophyll *a* concentration in mgm^3 (assumed uniform with depth), $\bar{I}$ is the average light intensity over the water column, and L is the rate of respiration and other oxygen loss terms including diffusion across the water surface. Assuming that light intensity declines exponentially with depth z as $I = I_0 \exp(-Kz)$, where I_0 is its intensity at the water surface, and K is the light extinction coefficient, then the average irradiance over a water column of depth H is:

Equation 7.2

$$\bar{I} = I_0 \frac{1-\exp(-KH)}{KH}$$

We estimate K from the measured TSS at each station. It ranges from 0.15 m^{-1} at Stn A in central-western Keppel Bay to 3.8 m^{-1} in the mouth of Casuarina Creek. Reynolds (1984) notes that Ŭ, which is the photosynthetic efficiency, has been observed to fall within the range 2–37 mgC(mgchla)$^{-1}$E^{-1}m^2 for phytoplankton, with the peak falling in the range 6–18 mgC(mgchla)$^{-1}$E^{-1}m^2. We initially chose a median value of Ŭ= 10 mgC(mgchla)$^{-1}$E^{-1}m^2. We will further assume that 1 mole of oxygen is released when one mole of carbon is taken up

during photosynthesis so that ɗ = 32 mg/12 mg = 2.67. As with temperature, we will assume that the loss rate during 24 h is uniform and that the net oxygen production is zero. So, $L = \alpha C\bar{\bar{I}}$ where $\bar{\bar{I}}$ is the radiation intensity averaged over 24 h as well as over depth. The radiation intensity is calculated from the height of the sun and assuming clear conditions.

From Equation 7.1 we calculate a modelled time series of oxygen concentration assuming that the concentration at the start equals the measured concentration at that time. The concentration of chlorophyll *a* in the model is adjusted to obtain the optimal fit in a least-squares sense between modelled and measured oxygen concentration at each of the seven stations. Figure 7.6 compares the chlorophyll concentrations estimated this way to those measured at each of the stations. Generally, the modelled and measured concentrations increase together; the best-fit regression between model and measurements has a slope of 2.45.

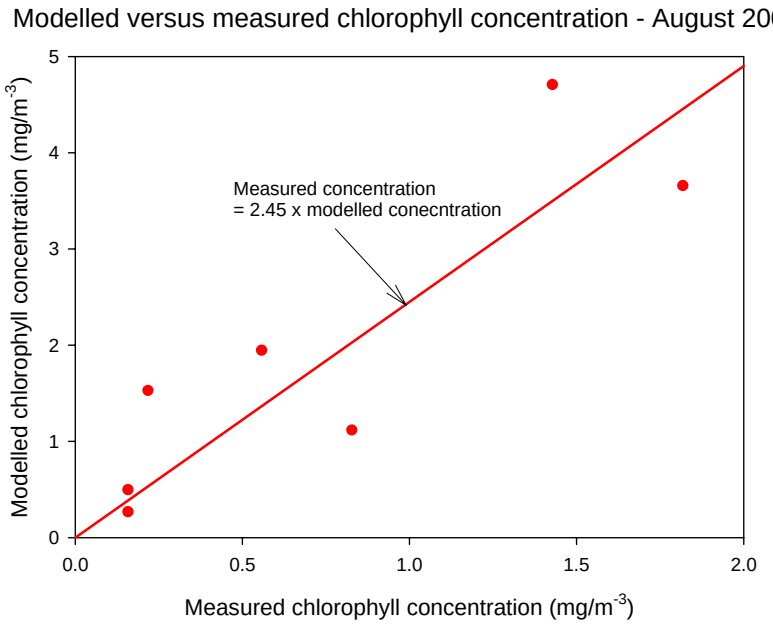

Figure 7.6: Modelled vs. measured chlorophyll concentrations at the time-series sampling stations in Keppel Bay and Casuarina Creek.

There are some several likely explanations for measured concentrations being lower than those predicted by the model. First, the analysis assumes that there is a local equilibrium between oxygen production and oxygen loss from the water column and does not consider the possibility of horizontal advection of oxygen or of oxygen gain and loss not being equal when averaged over a day. Second, at two of the stations (Stns A and B) the water is sufficiently clear that there could be significant oxygen production from benthic algae. At these two stations, the light on the bottom is estimated to be 20% and 18% respectively of that incident at the water surface. At the other stations, the bottom light intensity was

estimated to be less than 0.1% of that incident at the surface. Third, the photosynthetic efficiency in Keppel Bay may be larger than that assumed in the analysis. An assumed value for Ŭof 25 mgC(mgchla)$^{-1}$E^{-1}m^{2} would result in a much improved agreement between model and measurement and this value would still lie within the range that has been reported. A higher value of Ŭmight be expected to occur as a light adaptation of phytoplankton in the light-limited conditions in the inner parts of Keppel Bay and Casuarina Creek.

Using this analysis, we can calculate the estimated production rates (Table 7.3). In Table 7.3 the estimated production rates presented as mgm^{-3} of oxygen fixed through photosynthesis over 24 h use the best-fit modelled chlorophyll concentrations. Despite chlorophyll *a* concentrations varying by a factor of 18, estimated production only varies by a factor of ~3. It seems that the clearest water (lowest *K*) also tends to have the lowest chlorophyll *a* concentrations. In effect, in the parts of the bay having higher phytoplankton concentrations, production is more severely limited by the availability of light necessary for photosynthesis.

Table 7.3: Average water depth, light extinction coefficient, modelled chlorophyll concentration and estimated daily oxygen production at 7 time-series stations.

Station	Average depth (m)	*K*(m^{-1})	Chlorophyll (mg m^{-3})	Production (g-O /m^{-3}-d
A	7.6	0.21	0.26	0.22
B	5.1	0.34	0.49	0.38
C	14.0	0.91	1.11	0.12
D	10.9	0.87	1.94	0.29
E	14.5	0.57	1.52	0.26
F	9.5	2.6	4.7	0.28
G	6.4	5.5	3.65	0.15

We can compare the potential uptake rate of nutrients through photosynthesis to the available nutrient and determine a timescale of nutrient utilisation. Assuming that the photosynthetic ratio is unity, then 32 g of oxygen is released when 12 g of carbon is taken up. Using the atomic Redfield ratios 106:16:1 for C:N:P, then the release of 32 g of oxygen is associated with the uptake of 12 g × 14/12 × 16/106 = 2.11 g of nitrogen if all photosynthetic production results in cell growth, or equivalently that oxygen production of 1 g is associated with the uptake of 66 mg of nitrogen. The corresponding figure for phosphorus uptake is 9 mg. Table 7.4 shows the nitrogen uptake equivalent to the photosynthetic rate listed in Table 7.3. The average DIN and DON for each station are listed together with a calculated timescale for uptake (~concentration/photosynthetic rate).

Table 7.4: Photosynthetic rate expressed as equivalent nitrogen uptake rate, average DIN and DON concentrations, and estimated nutrient uptake timescale for 7 time-series stations.

Station	Photosynthetic N uptake (g-N /m^{-3}-d)	DIN(g/m^3)	Timescale DIN (d)	DON (g/m^3)	Timescale DON (d)
A	0.015	<0.0014	<0.1	0.099	7
B	0.025	<0.0014	<0.05	0.100	4
C	0.008	0.0013	0.2	0.097	12
D	0.019	0.0049	0.3	0.103	5
E	0.017	0.0004	0.2	0.091	5
F	0.018	0.0197	1	0.079	4
G	0.010	0.0271	3	0.148	15

From Table 7.4, at five of the seven stations, the available DIN could support photosynthetic production at the rate estimated from oxygen production for less than a day, whereas at the station close to the mouth Of the Fitzroy Estuary (Stn F) and in Casuarina Creek (Stn G), there was sufficient DIN to support production for a day or longer. For most stations, the filtered reactive phosphorus (FRP) concentration was below the detection limit of 0.002 gm^{-3}. At stations F and G though, FRP concentrations were high enough to sustain photosynthesis for 3 d and 8 d, respectively. The measurements are not able to tell us what the temporal dynamics of the phytoplankton are; that is, whether their local populations are growing or shrinking or whether nutrients are being imported and phytoplankton exported, but these results do suggest a moderately tight cycling between phytoplankton growth and the regeneration of nutrients from phytoplankton mineralisation.

Based on the chlorophyll *a* concentrations at the various sites, and the nitrogen content of the phytoplankton (calculated from the chlorophyll *a* content, a C:N of 50, and Redfield ratio) then the doubling of the standing stock of phytoplankton will require 17.6 μgNL^{-1} when the chlorophyll *a* concentration is 2 μgL^{-1}, and 4.4 μgNL^{-1} when there is 0.5 μgL^{-1} of chlorophyll *a*. From Table 7.4: we see that the inner stations such as F and G have sufficient DIN for a further doubling of the observed biomass of phytoplankton. In contrast, the stations such as 1 and 2 which have low chlorophyll *a* have, proportionately, even less DIN and thus have very limited potential for further growth using DIN. These DIN-depleted conditions more closely resemble the waters further off-shore, and these results explain the dominance of *Trichodesmium* spp., which is able to fix atmospheric nitrogen given an adequate supply of DIP as noted above.

Conceptual models

Transport and mixing processes

We have presented an analysis of features of the oceanography of Keppel Bay and we consider now its characteristics as they relate to the dispersal of material introduced to the system by discharges from the Fitzroy Estuary. The discharge from the Fitzroy River is highly episodic (Webster *et al.* 2004). Most of the discharge occurs during a series of flow events that last several weeks that are typically spread through the summer months January to March, but this is not universally the case. Flows of over 4000 m^3s^{-1} occurred in early September 1998. For most of the year, the flows in the Fitzroy are fairly modest and for a major proportion of the time they are small and sometimes measured to be zero. During times of zero or low discharge during the winter months, much if not most of the freshwater entering the upper end of the estuary is discharge from the Rockhampton Sewage Treatment Plant.

The delivery of nutrients by the Fitzroy River increases in approximate proportion to the discharge volume although delivery will be affected by the particular sub-catchments that are contributing to the flow in the Fitzroy. Fine-sediment deliveries increase at a greater rate than the discharge volume; that is, large flows contribute proportionally greater to total sediment delivery than smaller flows. The variability in annual discharge is very large (Figure 2.3). The year 1991 had an average discharge of 730 m^3s^{-1} whereas 1969 had an average discharge of only 4 m^3s^{-1}, more than two orders of magnitude smaller. The high average flows in 1991 were mostly due to a flood event with discharges of up to 15 000 m^3s^{-1}. This flood event lasted about two weeks. A second major flood occurred a month later.

If a flow event provides a discharge volume less than the volume of the estuary, it will be confined within the estuary, but if much greater, then the excess freshwater will flow into Keppel Bay rendering the estuary fresh all the way to its mouth. In most years, the flows were large enough to fill the estuary at least once. Figure 3.14 shows that in 2005 which was close to the 25%-ile for total annual discharge, the flows occurred as three events each of which had a volume that was similar to the estuary volume. Following the cessation of significant flows in the Fitzroy Estuary at the end of summer, the water in the estuary gradually becomes more saline as seawater is mixed up-estuary by the tidal flows.

During the times of Fitzroy discharge, salinity within Keppel Bay is reduced to a degree that depends on the volume of freshwater discharged. Large enough discharges would cause a brackish plume to spread out from the mouth of the

estuary that floats on more saline water underneath (Figure 8.1). The freshwater discharged into Keppel Bay during the flood of 1991 produced a surface plume approximately 3 m thick (O'Neil *et al.*, 1992) that extended at least as far as the Keppel Islands. Turbulent mixing caused by energetic tidal currents would gradually erode such a plume from below causing its salinity to gradually increase, and the thickness of the fresher water layer to decrease as saltwater from below was mixed into it. The longevity of the plume will be very much affected by the state of the spring-neap tidal cycle, and the volume and rate of freshwater delivery. The mixing power of tidal currents is proportional to the cube of the current speed (Simpson and Hunter, 1974). The doubling of current speed between neap and spring tides would result in an eight-fold increase in the rate at which tidal mixing would reduce stratification.

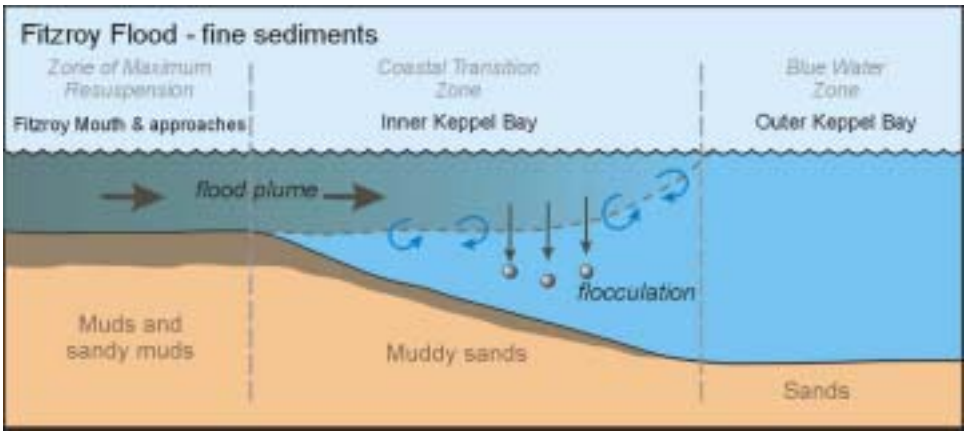

Figure 8.1: Conceptual model of Fitzroy flood plume penetrating into Keppel Bay showing flocculation of fine sediments.

In contrast to the flood of 1991, the much more modest discharge of February 2005 did not cause a distinct surface layer of brackish water to spread throughout Keppel Bay. Typically, surface salinities were only about 1 less than those near the bottom and average salinities through the water column gradually increased away from the mouth.. Thus, some stratification was evident, but it was unlikely to have had a major effect on the biogeochemistry of the system.

During times of low flow (most of the year) in the Fitzroy River, the circulation and mixing within Keppel Bay is dominated by the combined effects of tides and by the wind. Following the cessation of the flows, the salinity within Keppel Bay gradually increases as seawater is mixed or transported shoreward. Eventually, salinities along the western side of the bay exceed those of seawater due to evaporation. The observed enhancement of salinity in western Keppel Bay is consistent with an exchange time between these waters and water outside the bay of ~20 days. This time would also be the timescale for the replacement of dissolved nutrients such as DIN or DIP that are released into the water column

by mineralisation processes within the sediments or the water column. Most of the freshwater discharged into Keppel Bay during a minor flow event in February 2005 remained in the bay a week later.

Tidally averaged current directions along the coast seaward of Curtis Island mostly follow the wind direction. Although wind directions and wind speeds show continuous variation as weather systems pass over the Queensland Coast, the dominant wind direction is southeasterly which results in the current direction being most commonly towards the northwest. The southeasterly winds are strongest and most dominant in summer, which is the most likely time for flood discharges into Keppel Bay. Thus, we would expect that dissolved and particulate nutrients and fine sediments discharged into the GBR Lagoon by the Fitzroy or released into the water column during the dry season would probably be transported along the coast towards the north. However, winds from the north during summer do occur and these were responsible for blowing the plume from the flooding associated with Cyclone Joy in 1991 towards the Capricorn-Bunker Group of coral atolls to the southeast of Keppel Bay.

Fine-sediment dynamics

Fine sediments derived from the Fitzroy discharge are important for their potential to increase turbidity and thereby reduce the light necessary for photosynthesis, as well as for their role as carriers of attached organic matter and nutrients. During floods, the turbidity of the Fitzroy River is very high usually exceeding 1000NTU. This water discharging as a plume into Keppel Bay gradually becomes more saline as it mixes with seawater in the bay. At salinities above ~1.5, many of the particles aggregate through the process of flocculation. These flocs sink out from the water column at a rate very much greater than that of unflocculated particles found in river water and are deposited around the mouth of the Fitzroy Estuary (Figure 7.1). We estimate a characteristic sinking rate for fine sediments in Keppel Bay to be ~2 md^{-1} so that in a water column of 10 m depth, flocculation would tend to cause the water column to clear of fine particles in ~5 days.

However, the tidal currents within Keppel Bay are very strong particularly around the estuary mouth and the channels leading to it. They are capable of resuspending the deposited fine sediments. Thus fine sediment concentrations and turbidity in the water column throughout Keppel Bay are strongly correlated and mainly determined by the settling and resuspension dynamics of the fine particles under the action of tidal currents, and probably wind and waves. For most of the year, what appears in satellite images to be a post-flood plume of sediment emanating from the mouth of the Fitzroy Estuary is actually resuspended sediment and not the river plume itself. Although the instantaneous

flux of fine sediments may be into or out of the estuary or bay, it would seem that averaged over the tidal cycle the net flux of fine sediments is out of the estuary and out of the bay (Figure 8.2). Resuspension rate is a 'strong' function of current speed as long as the shear velocity at the sediment surface is above the critical shear velocity. Thus, we would expect that doubling of the current speed will increase the resuspension rate by many times more than double. One consequence of this dependency is that resuspension is much more effective and suspended sediment concentrations are much higher in the channels approaching the mouth of the Fitzroy Estuary than elsewhere in Keppel Bay. Also, resuspension rates and net sediment fluxes are much higher during times of spring tides than during neap tides.

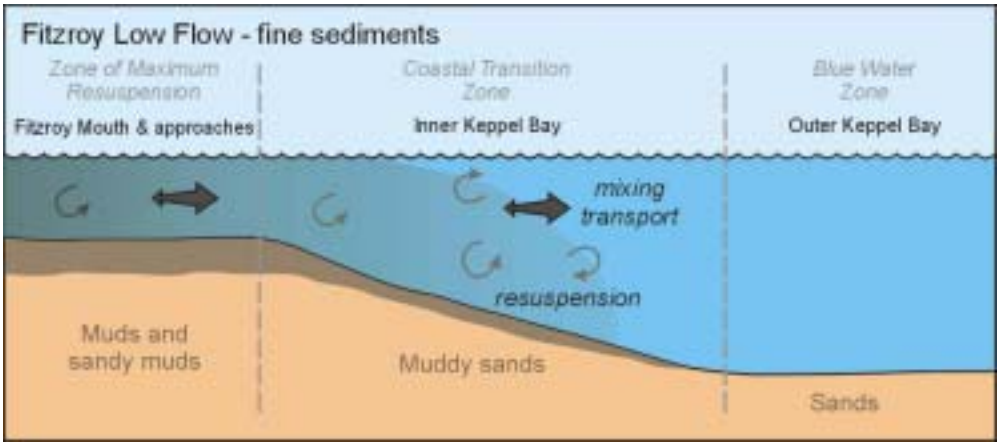

Figure 8.2: Conceptual model of mixing processes and fine sediment transport in The Fitzroy Estuary and Keppel Bay.

The flux of fine sediment through the main channel at Timandra Buoy to the northwest of Curtis Island was calculated to be the equivalent of 2.1 MYy^{-1} in August 2004, which is about half the estimated average annual delivery of fine sediment to the estuary. Close to the mouth at Buoy 1, the flux out of the estuary was calculated to be 0.5 MTy^{-1} immediately following the minor flood in January-February 2004 reducing to 0.24 MTy^{-1} in August of the same year. It would appear that the zone between the two buoys is one where deposition would have occurred during floods, but which was undergoing net erosion of fine sediments during the dry season. These transport estimates are for two sections of the main channel only and do not account for sediment transport over large areas of the rest of the system.

Much of the shallower region in the centre-western side of Keppel Bay has bottom sediments with a high proportion of mud. Satellite images show higher suspended sediment concentrations on the western side of the bay than in the deeper water further east. Tidal currents in the centre and northern parts of the bay are a lot smaller than they are in the approaches to the Fitzroy.

Nevertheless, we might suppose that fine sediments that are suspended in the more active resuspension zone in the Fitzroy mouth are carried northward by wind-currents. In addition, this area is subject to waves propagating from the east. Waves could be effective agents for sediment resuspension along the relatively shallow western side of Keppel Bay. High waves having significant heights greater than 2 m occur several times a year and have durations of a few days (QEPA 2002, 2003, 2004). These events are more likely to occur in the summer months. Due to the highly non-linear dependence of sediment resuspension on bottom current speed, it is probable that these wave events cause a disproportionate movement of fine sediments in the region. The effects of cyclone passage over the bay when it occurs are likely to be even more profound.

Nutrient dynamics and primary production

Sediment and nutrients are discharged from the Fitzroy River into Keppel Bay. As mentioned previously, the time taken for salinity near the head of the estuary to approach that of seawater is ~100 d (Webster *et al.* 2004). Thus for flows that do not exceed the estuary volume, the nutrient inputs associated with the discharge can be subject to transformation reactions and storage processes within the estuary or significant periods of time that can potentially reduce the amounts eventually exported to Keppel Bay. Conversely, the proportion of the flow larger than the estuary volume would pass quickly through the estuary and input nutrients and sediments directly into Keppel Bay. The analysis of TN in the Fitzroy Estuary by Webster *et al.* (2005) showed that export efficiency of nitrogen in the summer of 2000/2001 was 95% versus only 55% the following summer. The flows in the first summer were large enough to fill the estuary 13 times, whereas during the second summer the estuary would have been filled less than twice. For the purposes of this section, we consider only the low-flow condition because we did not have the opportunity to study a large flood event.

Nutrient dynamics in Keppel Bay under low-flow conditions reflects the interplay of internal biogeochemical processes, biological utilisation and hydrodynamic factors which govern the distribution and concentrations of fine-grained sediments in the seabed and overlying water column (i.e. dispersion, mixing and resuspension). In Chapter 5 it was shown that Keppel Bay can be divided into three biogeochemical zones based on the nature of the underlying sediment, TSM levels and on behaviour of dissolved inorganic nutrients in the dry season mixing diagrams. Accordingly, the conceptual model of dissolved nutrient dynamics (Figure 8.3) under low flow conditions is divided into three segments based on these zones i.e. the: Zone of Maximum Resuspension (ZMR), the Blue Water Zone (BWZ) and the Coastal Transitional Zone (CTZ).

Ultimately, these zones derive from the hydrodynamics of the bay. The ZMR encompassing the approaches to the Fitzroy Estuary and tidal creeks has high tidal currents causing active resuspension of fine particles and high turbidity. The CTZ, which covers most of the western side of Keppel Bay, is characterised by smaller tidal currents but being relatively shallow is subject to some resuspension due to the combined effects of tidal currents and waves. In the deeper BWZ further offshore, the effects of waves on resuspension is diminished. Also, the water in this zone is subject to exchange with clearer water from across the seaward boundary of Keppel Bay.

A range of different phytoplankton functional groups are present in Keppel Bay but their relative abundance reflects the adaptive capabilities of the various groups and the different physical and chemical conditions in the different parts of the Bay. These differences are highlighted in Figure 8.4.

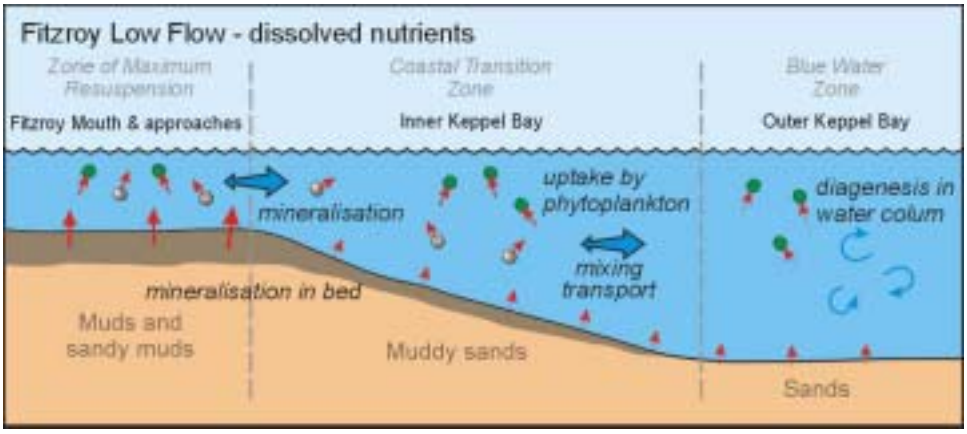

Figure 8.3: Conceptual model of dissolved nutrient dynamics under low-flow conditions in Keppel Bay.

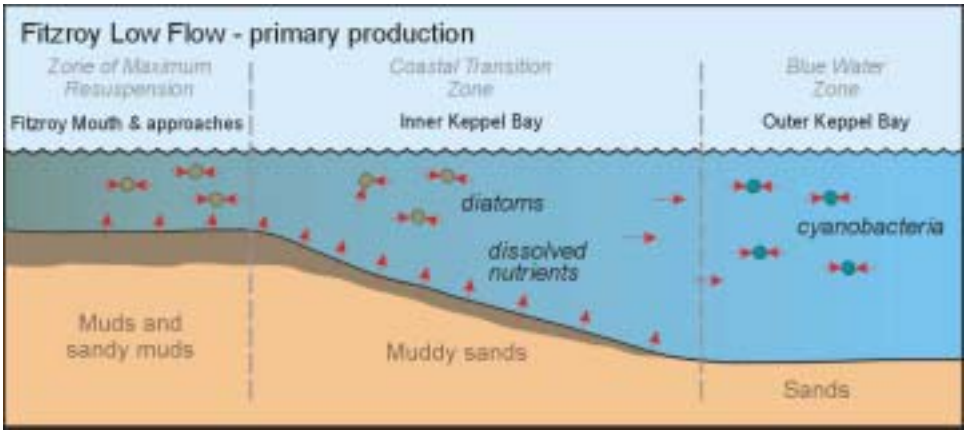

Figure 8.4: Conceptual model of primary production under low-flow conditions in Keppel Bay

About l of nutrients are delivered to the Keppel in the particulate form, and mainly as organic constituents on soil particles while the remainder is in dissolved forms (Douglas *et al.*, 2005). The dissolved materials move with the

plume and are mixed into the saline waters as the plume dissipates. Usually about 10 days after the end of a flood event, the water clears sufficiently (see below) and a phytoplankton bloom occurs consuming the available dissolved nutrients (Brodie and Mitchell, 1992). Most of the soil particles contained in the flood are deposited near the mouth of the estuary in the ZMR due to flocculation (Figure 8.1). Over time, the strong tidal currents near the mouth of the estuary cause the resuspension, entrainment and transport of a large component of this fine sediment to deeper into the tidal creeks where much of it is ultimately deposited. Burial of sediment in the tidal creeks is an important sink for nutrients in the ZMR (Tables 5.2 and 5.3).

The large concentrations of suspended sediment in the ZMR limit the extent to which primary producers can utilise the available nutrients. Results in Chapter 7 indicate that there is at least enough dissolved inorganic nitrogen to support two days further growth. Therefore, dissolved nutrients build up in the water column in the ZMR, and they behave conservatively with respect to salinity (Figure 5.12). This is despite the fact that maximum chlorophyll *a* concentrations occur near the ZMR. Diatoms were the main taxonomic group in the ZMR, also due to the energetics of the region. Because diatoms sink, the need to be actively resuspended and mixed through the water column in order to access the light near the water surface that they need for photosynthesis.

Under the dry season conditions, the dissolved nutrients are mainly derived from the mineralisation/diagensis of algae as well as soil particles deposited during a previous flood event (Figure 5.3). Sediment mixing and re-working in energetic coastal environments enhances overall mineralisation rates by transporting previously reduced Mn and Fe compounds to zones where they can be re-oxidised and thus be used again in the degradation of organic matter (Chapter 5).

Dissolved nutrients are moved by tidal mixing and wind currents from the ZMR to the CTZ where the light climate is more conducive to their biological utilisation (i.e. TSM levels are usually < 10 mg L^{-1}). Indeed, the CTZ is probably the zone of maximum biological uptake based on the results of this study. As FRP was detectable in more samples than NO_X in the CTZ, it is likely that nitrogen was the limiting nutrient in this zone (Figure 5.9; Table 5.7). There is evidence that that abundant nitrogen is added to the CTZ through the activity of nitrogen fixing organisms (Figure 5.7b) to compensate for nitrogen limitation. As shown in Chapter 7, cyanobacteria (both the filamentous *Trichodesmium* and the smaller unicellular species) were the main phytoplankton groups present in the CTZ, and seasonal shoreline accumulations of *Trichodesmium* occurred in spring due to prevailing onshore wind direction. Their significance on a Keppel Bay scale is

limited however. As with the ZMR, the degradation of algae (and a smaller component of soil) can occur in the water column or bottom sediment. Burial has been shown to be a relatively minor sink for nutrients along the western shore of Keppel Bay (Tables 5.2 and 5.3), where the under-lying sediments consist mainly of muddy-sands.

Tidal mixing and wind-driven current may move phytoplankton from the CTZ to the BWZ further out in Keppel Bay. As dissolved inorganic nutrients were always below detection limits in this zone, it is likely that primary productivity was nutrient limited and that nutrients are subject to rapid re-cycling. In fact, the bulk of the N and P demand in this zone is probably met by microbial breakdown of organic matter in the water column because pico-phytoplankton (mainly cyanobacteria) do not sink readily, and because the water column is much deeper here. Pico-phytoplankton (mainly cyanobacteria) are frequently P-limited, and are known to utilise available components within the DOP pool. This might explain why TN:TP ratios were at their highest in the BWZ (Table 5.7). Despite the pre-dominance of cyanobacteria in the BWZ, denitrification was found to prevail over N-fixation in our benthic measurements. This is presumably due to the low Fe concentrations of the underlying sediments. These relict sediments have been in the marine environment for a long time and consequently much of the mud has been winnowed out of them. However, N-fixation probably occurs in the water column.

Preliminary N and P budgets

Based on the results of this study we can derive preliminary N and P budgets for Keppel Bay. Some estimates of sediment and nutrient loads to Keppel Bay under low flow conditions are presented in Table 8.1, and there is good correspondence between the TN and TP loads for 1994–1998 (Douglas *et al*., 2005), those estimated by Furnas (2001) and those calculated on the basis of Figure 5.3 in this study (Table 5.4). The range and median values from Table 8.1 are used to define the catchment loads of TN and TP to Keppel Bay These are presented in the form of simplified nutrient budgets in Figure 8.5 and Figure 8.6. The overall conclusion is that a fraction of the incoming material is retained within Keppel Bay with the retention efficiency declining as the load goes up. It also appears that proportionately more of the sediments than the attached nutrients are exported from Keppel Bay, assuming that the annual average sediment load is 4.7 MT. Nutrient and sediment loads based on different management scenarios are presented in Robson *et al.*, (2006).

Table 8.1: Estimates of sediment and nutrient inputs to Keppel Bay. All units are tonnes except for TSS which is in kilo-tonnes.

Year	SOURCE	DIN	DON	PN	TN	DIP	DOP	PP	TP	TSS
Multiple	Furnas (2003)[a]	1198	845	3058	5101	157	54	790	1001	2230
1994	Douglas *et al.* (2005)				5835				1362	
1995	Douglas *et al.* (2005)				5834				117	
1996	Douglas *et al.* (2005)				6240				1454	
1997	Douglas *et al.* (2005)				3055				844	
1998	Douglas *et al.* (2005)				5744				1838	
2003-2005	Figure 5.3 & Table 5.4 (this report)				5440				2000	
Multiple	Dougall (2005)[b]									4575
2003-2005	Margvelashvili *(in prep)*[c]									1700
Multiple	Joo *et al.*, (2005)									3090

a) From Furnas (2001), Table 32, pg. 209. These were calculated by multiplying volume specific sediment export coefficients my mean annual freshwater discharges.

b) Based on improved SedNet estimates

c) Loads were derived from a regression between TSS concentrations near the barrage and river flow 1990-1994: TSS = (0.5*RiverFlow +15)/1000).

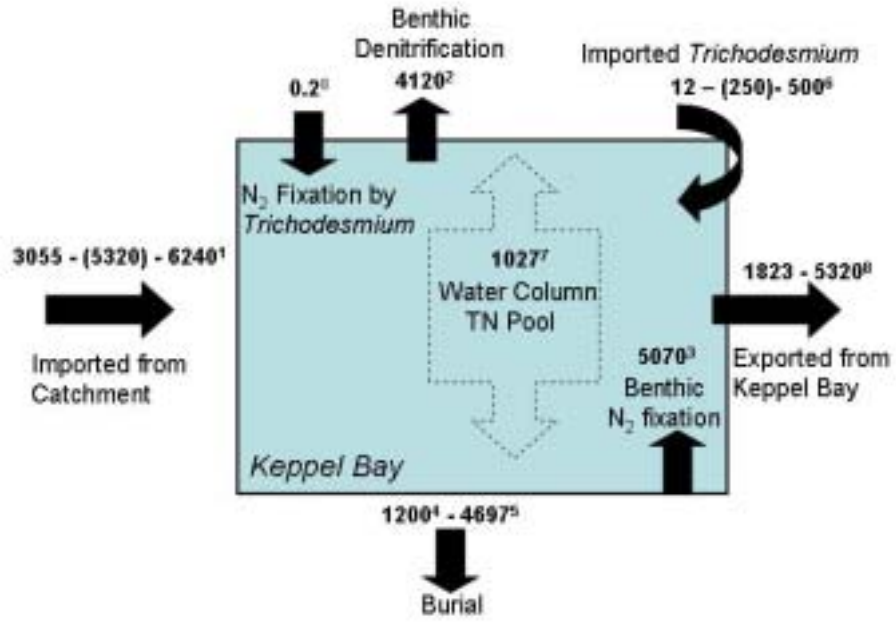

Figure 8.5: A preliminary N budget for Keppel Bay. All inputs and outputs are in tonnes: 1. N inputs from the catchment are derived from Table 8.1 (the median and range are shown); 2&3. Benthic denitrification and N-fixation rates are derived from Figure 5.7; 4&5. Burial rates are derived from Tables 5.2 and 5.3; 6. Imported N in Trichodesmium values are derived from Chapter 7 (the approximate median is shown in brackets); 7. Water column inventory is based on the average of dry season TN values in Table 5.6; 8. Export rates are based on the sum of the inputs (medians are used when shown) minus denitrification minus burial. Two values are shown to account for the range of burial rates.

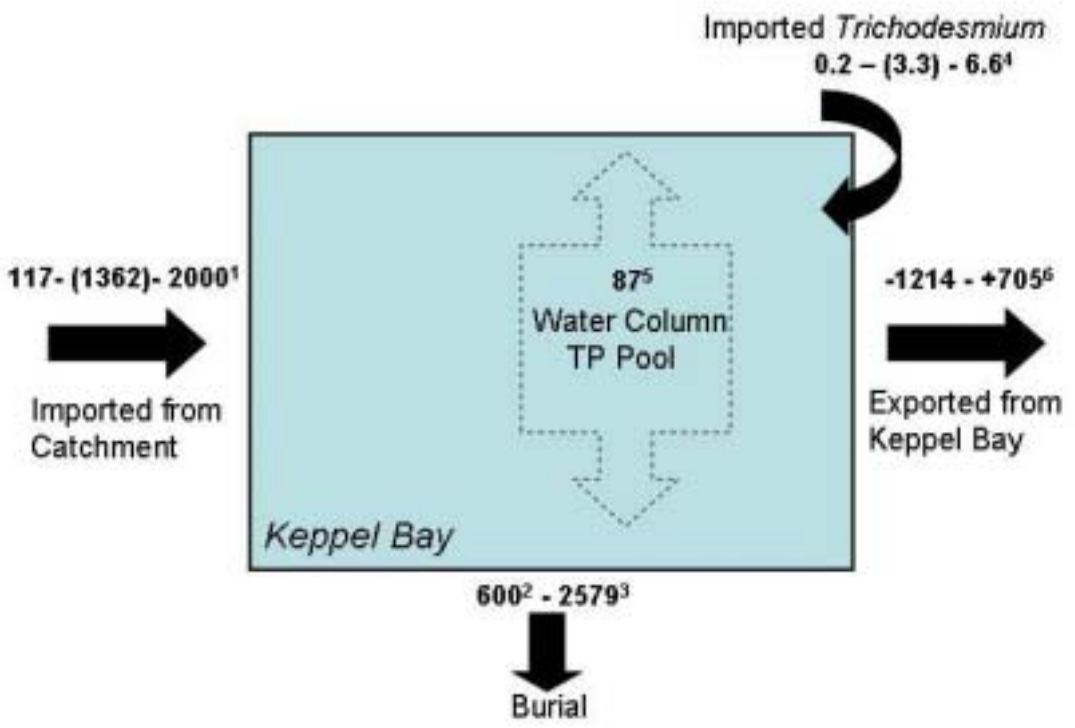

Figure 8.6: A preliminary P budget for Keppel Bay. All inputs and outputs are in tonnes: 1. P inputs from the catchment are derived from Table 8.1 (the median and range are shown); 2&3. Burial rates are extracted from Tables 5.2 and 5.3; 4. Imported N in Trichodesmium values are taken from Chapter 7 (the approximate median is shown in brackets); 5. Water column inventory is based on the average of dry season TP values in Table 5.6; 6. Export rates are based on the sum of the inputs (medians are used when shown) minus burial. Two values are shown to account for the range of burial rates.

References

Abril, G., Riou, S.A., Etcheber, H., Frankignoulle, M., de Wit, R. and Middelburg, J.J. 2000. Transient, tidal time-scale, nitrogen transformations in an estuarine turbidity maximum-fluid mud system (The Gironde, South-west France). *Estuarine, Coastal and Shelf Science* 50, 703–715.

Affourtit, J., Zehr, J.P. and Paerl, H.W. 2001. Distribution of nitrogen-fixing microorganisms along the Neuse River estuary, North Carolina. *Microbial Ecology* 41, 114–123.

Agawin, N.S., Duarte, C.M., Agusti, S. and Vaque, D. 2004. Effect of N:P ratios on the response of Mediterranean picophytoplankton to experimental nutrient inputs. *Aquatic Microbial Ecology* 34, 57–67.

Aller, R.C., Mackin, J.E. and Cox, R.T. 1986. Diagenesis of Fe and S in Amazon inner shelf muds: apparent dominance of Fe reduction and implications for the genesis of ironstones. *Continental Shelf Research* 6(1/2) 263–289.

Aller, R.C., Blair, N.E., Xai, Q. and Rude, P.D. 1996. Remineralisation rates, recycling, and storage of carbon in Amazon shelf sediments. *Continental Shelf Research* 16, 753–786.

Aller, R.C. 1998. Mobile deltaic and continental shelf muds as suboxic, fluidized bed reactors. *Marine Chemistry* 61, 143–155.

Aller, R.C. and Blair, N.E. 2004. Early diagenetic remineralisation of sedimentary organic C in the Gulf of Papua deltaic complex (Papua New Guinea): Net loss of terrestrial C and diagenetic fractionation of C isotopes. *Geochimica et Cosmochimica Acta* 68(8), 1815–1825

Alongi, D. 1995. Decomposition and recycling of organic matter in muds of the Gulf of Papua , northern Coral Sea. *Continental Shelf Research* 15, 1319–1337.

Alongi, D. and Robertson, A.I. 1995. Factors regulating benthic food chains in tropical river deltas and adjacent shelf area. *Geo-Marine Letters* 15, 145–152.

Alongi, D.M. and McKinnon, A.D. 2005. The cycling and fate of terrestrially-derived sediments and nutrients in the coastal zone of the Great Barrier Reef. *Marine Pollution Bulletin* 51, 239–252.

Anonymous 1979. Beaches of the Capricorn Coast. Beach Protection Authority, Brisbane.

Anonymous 2005. Long term monitoring of chlorophyll *a* concentrations in the Great Barrier Reef Marine Park. Reef CRC, Townsville. http://adc.aims.gov.au:9555/chloro/do/gotoStart.do

Aufdenkampe, A.K., Hedges, J.I., Richey, J.E., Krusche, A., V. and Llerena, C.A. 2001. Sorptive fractionation of dissolved organic nitrogen and amino acids onto fine sediments within the Amazon Basin. *Limnology and Oceanography* 46(8), 1921–1935.

Bell, P.R.F., Elmetri, I. and Uwins, P.J.R. 1999. Nitrogen fixation of *Trichodesmium* spp. In the Central and Northern Great Barrier Reef Lagoon: relative importance of the fixed-nitrogen load. *Marine Ecology Progress Series* 186, 119–126.

Bell, P.R.F., Uwins, P.J.R., Elmetri, I., Phillips, J.A., Fu, F-X. and Yago, J.E. 2005. Laboratory culture studies of Trichodesmium isolated from the Great Barrier Reef Lagoon, Australia. *Hydrobiologia* 532, 9–21.

Berg, G.M., Glibert, P.M., Lomas, M.W. and Burford, M.A. 1997. Organic nitrogen and growth by the chrysophyte *Aureococcus anophagefferens* during a brown tide event. *Marine Biology* 129, 377–387.

Berman, T. and Bronk, D.A. 2003. Dissolved organic nitrogen: a dynamic participant in aquatic ecosystems. *Aquatic Microbial Ecology* 31, 279–305.

Bird, M.I., Brunskill, G.J. and Chivas, A.R. 1995. Carbon-isotope composition of sediments from the Gulf of Papua. *Geo-Marine Letters* 15,153–159.

Bostock, H., Brooke, B., Ryan, D.A. and Hancock, G.J. 2005a. *Keppel Bay vibracores and sediment accumulation rates.* Cooperative Research Centre for Coastal Zone, Estuary and Waterway Management Agricultural (Fitzroy) Project, Contaminants Dynamics Sub-project, Milestone Report AC48.

Bostock, H., Radke, L., Brooke, B. and Ryan, D. 2005b. *Report on sediments in lagoons on the Fitzroy River lower floodplain and tidal creeks.* Cooperative Research Centre for Coastal Zone, Estuary and Waterway Management Agricultural (Fitzroy) Project, Contaminants Dynamics Sub-project, Milestone Report AC5supp6.

Bostock, H.C., Ryan, D., Brooke, B., Hancock, G., Piestch, T., Harle, K. and Moss, P. *in prep*., *Sediment accumulation in the Fitzroy River floodplain, estuary and billabongs, southeast Queensland, Australia.* Cooperative Research Centre for Coastal Zone, Estuary and Waterway Management Agricultural (Fitzroy) Project, Contaminants Dynamics Sub-project, Milestone Report AC65.

Brando V.E., Dekker A.G., Marks A., Qin Y. and Oubelkheir, K. 2006. *Chlorophyll and Suspended Sediment Assessment in a Macro-Tidal Tropical Estuary Adjacent to the GBR: Spatial and Temporal Assessment Using Remote Sensing.* A Report to the Cooperative Research Centre for Coastal Zone, Estuary and Waterway Management (in preparation).

Brodie, J.E. and Mitchell, A. 1992.Nutrient composition of the January 1991 Fitzroy River plume. In: Proceedings of a workshop on the impacts of flooding (Ed; G. T. Byron) Workshop Series 17, Great Barrier Reef Marine Park Authority, Townsville, pp. 56–74.

Brooke B., Ryan, D.A. and Radke, L. 2005. *Report on the Capricorn Coast Beach Sediments Milestone Reports AO03 and AO13.* Cooperative Research Centre for Coastal Zone, Estuary and Waterway Management. pp. 17.

Brooke, B., Ryan, D., Radke, L., Pietsch, T., Olley, J., Douglas, G., Flood, P. and Packett, B. *in prep*. *Records of changes in climate, sea level and landuse over the last 1,500 years preserved in beach deposits at Keppel Bay, Queensland, Australia.*

Burban, P.-Y., Lick, W. and Lick, J. 1989. The flocculation of fine-grained sediments in estuarine waters. *Journal of Geophysical Research*. 94(C6) 8323–8330.

Burns, J.A., Zehr, J.P. and Capone, D.G. 2002. Nitrogen-fixing phylotypes of Chesapeake Bay and Neuse River Estuary Sediments. *Microbial Ecology* 44, 336–343.

Burrage, D.M., Steinberg, C.R., Skirving, W.J. and Kleypas, J.A. 1996. Mesoscale circulation features of the Great Barrier Reef Region inferred from NOAA satellite imagery. *Remote Sensing of the Environment*, 56:21–41.

Burrage, D., Steinberg, C., Bode, L. and Black, K. 1997. Long-term current observations in the Great Barrier Reef. In Wachenfeld, D., Oliver, J. and Davis, K. (eds), State of the Great Barrier Reef World Heritage Area Workshop. Proceedings of a technical workshop held in Townsville, Queensland, Australia 27–29 November 1995. (GBRMPA Workshop Series; 23). Great Barrier Reef Marine Park Authority, Townsville, 21–45.

Bureau of Meteorology 2005. Climate averages for Australian Sites: http://www.bom.gov.au/climate/averages/tables/ca_qld_names.shtml

Carpenter, E.J., and Capone, D.G. 1992.Nitrogen fixation in Trichodesmium blooms. In: Carpenter, E.J., D.G. Capone, and J.G. Reuter (eds). Marine pelagic cyanobacteria: Trichodesmium and other diazotrophs. Kluwer Academic publishers, Dordrecht, pp. 211–217.

Carpenter, E.J., Harvey, H.R., Fry, B. and Capone, D.G. 1997. Biogeochemical tracers of the marine cyanobacterium *Trichodesmium*. *Deep-Sea Research I* 44:27–38.

Claustre, H. 1994. The trophic status of various oceanic provinces as revealed by phytoplankton pigment signatures. *Limnology and Oceanography* 39:1206–1210.

Currie, D.R. and Small, K.J. 2002. *Macrobenthic community structure in the Fitzroy River Estuary.* Report to Cooperative Research Centre for Coastal Zone, Estuary, and Waterway Management.

Devlin, M., Waterhouse, J., Taylor, J. and Brodie, J. 2001. Flood plumes in the Great Barrier Reef: Spatial and temporal patterns in composition and distribution. Great Barrier Reef Marine Park Authority Research Report No. 68, Great Barrier Reef Marine Park Authority, Townsville.

Devlin, M.J. and Brodie, J. 2005. Terrestrial discharge into the Great Barrier Reef Lagoon: nutrient behaviour in coastal waters. *Marine Pollution Bulletin* 51, 9–22.

Dore, J., Brum, J.R., Tupas, L.M. and Karl, D.M. 2002. Seasonal and inter annual variability in sources of nitrogen supporting export in the oligotrophic subtropical North Pacific Ocean. *Limnology and Oceanography* 47:1595–1607.

Douglas, G., Ford, P., Palmer, M., Noble, R. and Packett, R. 2005a. *Identification of sediment sources in the Fitzroy River Basin and Estuary, Queensland, Australia Nutrient and carbon cycling in subtropical estuaries (Fitzroy) – FH1.* Cooperative Research Centre for Coastal Zone, Estuary and Waterway Management. Technical Report No 13, 32 pp. (www.coastal.crc.org.au/pdf/TechnicalReports/13-Fitzroy_geochemistry.pdf).

Douglas, G. D., Ford, P. W., Moss, A. J., Noble, R. M., Packett, R., Palmer, M., Revill, A., Robson, B., Tillman, P. and Webster, I. T. 2005b. *Carbon and nutrient cycling in a subtropical estuary (the Fitzroy), Central Queensland.* Cooperative Research Centre for Coastal Zone, Estuary and Waterway Management. Technical Report 14. 72 pp.

Donald K.M., Scanlan D.J., Carr N.G., Mann N.H., Joint, I. (1997). Comparative phosphorus nutrition of the marine cyanobacterium *Synechococcus* WH7803 and the marine diatom *Thalassiosira weissflogii. J Plankton Res* 19: 1793–1813.

Dore, J., Brum, J.R., Tupas, L.M. and Karl, D.M. 2002. Seasonal and inter annual variability in sources of nitrogen supporting export in the oligotrophic subtropical North Pacific Ocean. *Limnology and Oceanography* 47:1595–1607.

Dougall, C., Packett, R. and Carroll, C. 2005. Application of the SedNet model in partnership with the Fitzroy Basin community. In Zerger, A. and Argent, R.M. (eds) MODSIM 2005 International Congress on Modelling and Simulation. Modelling and Simulation Society of Australia and New Zealand, December

2005, pp. 170–176. ISBN: 0-9758400-2-9. http://www.mssanz.org.au/modsim05/papers/dougall.pdf.

Easton, A. 1970. Tides of the Continent of Australia. Horace Lamb Centre, Research paper No. 37, The Flinders University of South Australia, 326 pp.

Eyre, B. 1994. Nutrient biogeochemistry in the tropical Moresby River Estuary System North Queensland, Australia. *Estuarine, Coastal and Shelf Science* 39, 15–31.

Eyre, B.D. 2000. Regional evaluation of nutrient transformation and phytoplankton growth in nine river-dominated sub-tropical east Australian estuaries. *Marine Ecology Progress Series* 205, 61–83.

Eyre, B. and Ferguson, A.J.P. 2002. Sediment biogeochemical indicators for defining sustainable nutrient loads to coastal ecosystems, Proceedings of Coast to Coast 2002 – "Source to Sea", Tweed Heads, pp. 101–104.

Folk, R.L., Andrews, P.B. and Lewis, D.W., 1970. Detrital sedimentary rock classification and nomenclature for use in New Zealand. NZ J. *Geol. and Geophys*. 13, 937–968.

Ford, P., Tillman, P., Robson, B. and Webster, I.T. 2005a. Organic carbon deliveries and their flow related dynamics in the Fitzroy estuary. *Marine Pollution Bulletin* 51, 119–127.

Ford, P. W., Radke, L.C., Webster, I.T., Robson, B., Atkinson, I., Tindall, C., Verwey, P., Steven, A., Hodge, J., Thornton, P. and Ferris, J. 2005b. *Pelagic primary production and nutrient dynamics in coastal creeks delivering into Keppel Bay.* Cooperative Research Centre for Coastal Zone, Estuary and Waterway Management. Milestone Report AC 32. 44 pp.

Froelich, P.N. 1988. Kinetic control of dissolved phosphate in natural rivers and estuaries: A primer on the phosphate buffer mechanism. *Limnology and Oceanography* 33, 649–668.

Fukuda, R., Ogawa, H., Nagata, T. and Koite, I. 1998. Direct determination of carbon and nitrogen contents of natural bacterial assemblages in marine environments. *Applied and Environmental Microbiology* 64(9), 3352–3358.

Fuller, N.J., West, N.J., Marie, D., Yallop, M., Rivlin, T., Post, A.F. and Scanlan, D.J. 2005. Dynamics of community structure and phosphate status of picocyanobacterial populations in the Gulf of Aqaba, Red Sea. *Limnology and Oceanography* 50(1), 363–375.

Furnas, M.J. and Brodie, J. 1996. Current status of nutrient levels and other water quality parameters in the Great Barrier Reef. In H.M. Hunter, A.G. Eyles

and G.E. Rayment, *Downstream Effects of Land Use*, Queensland Department of Natural Resources, pp. 9–21.

Furnas, M. 2003. Catchments and Corals. Australian Institute of Marine Science, pp. 334.

Furnas, M., Mitchell, A., Skuza, M. and Brodie, J. 2005. In the other 90%: phytoplankton responses to enhanced nutrient availability in the Great Barrier Reef. *Marine Pollution Bulletin* 51, 253–265.

Gagan, M.K., Sandstrom, M.W. and Chivas, A.R. 1987. Restricted terrestrial carbon input to the continental shelf during Cyclone Winifred: implications for terrestrial runoff to the Great Barrier Reef Province. *Coral Reefs* 6, 113–119.

Gentilli, J. 1971. Climates of Australia and New Zealand, (vol. 13. of World Survey of Climatology), Elsevier, Amsterdam, 1971.

Gentilli, J. 1972. Australian Climate Patterns, Thomas Nelson (Australia) Limited, Melbourne, 285 pp.

Glibert, P.M., and Bronk, D.A. 1994. Release of dissolved organic nitrogen by marine diazotrophic cyanobacterium, *Trichdesmium* spp. *Appl. Environ. Microbiol*. 60, 3996–4000.

Gippel, C.J. 1989. The Use of Turbidity Instruments to Measure Stream Water Suspended Sediment Concentration. Monograph Series No. 4, Department of Geography and Oceanography, University College, Australian Defence Force Academy, Canberra, 204 pp.

Gippel, C.J. 1995. Potential of turbidity monitoring for measuring the transport of suspended solids in streams. *Hydrological Processes*, 9: 83–97.

Goni, M.A., Cathey, M.W., Kim, Y.H. and Voulgaris, G. 2005. Fluxes and sources of suspended organic matter in an estuarine turbidity maximum region during low discharge condition. Estuarine, *Coastal and Shelf Science* 63, 683–700.

Grant, W.D. and Madsen, O.S. 1979. Combined wave and current interaction with a rough bottom, *Journal of Geophysical Research*, 84(C4) 1797–1808.

Griffin, D.A., Middleton, J.H. and Bode, L. 1987. The tidal and longer-period circulation of Capricornia, Southern Great Barrier Reef. *Australian Journal of Marine and Freshwater Research*, 38: 461–474.

Haese, R.R. 2000. The reactivity of iron. In Schultz, H.D and M Zabel (Eds). Marine Geochemistry. Springer-Verlag, Berlin.

Hamon, B.V. and Greig, M.A. 1972. Mean sea level in relation to geodetic land leveling around Australia. *Journal of Geophysical Research*, 77(36), 7157–7162.

Hancock, G.J. and Ford, P.W. 2004. *Suspended sediment deposition and transport ion Keppel Bay: 2004 dry season sample collection and analysis.* Cooperative Research Centre for Coastal Zone, Estuary and Waterway Management. Milestone Report AC34.

Harris, G.P. 2001. Biogeochemistry of nitrogen and phosphorus in Australia catchments, rivers and estuaries: effects of land use and flow regulation and comparison with global patterns. *Marine and Freshwater Research* 52, 139–149.

Hedges, J.I., Keil, R.G. and Benner, R. 1997. What happens to terrestrial organic matter in the ocean. *Organic Geochemistry* 27 (5/6), 195–212.

Heggie, D.T., Skyring, G.W., O'Brien, P., Reimers, C. Herczeg, A., Moriarty, D.J., Burnett, W.C. and Milnes, A.R. 1990. Organic carbon cycling and modern phosphorite formation on the east Australian continental margin: an overview. In *Phosphorite Research and Development.* Geol. Soc. Spec. Publ. 52 (eds. A.G. Notholt and I Jarvis), pp. 87–117.

Hedges, J.I. and Keil, R.G. 1995. Sedimentary organic matter preservation: an assessment and speculative synthesis. *Marine Chemistry* 49, 81–115.`

Hedges, J.I. and Keil, R.G. 1999. Organic geochemical perspectives on estuarine processes: sorption reactions and consequences. *Marine Chemistry* 65, 55–65.

Herzfeld, M., Andrewartha, J.R., Sakov, P. and Webster, I. 2006. *Numerical Hydrodynamic Modelling of the Fitzroy Estuary.* Cooperative Research Centre for Coastal Zone, Estuary & Waterway Management. Technical Report No. 38.

Hutchins, D.A. 1995. Iron and the marine phytoplankton community. Progress in *Phycological Research* 11, 1–49.

Joint, I.R. 1986. Physiological ecology of pico-phytoplankton in various oceanographic provinces. In Platt, T. and Li, W.K.W. (Eds) Photosynthetic Pico-phytoplankton, *Canadian Bulletin of Fisheries and Aquatic Sciences* 214, 287–309.

Joo, M., Yu, B., Carroll, C. and Fentie, B. 2005. Estimating and modelling suspended sediment loads using rating curves in the Fitzroy River catchment Australia. International Congress on Modelling and Simulation. Modelling and Simulation Society of Australia and New Zealand, December 2005.

Karl, D.M., Letelier, R., Hebel, D., Tupas, L., Dore, J., Christian, J. and Winn, C. 1995. Ecosystem changes in the North Pacific subtropical gyre attributed to the 1991–92 El Nino. *Nature* 373, 230–234.

Karl, D. M., Letelier, R., Tupas, L., Dore, J., Christian, J and D. Hebel, D. 1997. The role of nitrogen fixation in biogeochemical cycling in the subtropical North Pacific ocean. *Nature* 388:533–538.

Karl, D.M., Bidigare, R.R. and Letelier, R.M. 2001. Long-term changes in plankton community structure and productivity in the North Pacific Subtropical Gyre: The domain shift hypothesis. *Deep-Sea Research II* 48, 1449–1470.

Keil, R.G., Mayer, L.M., Quay, P.D., Richey, J.E. and Hedge, J.I. 1997. Loss of organic matter from riverine particles in deltas. *Geochimica et Cosmochimica Acta* 61 (7), 1507–1511.

Kinsman, B., 1965. Wind Waves – Their Generation and Propagation on the Ocean Surface. Prentice-Hall, Englewood Cliffs N.J., 676 pp.

Kirchman, D.L. 2000. Uptake and regeneration of inorganic nutrients by marine heterotrophic bacteria. In D.L. Kirchman (Ed.), Microbial Ecology of the Oceans. Wiley-Liss Inc, pp. 261–288.

Kleypas, J.A. and Burrage, D.M. 1994. Satellite observations of circulation in the southern Great Barrier Reef, Australia. *Int. J. Remote Sensing*, 15(10) 2051–2063

Krull, E.S., Baldock, J.A. and Skemstad, J.O. 2003. Importance of mechanisms and processes of the stabilisation of soil organic matter for modelling carbon turnover. *Functional Plant Biology* 30, 207–222.

Kuhnen, M. 2004. Constraining the source areas and nutrient transport of sediment entering the Fitzroy Estuary since European arrival. Honours Thesis (The Australian National University)

Kustka, A., Carpenter, E.J. and Sanudo-Wilhelmy, S.A. 2002. Iron and marine nitrogen fixation: progress and future directions. *Research in Microbiology* 153, 255–262.

LeBlond, P.H. and Mysak, L.A. 1978. Waves in the Ocean. Elsevier, New York, 602 pp.

Lenes, J.M., Darrow, B.P., Cattrall, C., Heil, C.A., Callahan, M., Vargo, G.A. and Byrne, R.H. 2001. Iron fertilization and the Trichodesmium response on the west Florida shelf. *Limnology and Oceanography* 46(6), 1261–1277.

Lewis, W.M., Melack, J.M., McDowell, W.H., McClain, M. and Richey, J.E. 1999. Nitrogen yields from undisturbed watersheds in the Americas. *Biogeochemistry* 46, 149–162.

Lourey, M.J., Alongi, D.M., Ryan, D.A.J. and Devlin, M.J. 2001. Variability of nutrient regeneration rates and nutrient concentrations in surface sediments of the northern Great Barrier Reef shelf. *Continental Shelf Research* 21, 145–155.

Margvelashvili, N. Robson, B., Sakov, P., Webster, I.T., Parslow, J.S., Herzfeld, M. and Andrewartha, J.R. 2003. *Numerical modelling of hydrodynamics, sediment transport and biogeochemistry in the Fitzroy Estuary.* Final Report to the Cooperative Research Centre for Coastal Zone, Estuary, and Waterway Management for project CM-2.

Margvelashvili, N., Herzfeld, M. and Webster, I. 2006. *Modelling of Fine Sediment Transport in Fitzroy Estuary and Keppel Bay.* Cooperative Research Centre for Coastal Zone, Estuary and Water Management Technical Report No. 39.

Massey, B.S. 1980. Mechanics of Fluids. Van Nostrand Reinhold, New York, 543 pp.

Maxwell, W.G.H. 1968. Atlas of the Great Barrier Reef. Elsevier, New York, 258pp.

McCarthy, M., Pratum, T., Hedges, J. and Benner, R. 1997. Chemical composition of dissolved organic nitrogen in the ocean. *Nature* 390, 150–154.

Middleton, J.H., Buchwald, V.T. and Huthnance, J.M. 1984. The anomalous tides near Broad Sound. *Continental Shelf Research* 3(4), 359–381.

Middleton, J.H., Cotis, P., Griffin, D.A., Macks, A., McTaggart, A., Merrifield, M.A. and Nippard, G.J. 1994. Circulation and water mass characteristics of the southern Great Barrier Reef, *Australian Journal of Marine and Freshwater Research*, 45: 1–18.

Mitsui, A., Kumazawa, S., Takahashi, H., Ikemoto, H., Cao, S. and Arai, T. 1986. Strategy by which nitrogen-fixing unicellular cyanobacteria grow photoautotropically. *Nature* 323, 720–722.

Montoya, J.P., Holl, C.M., Zehr, J.P., Hansen, A., Villareal, T.A. and Capone, D.G. 2004. High rates of N2 fixation by unicellular diazotrophs in the oligotrophic Pacific Ocean. *Nature* 430,1027–1031.

Neumann, L.E. 2004. Modelling of Flocculation and Settling of Suspended Sediments Using Population Balances, PhD thesis, University of Queensland, 179 pp.

O'Neill, J.P., Byron, G.T. and Wright, S.C. 1992. Some physical characteristics and movement of the 1991 Fitzroy river flood plume. In Proceedings of a

Workshop held in Rockhampton, Australia, 27 September, 1991. Ed. G.T. Byron. GBRMPA.

Oubelkheir, K., Clementson, L., Webster, I., Ford, P., Dekker, A., Radke, L, and Daniel, P. *in press.* Using inherent optical properties to investigate biogeochemical dynamics in a tropical macro-tidal coastal system. Accepted for publication in *Journal of Geophysical Research*.

Owens, N.J.P. 1986. Estuarine nitrification: a naturally occurring fluidised bed reaction? *Estuarine, Coastal and Shelf Science* 22, 31–44.

Palenik, B. and Morel, F.M.M. 1990. Amino acid utilisation by marine phytoplankton: A novel mechanism. *Limnology and Oceanography* 35(2), 260–269.

Perakis, S.S. and Hedin, L.O. 2002. Nitrogen loss from unpolluted South American forests mainly via dissolved organic compounds. *Nature* 415, 416–419.

Piorewicz, J. and Massel, S.R. 2001. Prediction of Ocean Waves in Shallow Water. Keppel Bay, Queensland , Recorded Data Analysis. Proceedings 15th Australasian Coastal and Ocean Engineering Conference , Gold Coast, Qld, 25–28 September 2001, pp. 528–533.

Pickard, G.L., Donguy, J.R., Henin, C. and Rougerie, F. 1977. A Review of the Physical Oceanography of the Great Barrier Reef and Western Coral Sea. Australian Government Publishing Service, Canberra.

Queensland Environmental Protection Agency (2002) http://www.epa.qld.gov.au/publications/p01315aa.pdf/Wave_data_recording_program_Queensland_wave_climate_annual_summary_for_season_200102.pdf

Queensland Environmental Protection Agency (2003) http://www.epa.qld.gov.au/publications/p01270aa.pdf/Wave_data_recording_program_Queensland_wave_climate_annual_summary_for_season_200203.pdf

Queensland Environmental Protection Agency (2004) http://www.epa.qld.gov.au/publications/p01612aa.pdf/Wave_data_recording_program_Queensland_wave_climate_annual_summary_for_season_20032004.pdf

Radke, L.C., Atkinson, I. and Tindall, C. 2004a. *Dry season water column and sediment properties in the Fitzroy Estuary and Keppel Bay, Rockhampton Queensland: Report on methods and raw data from the September 2003 Survey.* Cooperative Research Centre for Coastal Zone, Estuary and Waterway Management Agricultural (Fitzroy) Project, Contaminants Dynamics Sub-project, Milestone Report AC16.

Radke, L.C., Atkinson, I. and Tindall, C. 2005a. *Report on methods and raw data from the second (August 2004) dry season water column and sediment properties of Keppel Bay.* Cooperative Research Centre for Coastal Zone, Estuary and Waterway Management Agricultural (Fitzroy) Project, Contaminants Dynamics Sub-project, Milestone Report AC56.

Radke, L.C., Atkinson, I. and Tindall, C. 2005b. *Report on methods and raw data from the Vibracoring survey of Keppel Bay:* Biogeochemical Component, Cooperative Research Centre for Coastal Zone, Estuary and Waterway Management Agricultural (Fitzroy) Project, Contaminants Dynamics Sub-project, Milestone Report ACsupp2.

Radke, L.C., Ford, P.F., Webster, I., Douglas, G., Oubelkheir, K., Atkinson, I., Robson, B., Verwey, P., MacKenzie, K. and Clementson, L. 2005c. Results of two dry-season surveys of Keppel Bay and Casuarina Creek: Biogeochemical properties of the water column and underlying sediments. Geoscience Australia, Record 2005/18, 121pp.

Radke, L.C., Ford, P., Verwey, P. and Webster, I. 2005d. *Field report on the first wet season water column and sediment properties in the Fitzroy Estuary and Keppel Bay, Rockhampton, Queensland.* Cooperative Research Centre for Coastal Zone, Estuary and Waterway Management Agricultural (Fitzroy) Project, Contaminants Dynamics Sub-project, Milestone Report AC17, AC18, and AC 19

Ransom, B., Bennett, R.H., Baerwald, R. and Shea, K. 1997. TEM study of in situ organic matter on continental margins: occurrence and the “monolayer hypothesis”. *Marine Geology* 138, 1–9.

Redfield, A.C., Ketchum, B.J. and Richards, F.A. 1963. The influence of organisms on the composition of sea water. In M.N. Hill (Ed.), The Sea, Vol 2, Wiley-Interscience, New York, pp. 26–77.

Revill, A., Leeming, R. and Smith, C.S 2005. *Fitzroy River: Intertidal Mudflat Biogeochemistry.* Cooperative Research Centre for Coastal Zone, Estuary and Waterway Management Milestone report AC64 as part of the Final Report for Coastal CRC Project AC – Fitzroy Contaminants. (in preparation)

Reynolds, C.S. 1984. The Ecology of Freshwater Phytoplankton. Cambridge

Ridd, P.V., Heron, M.L., Steiglitz, T.C. and Orpin, A*. in submission*. The cross-shelf diffusion coefficient and flushing time of the Great Barrier Reef lagoon estimated from cross-shelf salinity transects, submitted to *Journal of Geophysical Research*.

Robson, B.J., Webster, I.T., Margvelashvili, N. and Herzfeld, M. 2006. *Scenario Modelling: Simulating the Downstream Effects of Changes in Catchment Land*

Use. Cooperative Research Centre for Coastal Zone, Estuary and Waterway Management. Technical Report No. 41.

Ruttenberg, K.C. 2005. The Global Phosphorus Cycle. In Schlesinger, W.H. (ed.) Biogeochemistry, Treatise on Geochemistry, Vol 8, Elsevier Ltd, pp. 585–645.

Ryan, D., Skene, D., Brooke, B., Kuhnen, M., and Radke, L. 2004. *Report on floodplain and estuarine sediment data.* Cooperative Research Centre for Coastal Zone, Estuary and Waterway Management. Milestone AC40. 62 pp.

Ryan, D.A., Bostock, H. Brooke, B.P. and Skene, D. 2005. *Synthesis of sediment and acoustic data for Keppel Bay – Report on the analysis of cores and sub-bottom profiles.* Cooperative Research Centre for Coastal Zone Estuary and Waterway Management Agricultural (Fitzroy) Project, Contaminants Dynamics Sub-project, Milestone Report AC54.

Ryan, D.A., Bostock, H., Brooke, B., Collins, L.B., Buchanen, C., Siwabessy, J., Margvelashvili, N., Radke, L. and Hamilton, L. *in prep*. *Geomorphology, sediment transport, and process-related seabed classification in Keppel Bay, south-east Queensland, Australia.*

Seitzinger, S.P., Saunders, R.W. and Styles, R. 2002. Bioavailability of DON from natural and anthropogenic sources to estuarine plankton. *Limnology and Oceanography* 47(2), 353–366.

Simpson, J.H. and Hunter, J.R. 1974 Fronts in the Irish Sea. Nature, 250: 404–406.

Skene, D., Ryan, D. and Brooke, B. 2004. *Subbottom profiling, surface sediment sampling, vibracoring and mapping with sidescan and multibeam sonar systems in the Fitzroy Estuary and Keppel Bay.* Cooperative Research Centre for Coastal Zone, Estuary and Waterway Management Coastal Habitat Mapping Project Milestone Report CG04.01.

Smith, C. 2004. *Report on the Sampling of the Intertidal Zone of the Fitzroy River.* Cooperative Research Centre for Coastal Zone, Estuary and Waterway Management Milestone Report AC45.11 pp.

Smith, J., Douglas, G., Radke, L., Palmer, M. and Brooke, B. *in prep*. *Identifying sources of catchment-derived sediments to Keppel Bay and the Fitzroy River floodplain in tropical Queensland, Australia.* Cooperative Research Centre for Coastal Zone, Estuary and Waterway Management Report toward the partial fulfilment of milestone AC66.

Smith, S. V. and M. J. Atkinson 1983. Mass balance of carbon and phosphorus in Shark Bay, Western Australia. *Limnology and Oceanography* 28:625–639.

Stal, M., Meysman, F.J.R. and Stal, L.J. 2003.Temperature excludes N_2 fixing heterocystous cyanobacteria in the tropical oceans. *Nature* 525: 504–507.

Suttle, C.A. and Harrison, P.J. 1988. Ammonium and phosphate uptake rates, N:P supply ratios, and evidence for N and P limitation in some oligotrophic lakes. *Limnology and Oceanography* 33(2), 186–202.

Takamura, N. and Nojiri, Y. 1994. Picoplankton biomass in relation to lake trophic state and the TN:TP ratio of lake water in Japan. *Journal of Phycology* 30, 439–444.

Taylor, B. and Jones, M. 2000. National Land and Water Resources Audit, Fitzroy Audit Summary Report.

Thomas, D.N., Judd, S.J. and Fawcett, N. 1999. Flocculation modelling: A review. *Water Research*, 33(7) 1579–1592.

Ullman, W.J. and Sandstrom, M.W. 1987. Dissolved nutrient fluxes from the nearshore sediments of Bowling Green Bay, Central Great Barrier Reef Lagoon (Australia). *Estuarine, Coastal and Shelf Science* 24, 289–303.

Vainshtein, P. Shapiro, M. and Gutfinger, C. 2002. Creeping flow past and within a permeable spheroid. *International Journal of Multiphase Flow*, 28, 1945–1963.

van Rijn, LC 1993, Principles of Sediment Transport in Rivers, Estuaries and Coastal Seas, Aqua Publications, Amsterdam.

Vidussi, F., Marty, J-C. and Chiaverini, J. 2000. Phytoplankton pigment variations during the transition from spring bloom to oligotrophy in the northwestern Mediterranean sea. *Deep-Sea Research I* 47: 423–445.

Vidussi, F., Claustre, H., Manmca, B.B., Luchetta, A. and Marty, J-C. 2001. Phytoplankton pigment distribution in relation to upper thermocline circulation in the eastern Mediterranean Sea during winter. *Journal of Geophysical Research* 109: 19,939–19,956.

Walker, T. A. 1981. Dependence of phytoplankton chlorophyll on bottom resuspension in Cleveland Bay, northern Queensland. *Australian Journal of Marine and Freshwater Science* 32, 981–986.

Webster, I.T., Ford, P.W., Robson, B., Margvelashvili, N. and Parslow, J. 2004. *Conceptual models of the hydrodynamics, fine sediment dynamics, biogeochemistry and primary production in the Fitzroy Estuary.* Cooperative Research Centre for Coastal Zone Estuary and Waterway Management Technical Report No. 8.

Webster, I.T., Ford, P.W. and Tillman, P. 2005. Estimating Nutrient Budgets in Tropical Estuaries Subject to Episodic Flows. Marine Pollution Bulletin, 51: 165–173.

Wilhelm, S.W. 1995. Ecology of iron-limited cyanobacteria: a review of physiological responses and implications for aquatic systems. *Aquatic Microbial Ecology* 9, 295–303.

Woodhead, P.M. 1970. Sea-surface circulation in the southern region of the Great Barrier Reef, spring 1966. *Aust. J. Mar. Freshwat. Res*. 21: 89–102.

Yoshida, T., Ken-ichiro, H. and Ohmoto, H. 2002. Dissolution of iron hydroxides by marine bacterial siderophore. *Chemical Geology* 184, 1–9.

Zehr, J.P., Carpenter, E.J. and Villareal, T.A. 2000. New perspectives on nitrogen-fixing organisms in tropical and subtropical oceans. *Trends in Microbiology* 68(8), 68–73.

Zehr, J.P. Waterbury, J.B., Turner, P.J., Motoya, J.P., Omoregie, E., Steward, G.F., Hansen, A. and Karl, D.M. 2001. Unicellular cyanobacteria fix N_2 in the subtropical North Pacific Ocean*. Nature* 412, 635–638.

Zehr, J.P. and Ward, B.B. 2002. Nitrogen cycling in the ocean: New perspectives on processes and paradigms. *Applied and Environmental Microbiology* 68(3), 1015–1024.